GEOLOGIC EVOLUTION OF THE ARCHEAN BUHWA GREENSTONE BELT AND SURROUNDING GRANITE-GNEISS TERRANE, SOUTHCENTRAL ZIMBABWE

by

Christopher M. Fedo

Dissertation submitted to the Faculty of the

Virginia Polytechnic Institute and State University

in partial fulfillment of the requirements for the degree

DOCTOR OF PHILOSOPHY

in

Geological Sciences

APPROVED:

K.A. Eriksson, Chairman

T.G. Blenkinsop

R.D. Law

J.F. Read

R.J. Tracy

September, 1994

Blacksburg, Virginia

GEOLOGIC EVOLUTION OF THE ARCHEAN BUHWA GREENSTONE BELT AND SURROUNDING GRANITE-GNEISS TERRANE, SOUTHCENTRAL ZIMBABWE

by

Christopher M. Fedo

Kenneth A. Eriksson, Chairman

Geological Sciences

(ABSTRACT)

The Archean (~3.0 Ga) Buhwa Greenstone Belt, and surrounding granite-gneiss terrane, is the least understood major greenstone belt in the Archean Zimbabwe Craton, despite occupying a critical position between an early Archean continental nucleus and the Limpopo Belt. The cover succession in the Buhwa Greenstone Belt, which was probably deposited on the margin of this nucleus, is divisible into shelfal and basinal facies associations separated by a transitional facies association. The shelfal association consists mostly of quartzarenite and shale, but also contains a thick succession of iron-formation. Geochemical characteristics of the shales indicate that the source terrane consisted of several lithologies including tonalite, mafic-ultramafic volcanic rocks, and granite that underwent intense chemical weathering. Basinal deposits consist dominantly of greenstones, with less abundant chert and iron-formation. The cover succession, which was deposited on a stable shelf transitional to deep water, has no stratigraphic equivalents elsewhere on the Archean Zimbabwe Craton. However, time and lithologic correlatives in the central zone of the Limpopo

Belt and on the Kaapvaal Craton suggest a period of tectonic stability between ~3.0 Ga and ~2.9 Ga in southern Africa.

At ~2.9 Ga, the northern margin of the greenstone belt experienced kilometer-scale, oblique-slip dextral shearing. This shear zone and the surrounding margins of the greenstone belt were later intruded by the ~2.9 Ga Chipinda batholith, which ranges from granitic to tonalitic in composition.

A number of events occurred during the time period spanning 2.9-2.5 Ga and current geochronology cannot separate their order; some are known to be coeval. Crustal shortening to the northwest, which resulted in map-scale folding of the cover succession (and surrounding batholith) and greenschist-facies metamorphism, occurred along a set of discrete high-angle reverse-sense shear zones in response to uplift the Northern Marginal Zone of the Limpopo Belt over the Zimbabwe Craton. Two suites of potassic granites were intruded into the area near the end of reverse shearing. Analysis of a conjugate fault pair that is developed within one of the potassic granite suites, yields a principal compressive stress consistent with continued northwest-directed crustal shortening. The region was stabilized by ~2.5 Ga, with intrusion of the Great Dyke of Zimbabwe. It is possible that the last events to affect the area, which include sinistral shearing, transecting cleavage development, and northwest-striking open folding, took place during the 2.9-2.5 Ga time interval. These structures post-date regional folding and metamorphism, but because of limited magnitude and extent, do not show obvious cross-cutting relationships with other rocks or structures. A tenable alternative is that these late structures formed at ~2.0 Ga, an age that is proving to be of great significance in the evolution of the Limpopo Belt and along parts of the southern margin of the Zimbabwe Craton.

To Mom, Dad, and Shannon

Acknowlegments

I am fortunate to have many people to thank. As my undergraduate advisor at Cal State Fullerton, John Cooper excited my interest in Geology many years ago. Thus, it is his fault I had to write this dissertation. I have learned a great deal about rocks and life from him, and am fortunate that our friendship and scientific collaboration are as fresh as ever. I am nervous to bear the responsibility of "colleague" now. Sparky, John, and DH, my friends from undergrad days, kept me interested in structure and hard rocks even though I like cross-bedded quartzites, and I am thankful now to have gained a healthy regard for "interdisciplinary" geology from them.

Ken Eriksson, my advisor, offered me the possibility to see, and do research in, Zimbabwe. Ken's expertise on Archean geology, both in the field and lab, has been a tremendous asset to my project and I am most greatful to have been presented so many opportunities during my tenure in his lab. It is difficult to say how much I have appreciated all of his efforts to critically evaluate the different papers and keep the science of the highest caliber. Sorry about the scorpion sting! My other committee members at Tech: Fred Read, Rick Law, and Bob Tracy always made time to see me on mostly unannounced visits to their offices; their advise on a diverse array of topics has been invaluable to my education and mental well-being. Richard Bambach always had a nice thing to say and an ear to lend. My thanks to Sam Bowring and Clark Isachsen at MIT for providing the preliminary zircon dates mentioned herein. Eirik Krogstadt welcomed me into the isotope lab at University of Maryland for REE analyses; Paul Tomascak patiently guided me through the chemistry and mass spectrometry.

It is impossible to count the number of times Mary, Dean, Linda, and Carolyn, have extracted me from difficult situations, and their bright spirits always put a smile

on my face. Karen's help over the years could never be repaid in full. My friends here have made me a better person and made life ejoyable. Those mostly responsible include: Eric and Jane, Cole, Mike and Pauline, Mike and Karen, Bret, Tom and Kathleen, Sven and Jen, Rich, Taury and Sharon, Aus, Scott, Anna, Dave, Ron and Barb, Jim, Sam, Pat, John and Sara, Matt, and Charlie. John Hanchar has lifted my spirits for what seems like ever.

Tom Blenkinsop showed a tremendous enthusiasm for my project upon my arrival in Zimbabwe. Tom graciously let me live in his house when I stayed in Harare and coconspired in many incredible dinners. Thanks for all the avo's! When it was clear that Buhwa could not offer the kind of sedimentology study I intended to do, he supported and encouraged me to stay there and undertake the structural details, rather than search for different sediments. The staff at Buchwa Mine provided me with superlative friendship so far from home and superlative field accommodations. I thank the entire Buchwa community through mine manager Zacheus Ncube. My good friend Derek Mudzamba spent five months chasing around after cross-beds and stretching lineations in the bush with me during my first field season. Gift Nyirenda followed suit the next year. Ndatenda to everyone who let me trespass on their farms, waved, and smiled while I inhabited Mberengwa District. In Harare, all at University of Zimbabwe did what they could to help. I am especially fortunate to have been able to discuss the evolution of the Zimbabwe Craton with Jim Wilson. John Grotzinger took time out of an African holiday to spend a few days in the field with me and offer his insights. I was also lucky to have overlapping field seasons with Balz Kamber and others from Jan Kramer's isotope lab in Switzerland. Balz and Jan have started dating garnets and other phases from my field area. Steve McCourt added many helpful

comments regarding structural geology during a visit to Buhwa and graciously offered me wonderful accommodations in Pretoria.

I made a lengthy stay at the University of Cambridge under the guidance of Mike Bickle and made many friends there. My thanks go to Mike, Morag, Claire, Maurice, Gideon, and Hazel.

I met Kate during my last year at Tech, and since then she has become about the most important facet of my life. How or perhaps why, she has managed to stay with me during the final stretch baffles me, although I sure am glad. I'm looking forward to our future together.

My family has been my backbone. Merely to say thanks would cheapen their efforts to see me be happy. They have stuck by me through this whole ordeal in a way anyone would be envious of and I love them dearly for it. A better Mom, Dad, sister, and brother-in-law cannot be found.

This research was funded by a National Science Foundation grant (910-4876) to Ken Eriksson and a grant from the Geological Society of America to me.

Table of Contents

List of Figures

List of Tables

CHAPTER 1

PREFACE

This dissertation is a collection of four papers that focus on different facets of the geologic evolution of the Archean Buhwa Greenstone Belt and surrounding granite-gneiss terrane in southern Zimbabwe, Africa. Archean-age rocks in southern Africa are found on both the Kaapvaal (South Africa) and Zimbabwe cratons (Zimbabwe) and in the granulite-facies Limpopo Belt, which separates the two cratons. Much of what is known regarding Archean cratonic evolution, the Limpopo Belt, and the joining of the Limpopo Belt to low-grade cratonic rocks comes from detailed studies in South Africa, despite the fact that most of the Limpopo Belt lies within Zimbabwe and rocks of the Zimbabwe Craton are equally well exposed. Although much has been learned regarding the Archean evolution of southern Africa, the "one-sided" pool of data has limited all genetic models for the region. The Buhwa Greenstone Belt provides a unique opportinity in Zimbabwe to study cratonic supracrustal deposition and later deformation associated with uplift of the Limpopo Belt because this greenstone belt lies at the southern margin of the craton directly adjacent to the Limpopo Belt.

There has been little in the way of previous geologic work to build on. As a result, much of what is presented in this dissertation represents the first critical analysis regarding the geology of the area. The only study of significance is that of Worst (1962). His work in the Buhwa area established a preliminary geologic map at 1:100 000 showing the distribution of lithologies across an area of ~1200 km^2 and delineated

the extent of high-grade iron ores that occur at Buhwa. Even at that scale, I found little need for major repositioning of lithologic contacts during my mapping, which was mostly at 1:25 000. Most of my repositioning of contacts has come from separating out new lithologic units based on protolith analysis.

The first paper (Chapter 2) discusses the stratigraphic succession that comprises the Buhwa Greenstone Belt. Unlike other greenstone belts in Zimbabwe, which dominantly comprise thick volcanic piles, the cover succession at Buhwa consists of marine-shelf and basinal facies associations separated by a transitional association. Marine-shelf rocks include cross-stratified quartzarenites, shales, and iron-formation. Basinal rocks are dominantly metagreenstones, but have thick accumulations of iron-formation and thoroughly recrystallized metachert. Metamorphic grade of the shelfal association is quite low (greenschist) and sedimentary features are well preserved. However, the same is not true for the basinal association, which at the margins of the belt are ductilely deformed at amphibolite facies. A depositional unconformity at the base of the section was not located, but the early Archean Tokwe segment gneisses further north in the craton are thought to be the basement. Based on available geochronology and cross-cutting relationships, the cover succession has a depositional age between ~2.9 Ga and ~3.05 Ga, which is again unique with respect to other Zimbabwean greenstone belts that were deposited mostly after ~2.9 Ga. While there are no other stable-shelf successions deposited at ~3.0 Ga in Zimbabwe, the cover succession at Buhwa resembles the lower part of the Witwatersrand Supergroup and the Mozaan Group in the Kaapvaal Craton and the granulite-facies Beitbridge Group in the Limpopo Belt all of which were deposited at approximately the same time. The time period 2.9-3.0 Ga in southern Africa was dominated by stable-shelf sedimentation.

The main purpose of the second paper (Chapter 3) is to document the historical geology of the area, from basin formation through deformation and metamorphism. Prior to this study, virtually all aspects of the structural geology (and relative timing of structures) and metamorphism were unknown. The history is divisable into three, or possibly four, major time frames. The oldest events are related to assembly of the Tokwe segment at ~3.5 Ga, which is interpreted to be the basement for the cover succession of the Buhwa Greenstone belt (deposited at ~3.0 Ga). Ductile deformation and tonalitic-granitic plutonism dominate the events at ~2.9 Ga. Most of the geologic events that shaped the geology of the area occurred between 2.9 Ga and 2.5 Ga (probably between 2.7-2.5 Ga but current geochronology does not permit this interpretation), and are associated with the northwestward thrusting of the Northern Marginal Zone of the Limpopo Belt over the Zimbabwe Craton. Intrusion of two suites of potassic granites accompanied deformation and regional metamorphism. The end of major deformation is heralded by the emplacement of the Great Dyke of Zimbabwe at ~2.5 Ga. Some of the late structures could possibly have formed during a fourth period of deformation at ~2.0 Ga. Thusfar only some very preliminary Pb-Pb garnet dates provided by Jan Kramers hint at this late deformation. It is noteworthy that much of the deformation of the Central Zone of the Limpopo Belt is now interpreted to have occurred at this time and that isotopic dates of ~2.0 Ga have been reported from the edge of the Zimbabwe Craton in the past.

The purpose of the third paper (Chapter 4) is to evaluate source-area composition and weathering conditions by reviewing the major-, trace-, and rare-earth element geochemistry of shelf- and transitional-association shales. The abundance of quartzarenite in the lower part of the cover sucession (shelf association) is consistent with a source terrane dominated by felsic plutonic rocks. However, the inferred

basement (Tokwe segment) consists of a mixture of tonalite, mafic-ultramafic volcanic rocks, and less common granite. Incompatible/compatible element ratios of immobile elements are consistent with a mixed source of mafic and felsic components; rare earth element patterns also suggest this. The shales are nearly devoid of calcium and sodium, but have potassium concentrations that are elevated from average Archean crust. When plotted on an aluminum - calcium+sodium - potassium ternary diagram, Buhwa shales lie along the potassium-aluminum join in a position consistent with derivation from granite. However, these elements more accurately depict weathering conditions because they are subject to considerable mobility during chemical weathering in the source terrane. The nearly complete loss of calcium and sodium suggests that aggressive chemical weathering conditions prevailed. Elevated potassium concentrations best explained by later metasomatsm. In the Buhwa region, potassium enrichment could have occurred during emplacement of the two suites of potassic granites at ~2.6 Ga.

The fourth paper (Chapter 5) presents a brief look at the occurrence and origin of the significant iron-ore deposits with respect to the overall geologic setting of the Buhwa Greenstone Belt. The iron ores at Buhwa are amongst the richest in Zimbabwe. With over 6000 km of strike length of iron-formation in Zimbabwe, one question is: why are the ores there so high-grade? Hypogene fluids seem to be the cause of ore enrichment. Perhaps the unique stratigraphic/sedimentologic setting of the Buhwa Greenstone Belt at the edge of the Tokwe segment coupled with its geographic proximity to advancing Limpopo Belt ductile thrust faults combined to produce the high-grade ores at Buhwa.

CHAPTER 2

Stratigraphic Framework of the ~3.0 Ga Buhwa Greenstone Belt: a Stable-Shelf Succession Unique in the Zimbabwe Archean Craton

ABSTRACT

The ~3.0 Ga Buhwa Greenstone Belt is the least understood major greenstone belt in the Archean Zimbabwe Craton, despite occupying a critical position adjacent to the Limpopo Belt. The cover succession at Buhwa is divisible into western and eastern associations connected by a belt of transitional deposits. The western, shelf association is ~4 km thick and consists of, in ascending stratigraphic order, quartzarenite, interbedded quartzarenite and shale, shale, and iron-formation. Nested sets of trough cross-stratification are the most common sedimentary structure in the quartzarenites, with less common oscillatory and interference ripples. Shales have isolated trains of sand-starved ripples. Iron-formation consists of laterally persistent, alternating, mm-scale bands of white chert, red chert, and hematite. These lithologies and structures formed in inner-shelf through below-wave-base shelf settings. Transitional deposits are dominated by green, tan, and locally black shale (now phyllite), with less abundant iron-formation and muddy sandstone and represent more basinward lateral equivalents to the western association. Iron-formation deposits show characteristics similar to each of those present in the western and eastern associations. The eastern, deep-water basinal association has been subjected to ductile strain, which has obliterated primary textures. The association comprises metamorphosed mafic-ultramafic lavas (including spinifex-textured lavas), possible

carbonate, recrystallized metachert, and iron-formation that consists of alternating bands of black opaque minerals and white, recrystallized chert. The cover succession, which was deposited on a stable shelf transitional to deep water, has no equivalents elsewhere on the Archean Zimbabwe Craton. However, time and lithologic correlatives in the central zone of the Limpopo Belt and on the Kaapvaal Craton suggest a period of tectonic stability between 3.0 and 2.9 Ga in southern Africa.

INTRODUCTION

Widespread greenstone successions in the Zimbabwe Archean craton formed at three different times, namely ~3.5 Ga, ~2.9 Ga, and ~2.7 Ga (Wilson et al., 1978; Wilson, 1979). The foundation of this stratigraphy is the Belingwe Greenstone Belt (e.g. Bickle and Nisbet, 1993), located in the southern part of the craton (Fig. 1). Approximately 30 km southeast of the Belingwe Greenstone Belt is the Buhwa Greenstone Belt (BGB; Fig. 1), which to date has only been studied in reconnaissance in order to indentify the extent of rich iron-ore deposits (Worst, 1962). At many scales, the cover rocks at Buhwa differ markedly from the nearby cover succession in Belingwe. The purpose of this paper is to document and interpret, for the first time, the variety of lithologic associations that comprise the BGB. Two other papers will cover the structural evolution and assembly of the BGB (Chapter 3) and the geochemistry of shales in the cover succession (Chapter 4).

The BGB lies at the approximate southern edge of ~3.5 Ga Tokwe segment (Wilson, 1990), an early Archean cratonic nuclei and the BGB lies within a few kilometers of the inferred thrust front of the granulite-facies Limpopo Belt (e.g. Rollinson and Blenkinsop, in press). Thus, the BGB represents the closest Zimbabwean greenstone belt to this significant orogenic belt. This study investigates

Figure 1. Simplified geologic map showing the southern part of the Zimbabwe Craton, the Limpopo Belt, and the northern part of the Kaapvaal Craton. Greenstone belts in the Zimbabwe Craton: B - Buhwa, Be - Belingwe, Mw - Mweza, Ma - Masvingo. Inset map shows the southern horn of Africa and the regional geologic setting of the Zimbabwe and Kaapvaal Cratons and the Limpopo Belt. Redrawn from Rollinson and Blenkinsop (in press).

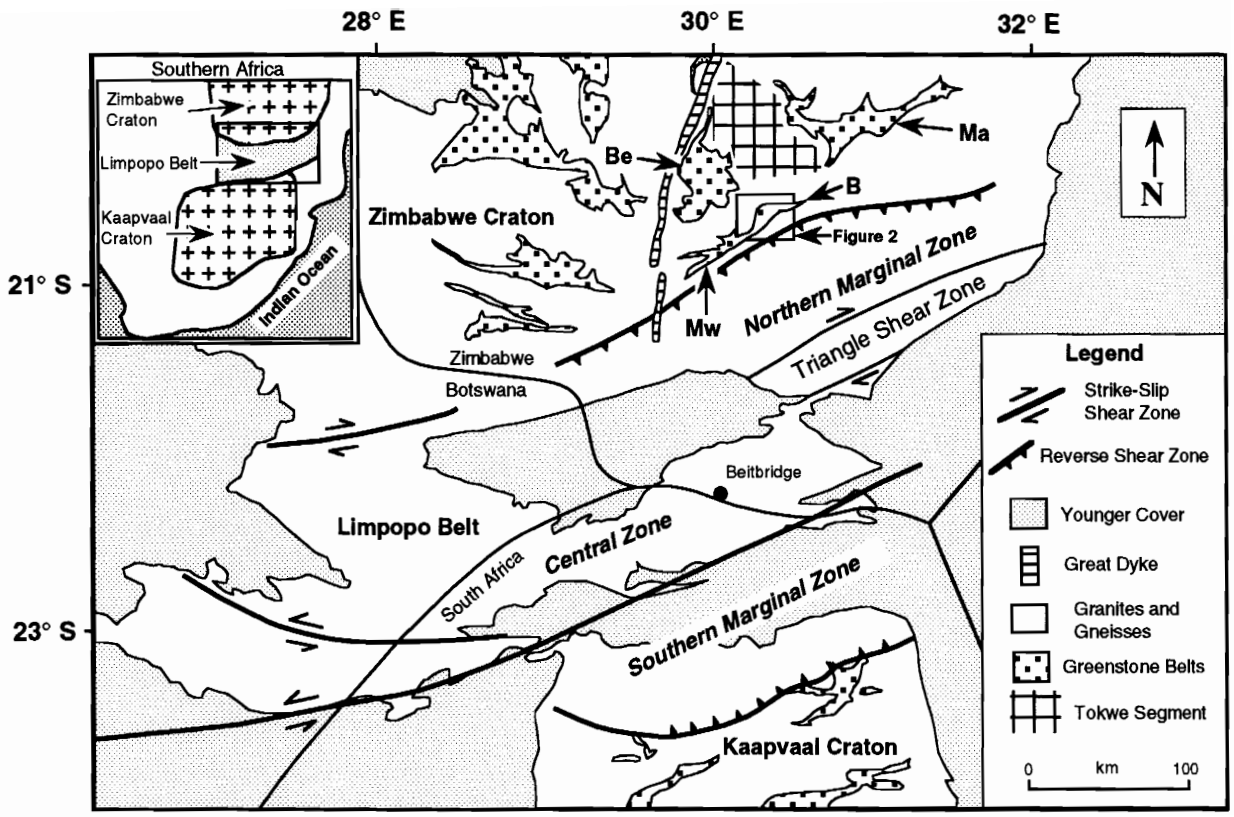
28° E
30° E
32° E
21° S
23° S
Southern Africa
Zimbabwe Craton
Limpopo Belt
Kaapvaal Craton
Indian Ocean
Zimbabwe Craton
Be
Ma
B
Figure 2
Mw
Northern Marginal Zone
Triangle Shear Zone
N
Zimbabwe
Botswana
Beitbridge
Limpopo Belt
South Africa
Central Zone
Southern Marginal Zone
Kaapvaal Craton
Legend
Strike-Slip Shear Zone
Reverse Shear Zone
Younger Cover
Great Dyke
Granites and Gneisses
Greenstone Belts
Tokwe Segment
0
km
100

the possibility that the sedimentary rocks preserved in the BGB were shed from the uplifted Limpopo orogen. Thus it is necessary to establish the relationship between the cover rocks in the BGB and Limpopo deformation and metamorphism. An understanding of the rocks at Buhwa is vital for interpretations regarding regional paleogeography and paleotectonic affinity.

GEOLOGIC SETTING

Lithologic Assemblage

An early Archean, triangular-shaped crustal domain termed the Tokwe segment crops out ~25 km north of the BGB (Fig. 1; Wilson,1990). This poorly understood fragment of sialic crust has been dated by Rb-Sr and Pb/Pb between 3.2 and 3.5 Ga (Hawkesworth et al., 1975; Taylor et al., 1991). No conclusive correlatives of the Tokwe segment have been located adjacent to the BGB. The development of the cover succession, which we interpret to have originally been deposited on the Tokwe segment, forms the topic of this paper and will be discussed below in detail.

Xenoliths of quartzarenite in adjacent plutons indicate that the Tokwe segment and the overlying sediments were intruded by a suite of plutons whose composition varies from granite to tonalite. This suite of plutonic rocks is here named the Chipinda batholith (Fig. 2). Primary minerals in these equigranular plutonic rocks are quartz, plagioclase, potassium feldspar, and biotite. Dominant accessory minerals consist of titanite (up to 4 mm and euhedral), apatite, allanite, and zircon. On the northern side of the BGB, these plutons show little evidence for strain; however, oriented biotites locally define a weak planar fabric that is concordant with bedding in the cover rocks (Fig. 2; Chapter 3). Lithologic similarity with the nearby Mashaba Tonalite (e.g. Hawkesworth et al., 1979; Bickle et al., 1993) and preliminary isotopic dates suggest

Figure 2. Geologic map and cross section of the Buhwa Greenstone belt and surrounding granite-gneiss terrane. Lithologic contacts modified from the mapping of Worst (1962).

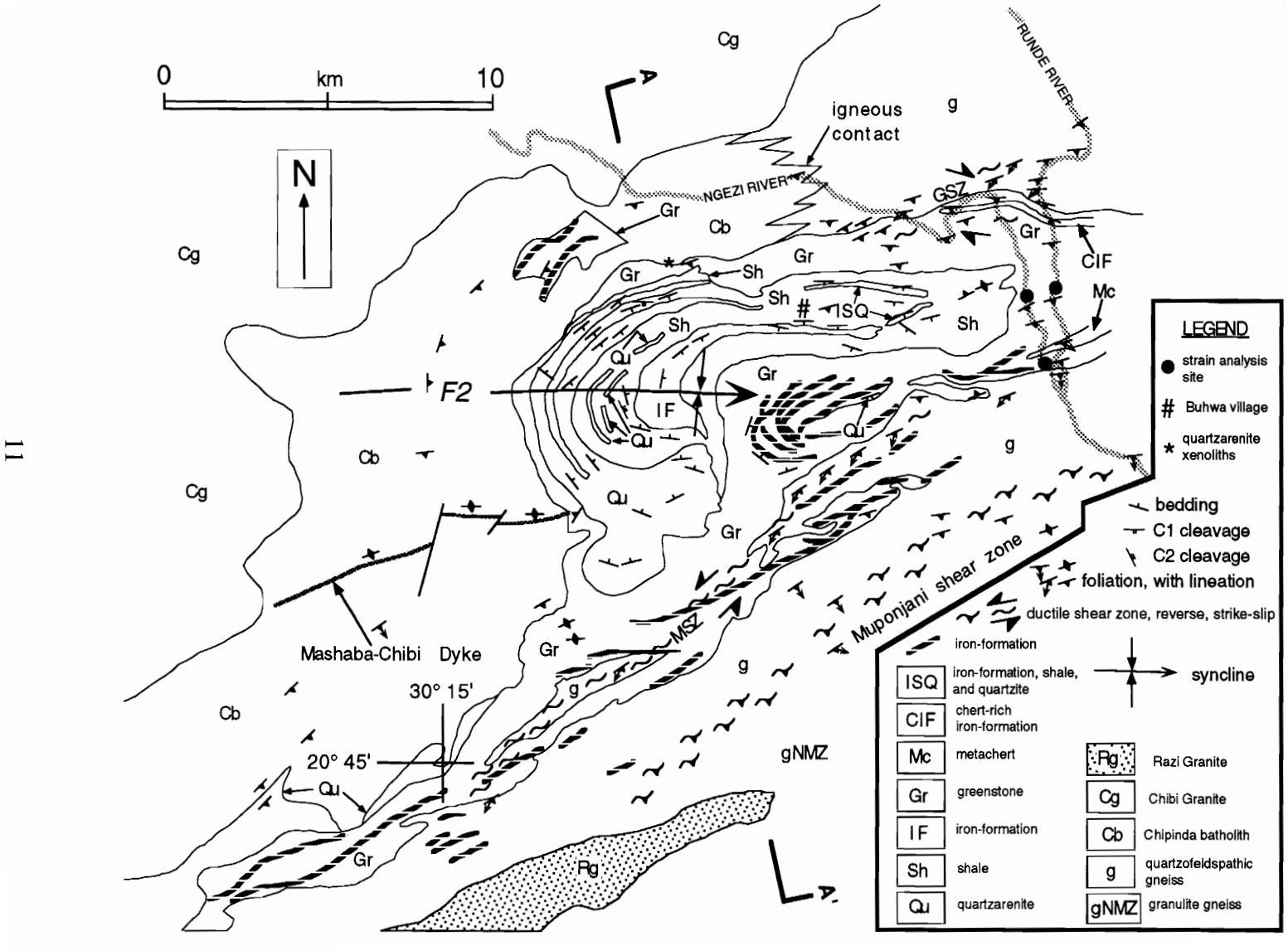
0
km
10
N
igneous
contact
RUNDE RIVER
NGEZI RIVER
GSZ
CIF
Mc
ISQ
Sh
Gr
Qu
IF
F2
Cg
Cb
g
gNMZ
Rg
MSZ
Muporjani shear zone
Mashaba-Chibi Dyke
30° 15'
20° 45'
LEGEND
strain analysis site
Buhwa village
quartzarenite xenoliths
bedding
C1 cleavage
C2 cleavage
foliation, with lineation
ductile shear zone, reverse, strike-slip
iron-formation
syncline
ISQ iron-formation, shale, and quartzite
CIF chert-rich iron-formation
Mc metachert
Gr greenstone
IF iron-formation
Sh shale
Qu quartzarenite
Rg Razi Granite
Cg Chibi Granite
Cb Chipinda batholith
g quartzofeldspathic gneiss
gNMZ granulite gneiss

Figure 2. Continued.

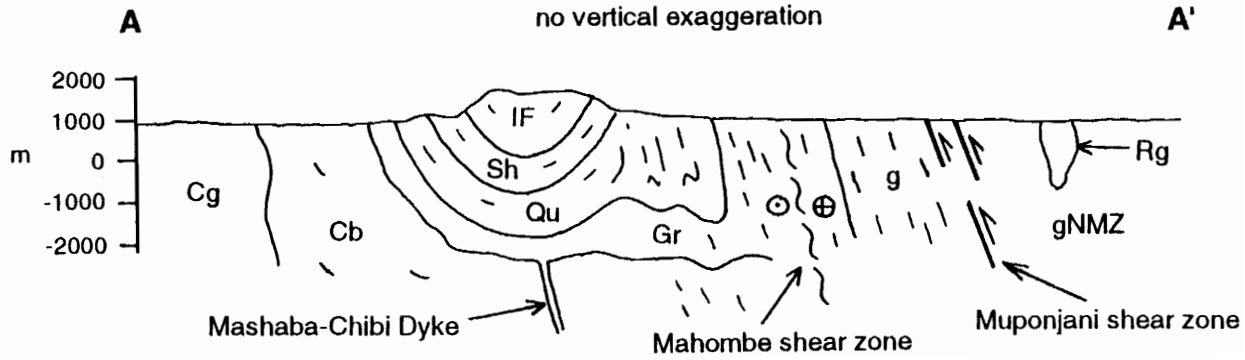
A
no vertical exaggeration
A'
2000
1000
0
-1000
-2000
m
IF
Sh
Qu
Gr
Cg
Cb
g
Rg
gNMZ
Mashaba-Chibi Dyke
Mahombe shear zone
Muponjani shear zone

that the Chipinda batholith was emplaced at ~2.9 Ga. Along most of the southern margin of the belt, rocks probably originally intrusive into the BGB have been mylonitized (Mahombe shear zone) during subsequent crustal shortening, which has obliterated primary field relationships (Fig. 2). The essential and accessory mineralogy of the mylonites is similar to that of the granitic rocks north of the belt, which we interpret as the mylonite protolith.

Gneiss that consists dominantly of alternating laterally persistent dm-thick bands of coarse-grained granitic rock (Ksp megacrysts + quartz + garnet) and dark fine-grained tonalitic gneiss (plagioclase + quartz + biotite) forms the primary lithology south of the Mahombe shear zone. This is a common lithology in the granulite-facies assemblage of the Northern Marginal Zone (NMZ) of the Limpopo Belt. No absolute dates come from the vicinity directly south of Buhwa; however, Hickman (1978) reported an inferred metamorphic age of 2880 ± 74 Ma (Rb-Sr whole-rock 13-point errorchron; recalculated using λ (^{87}Rb) = 1.42 x 10^{-11} a^{-1}) from granulite gneiss southeast of Buhwa. Berger et al. (in review) report ages spanning from 2.58-2.71 Ga from the charnockite-enderbite suite in the NMZ, SW of the Buhwa area.

A prominent, vertical, east-northeast striking mafic dyke that is offset by a north-northeast-striking apparent sinistral-sense strike-slip fault, cross-cuts the Chipinda tonalite and intersects the BGB near the fold-closure region where it spreads as a sill along the intrusive contact (Fig. 2). In several places, this dyke shows textural and compositional zonation from margin (fine-grained talc schist) to core (coarse-grained amphibole schist). Elsewhere along strike, dyke rock consists of highly sheared amphibole schist enclosing altered opaque-rich pyroxene porphyroclasts, or an altered mosaic of pyroxene crystals; pyroxenite was the likely unmetamorphosed equivalent. Ultramafic and mafic dykes of this orientation and relative age, regionally, have been

termed Mashaba-Chibi dykes and may represent filling of the feeder conduits to ~2.7 Ga Ngezi Group mafic and ultramafic lava flows (Wilson et al., 1987; Wilson, 1990). Toward the center of the craton, Mashaba-Chibi dykes are undeformed (Wilson et al., 1987); however, at Buhwa the locally present penetrative schistosity and metamorphic mineral assemblage indicate that this dyke has suffered the regional deformation and metamorphic event that affects the whole area (Chapter 3). This difference in deformaton and state of metamorphism is the result of the proximal position of the BGB with respect to major northwest-verging thrusts (Chapter 3). Worst (1962) shows the dyke cross-cutting the ~2.6 Ga Chibi Granite (see below), although we found no field evidence to support that interpretation.

Two suites of ~2.6 Ga K-feldspar granite, one north (Chibi Granite) of the BGB and the other south (Razi Granite), comprise the youngest major lithology in the Buhwa area (Fig. 2). The Chibi Granite forms an elongate batholith subparallel to orogenic strike of the Limpopo Belt and separates the BGB from the well studied Belingwe Greenstone Belt some 30 km northwest (Fig. 1). Hawkesworth et al. (1979) generated two Rb-Sr whole-rock isochrons for 15 samples of Chibi Granite, one at 2.52 ± 0.44 Ga and the other at 2.62 ± 0.22 Ga, which agrees with the 2.63 ± 0.02 Ga composite isochron for other nearby potassic granites (Hickman, 1978). There are at least two localities where undeformed Chibi Granite intruded undeformed Chipinda batholith, which is preserved as large xenoliths at the contact zone.

The Razi Granite occupies an important spatial position with respect to the BGB and the NMZ. Outcrops of Razi Granite are located directly north, straddle, and south of the the "orthopyroxene-in isograd." Traditionally this isograd has been used to demarcate the northern margin of the NMZ (Robertson, 1973, 1974), although recent detailed structural studies by Rollinson and Blenkinsop (in press), Mkweli et al. (in

press), and here (Chapter 3) have demonstrated the boundary to be a significant structural discontinuity. The Razi suite is identified by its ubiquitous K-feldspar megacrysts and cross-cutting relationships with all other lithologies. Although mostly undeformed, some plutons are sheared and indicate overthrusting of the NMZ to the northwest. An associated late-tectonic microgranite has been dated recently at 2627 ± 7 Ma by Mkweli et al. (in press; U-Pb zircon) and indicates the synchroneity age of thrusting and Razi Granite emplacement.

Structural Geology

Three major structures deform either part or all of the cover succession and surrounding granitoids at Buhwa: 1) a shear zone that bounds part of the northern margin of the BGB, 2) a shear zone that bounds the southern margin of the BGB, and 3) a regional-scale syncline that deforms the cover succession (Fig. 2; Chapter 3). Areally, both shear zones transfer considerable ductile strain into the margins of the cover succession.

The most significant structure is the major fold into which the cover succession is deformed. The fold is asymmetric in map view, with a short southern limb and a long northern limb. Rocks on the northern limb strike east/west and dip to the south, except where the rocks curve into the fold closure. The fold axis plunges 28° towards 088°, with a nearly vertical axial surface. Younging criteria in the quartzites and interbedded quartzites and shales show consistent younging directions toward the axial surface of the fold, which indicates the strata are not overturned and that the fold is a synformal syncline.

Metamorphism

Metamorphic conditions vary along and across strike of the BGB, with across strike variations the most significant. In a SE transect across the belt from near the fold closure, metamorphism increases from greenschist facies (dominant metamorphic grade) to granulite facies in ~5 km (Fig. 2). The increase in temperature and pressure is not likely to be continuous, in that metamorphic grade changes adjacent to two major ductile shear zones (Fig. 2).

Along-strike changes in metamorphism are the result of coverging ductile shear zones (Fig. 2), which reduce the outcrop width of the belt to < 1 km northeast of the study area (Fig. 1). As a result, increasingly higher strain, and rocks at higher metamorphic grades are found both toward the northeast and away from the core of the greenstone belt.

Age of the cover succession

The age of the cover succession at Buhwa is dated indirectly as between ~2.9 Ga and ~3.09 Ga. A maximum age for the cover succession is provided by ages of detrital zircons. Dodson et al. (1988) dated 43 detrital zircons extracted from the quartzite, which yielded concordant ages for the zircons that vary from 3.09 ± 0.08 Ga to 3.81 ± 0.01 Ga, with a major clustering of dates at ~ 3.25 Ga. At two localities, xenoliths of detrital quartzite are found within the the ~2.9 Ga Chpinda batholith, which provides a minimum age for the cover rocks. A depositional age greater than ~2.9 Ga indicates that sedimentation in the Buhwa region was not related to uplift associated with the Limpopo Orogeny, which is thought to have occurred between ~2.7-2.6 Ga (eg. Barton and van Reenen, 1992; Mkweli et al., in press).

STRATIGRAPHY AND DEPOSITIONAL CONDITIONS

Introduction

Worst (1962) briefly commented on the lithologies present in the BGB but focussed mainly on the distribution of iron ore at Buhwa. There is a wide range of lithologies present; these can be roughly divided into two distinct associations (eastern basinal and western shelf) separated by a transitional association.

Exposures are too poor to recognize individual marker units or unconformities that may serve as time lines to link the basinal and shelf associations. A lower unconformable contact with older crystalline basement was not observed. There could be significant disconformities within the succession, although the general continuity of the lithologies in vertical section suggests that multiple unconformity bounded successor-basin deposits are unlikely.

Kusky and Kidd (1992) commented that significantly allochthonous lithologic sections are transported along thin zones of dislocation, with little associated deformation, such as folding or cleavage development. Although a dislocation zone in the BGB could be concealed by the vegetative cover, we find it remarkable that where exposed, even the most easily deformable lithologies such as shale and iron-formation record no evidence of significant structural transport.

Shelf Association-Description

Rocks of the western association are best exposed in the fold-closure region of the main Buhwa syncline (Fig. 2), where a discontinuous section was measured (Fig. 3). The rocks in this area have been metmorphosed to greenschist facies. Structures include a very strong pressure solution cleavage in shale, a locally developed transecting spaced cleavage, and ductile deformation fabrics at the very base of the

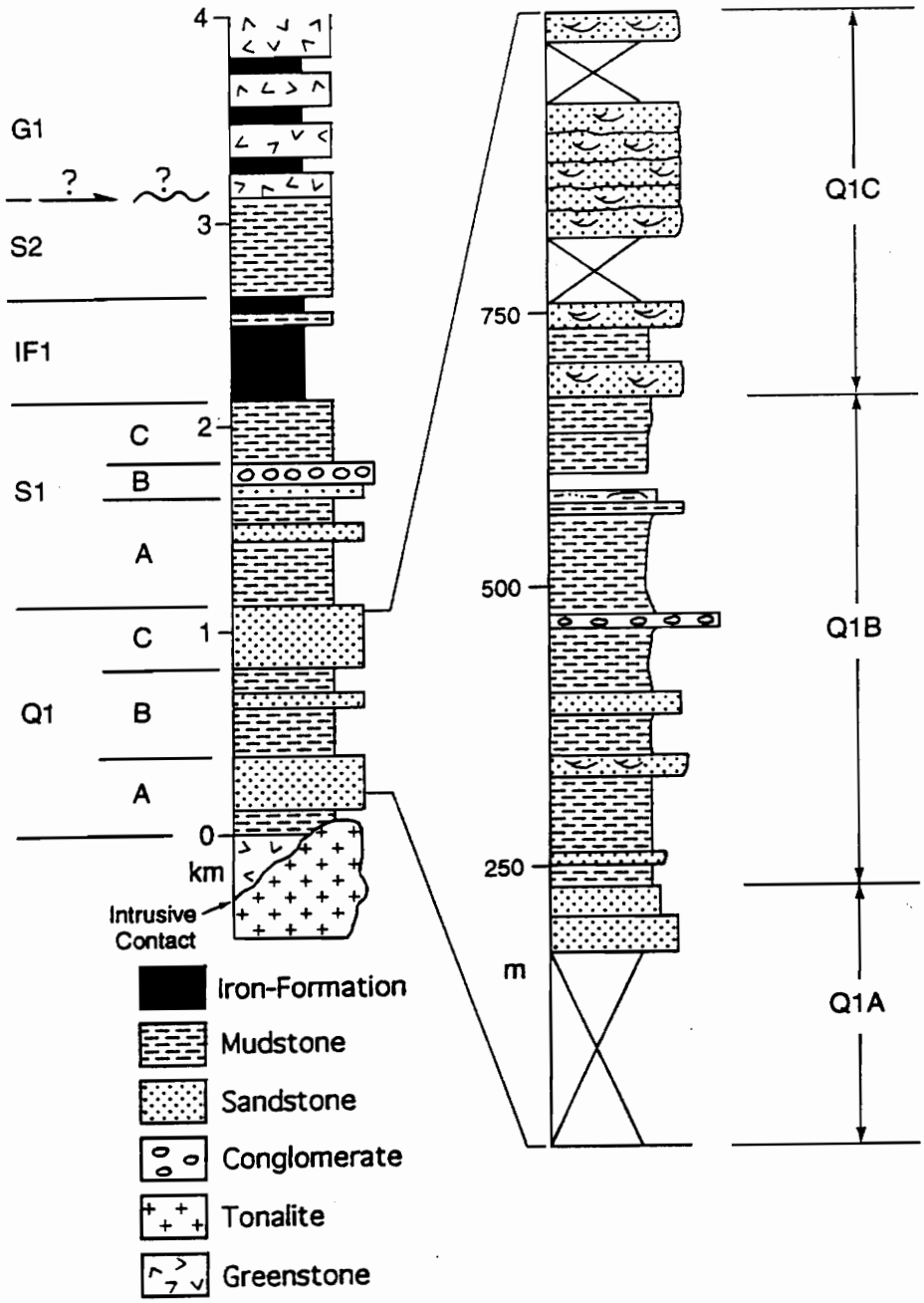

Figure 3. Lithologic column of the shelf association from just NW of the fold axis. Nature of the S2-G1 contact is uncertain. It may be a fault or an unconformity. Expanded column shows details of Q1.

section near the contact with younger granitoids. This association is divided into five subunits based on dominant lithology.

Quartzarenite (Q1)

Approximately 1 km of interbedded quartzarenite and shale form the base of the section of the western association. The quartzarenites are in contact with ~150 m of talc schist, which in turn is in contact with intrusive granitoids. Thickest accumulations of Q1 are in the fold-axis region; the quartzarenites gradually thin stratigraphically, and then disappear along strike to the east (Fig. 2). This succession has three subdivisions: 1) a lower quartzarenite, 2) a middle shale, and 3) an upper quartzarenite (Fig. 3).

The lower quartzarenite (Q1A), which forms prominent foothills, is ~240 m thick, although the lower 175 m is mostly covered with quartzarenite float. The quartzarenites are vitreous and bedding is difficult, but possible, to discern. In thin-section, medium-to-coarse quartz grains form a strongly interlocking mosaic with a deformation-induced grain shape preferred orientation; undulose extinction is common. Zircon is the dominant accessory phase. A poorly preserved primary clastic texture can be recognized and rare cross-stratification is present. Rare randomly oriented flakes of fuchsite are found along grain boundaries.

The middle shale (Q1B) consists of ~400 m of shale with interbeds of quartzarenite that gradationally overlie the basal sandstone. The lower 165 m and upper 130 m of this section section contains numerous sandstone interbeds, whereas the middle 205 m consists exclusively of fine-grained rock except for a 1 m-thick conglomerate unit.

Within the lower and upper intervals, shale forms the dominant lithology and is typically green, purple, red-brown, or gray. The most common structure is mm- to cm-scale flat alternations of mudstone (now chlorite ± sericite phyllite) and muddy siltstone or muddy very fine sandstone. Primary stratification is well preserved despite the pressure solution cleavage, which cross-cuts bedding at a low angle. Locally, the cm-thick sandstone layers are clay-free and organized into wavy laminations or into trains of sand-starved asymmetrical ripples. Interbeds of quartzarenite range from 30-100 cm thick and form accumulations 5-12 m thick. These medium- to coarse-grained sandstones commonly show 2-30 cm-thick nested sets of broad trough cross-stratification. A well-exposed example of hummocky cross-stratified very fine-grained sandstone occurs in the upper interval. Fuchsite is typically concentrated at the outer weathered edges of outcrops and is more common in the upper interval.

The middle interval consists of shales similar to those of the lower and upper intervals. A 1 m-thick, clast-supported, very fine-to-fine quartz-pebble conglomerate occurs about half way through this shale. The conglomerate displays a tightly interlocking mosaic of recrystallized quartz. Along strike, exposure is poor and in-place outcrops of this conglomerate are rare, although float is common.

The upper quartzarenite (Q1C) is ~400 m thick, although the upper ~50 m forms a densely covered dip-slope and the transition into overlying shales (S1) is not exposed. Medium- to coarse-grained, quartzarenite forms the dominant lithology of Q1C (Fig. 4). Beds range from 10-50 cm thick with an average of 25 cm and have flat, sharp basal contacts. Sets of trough cross-strata are commonly 10-15 cm thick and commonly are arranged into nested cosets that fill entire beds. Symmetrical ripple marks with mudstone drapes are present at several levels, with a single exposure of

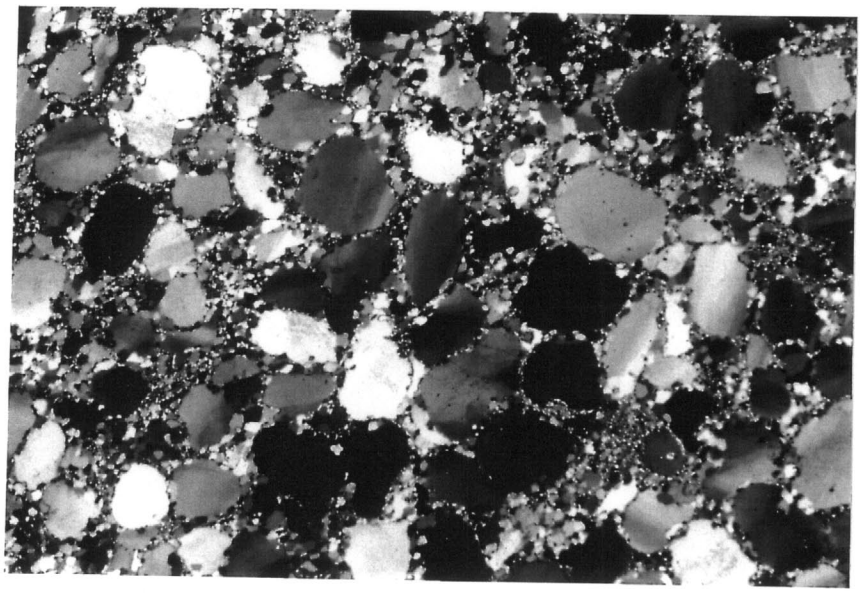

Figure 4. Photomicrograph of coarse-grained quartzarenite from Q1C. Note rounding of grains and recrystallized nature of quartz grains. Cross-polarized light. Length across bottom of photo is ~6 mm.

symmetrical megaripples. Rare meter-thick sections of mixed shale and quartzarenite similar to Q1B punctuate Q1C. Fuchsite is common.

Shale (S1)

An approximately 1 km-thick package of rock that dominantly consists of shale overlies Q1. This shale unit can be divided into three variably exposed subunits (Fig. 3), whose thicknesses have been determined geometrically utilizing bedding attitude and map pattern. The lowest subunit (S1A) is ~500 m thick and too poorly exposed to describe in detail. Rare exposures consist of green, fine-grained phyllite, and several small ridges of quartzarenite crop out through the shale. A small exposure of stromatolitic limestone is also present (L. Machiridza and T.G. Blenkinsop, personal communications, 1993). Contact relations between S1A and S1B are uncertain.

S1B is ~150 m thick and consists of two lithologies. The lower subdivision consists of ~20 m of medium-grained, thick-bedded quartzarenite. No sedimentary structures were seen. An ~130 m-thick section of very poorly sorted, matrix-supported conglomerate abruptly overlies the sandstone. The contact between the arenites and the conglomerate is covered, so that its geometry could not be resolved. This conglomerate unit is variably exposed in vertical section and along strike. A chaotic internal fabric dominates the deposit and a matrix of clays and chlorite forms up to and in excess of 50 % of the rock; this fabric is characteristic of cohesive debris flows (e.g. Bøe and Sturt, 1991). A dominantly bimodal intrabasinal clast assemblage consists of quartzarenite and chert/iron-formation; quartzarenite clasts are slightly more abundant than chert (55 % and 45 %, respectively). Rare resedimented clasts of this conglomerate, mudstone, and highly altered volcanic rock (?) are present. Clasts range from 2-130 mm in long dimension, with sandstone clasts typically having

compact to compact-bladed shapes and chert clasts having compact-bladed to bladed shapes. Clasts vary from rounded (sandstones) to angular (cherts). Sand-sized grains of monocrystalline quartz are common.

The contact between S1B and S1C is not exposed, but is inferred to be gradational based on observations at one exposure where rocks similar to S1C appear to be interbedded with S1B. S1C consists of ~350 m of laminated maroon and green mudstone/siltstone couplets. The laminations are typically 0.5-2 mm thick and very even, despite locally having irregular tops and bottoms. Flame structures are common and young in the same direction as the cross stratification. The laminations consist of alternations of clays plus chlorite or hematite and very fine sandy silt shale, which contains abundant clay and chlorite or hematite. Locally the laminations are wavy and develop into symmetrical ripples that young in the same direction as the flame structures. High in the section, dm-thick laterally discontinuous accumulations of iron-formation are intercalated with iron-rich laminated shales (30-40 % Fe_2O_3; Chapter 4).

Iron-Formation (IF1)

The prominent Buhwa summit ridge consists of iron-formation, which gradationally overlies S1. Overhanging cliffs and dense vegetative cover make it difficult to accurately measure the thickness of the iron-formation; however, geometric calculations based on map distribution and bedding attitude require a thickness in excess of 500 m in the vicinity of Buhwa summit. Along strike, the unit thins to less than 300 m. IF1, which hosts significant iron-ore deposits (Worst, 1962; Fedo and Eriksson, in press), consists of submillimeter- to cm-scale alternations of highly

recrystallized white or red chert and hematite, common to the oxide facies (James, 1954).

IF1 has a strike length of ~13 km and is best developed in the shelf association particularly above the thickest accumulation of the underlying phyllite-dominated succession and extends into the transitional deposits. Deformation fabrics in IF1 are weak, but include minor cleavage formation in some cherty laminations and cm- to dm-scale displacements on rare thrust faults.

Shale (S2)

Approximately 500 m of poorly exposed hematite-rich, quartz-silt shale (S2) overlies IF1. At the top of IF1, S2 is interbedded with IF1 through a stratigraphic interval of ~10 m. Shale beds in this gradational zone are ~1 m thick.

Greenstone (G1)

A succession dominated by greenstone occurs in the core of the major syncline. This succession may or may not be structurally concordant with all underlying lithologies (Q1-S2). At map scale, folded G1 lithologies, as highlighted by beds of iron-formation, strike into S2 (Fig. 2). Whether this discordancy represents an angular unconformity, or is related to mutiple folding events with similar axial surfaces, or disharmonic folding in one event could not be determined.

G1 has intercalations of iron-formation, and a single ~3 m-thick unit of quartzite. The quartzite, which is only exposed on the northern limb of the fold, is typically structureless; however, a possible example of cross-stratification, very faintly defined by fuchsite, was observed. Younging direction is to the south, and thus is consistent

with younging directions in underlying units. Alternatively, the quartzite could be a metachert, which is more consistent with the overall lithologic association.

Transitional Association-Description

Lithologies of the eastern and western associations do not interfinger with each other. Instead, individual lithologies similar to those developed in the east or west interfinger in a transitional association developed near Buhwa village (Fig. 2) and provide the critical connection. The rocks have a distinct pressure solution cleavage and are not well enough exposed to measure a representative section; however, many observations provide some insight to the lithologies. No unequivocal younging indicators were found.

Green and tan laminated phyllite (originally shale), similar to that of Q1B and S1A, is the most common rock type in the transitional zone. A number of occurrences of several-meter-thick intervals of black shale are present east of Buhwa village.

Fine- to medium-grained, muddy quartzose sandstone, that may represent lower energy versions of Q1A and Q1B, are found in the transitional zone. Matrix material is stained by hematite. These sands have a well-preserved clastic texture and are interbedded with shale.

Small, scattered exposures of a meter-thick, deformed, very fine-to-fine quartz pebble conglomerate resemble the conglomerate in Q1B. In thin section, the conglomerate exposed in the transitional zone has many more polycrystalline quartz grains and a finer-grained sand framework than the Q1B counterpart.

One of the most distinctive lithologies in the transitional association is iron-formation, which has two variants. The first variant, which consists of alternating bands of opaques, red cert, and white chert is the along-strike extension of IF1 from

the western association. IF1 terminates in the transition zone near Buhwa village (Fig. 2), where it is strongly folded and intensely microfaulted. The second variant consists of mm-scale alternations of recrystallized quartz and opaque iron oxides. Layering is flat and sharp. Quartz crystals have straight extinction and straight boundaries with 120° junctions. Opaques consist dominantly of anhedral and less common euhedral crystals; abundance of opaques varies significantly from <5 % to ~40 %. There is a striking similarity between these rocks and the iron-formations of the basinal association (Fig. 5). In one well-exposed outcrop, numerous beds of iron-formation, up to 4 cm thick, are interbedded with meter-thick intervals of gray-green shale.

Basinal Association-Description

The eastern association consists of steeply SE-dipping rocks that are best exposed in the Runde and Ngezi Rivers, which flow perpendicular to strike of the BGB (Fig. 2). Locally severe ductile deformation and metamorphism has obliterated most primary fabrics, thus a column depicting predeformed stratigraphic relationships cannot be assembled. The ~4.4 km thick column for the eastern association (Fig. 6) only represents the succession of lithologies from north (bottom of column) to south (top of column), which is consistent with the younging direction determined by the orientation of giant spinfex fans in a lava flow.

Greenstones

Greenstone is the most common lithology of the eastern association and is present in several varieties, each of which formed in response to different starting bulk composition and metamorphic conditions. Worst (1962) differentiated an "ultramafic complex" from "greenstones" based on the presence of hornblende, which defined the

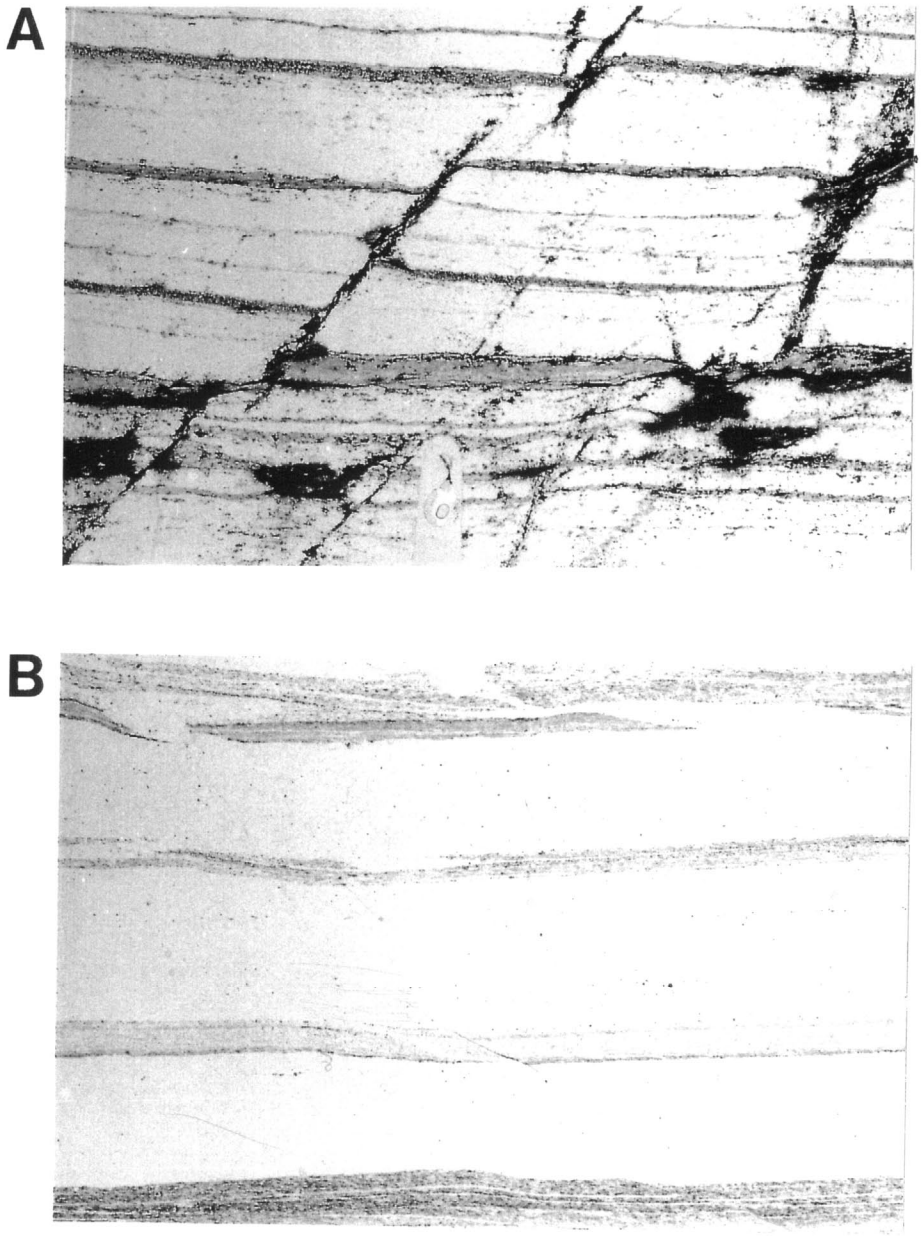

Figure 5 A. Photomicrograph of iron-formation (variant 2) from the transitional association. Plane-polarized light. Length across bottom of photo is ~40 mm. B. Photomicrograph of iron-formation from the basinal association. Note similaity with Figure 5A. Plane polarized light. Length across bottom of photo is ~40 mm.

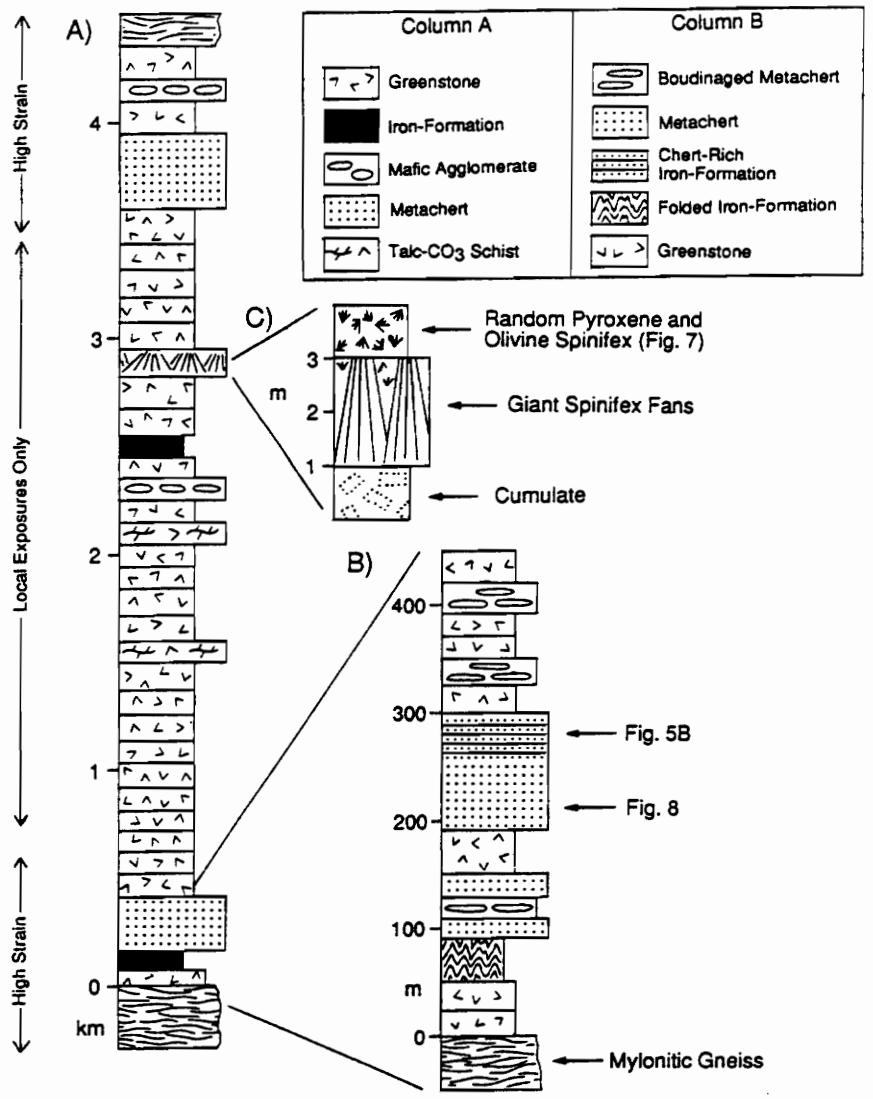

Figure 6 A. Lithologic column of the basinal association measured in the Runde and Ngezi rivers. Column is oriented so that the base represents the northern contact with gneiss and the top represents southern margin at the confluence of the Runde and Ngezi rivers. Note this is a structural thickness. Stratigraphic way up is neither implied nor inferred. B. Expanded column showing details of the lithologies. C. Expanded column showing details of the giant spinifex fan locality. Stratigraphic way up is inferred to be toward the apices of the fans.

"greenstones." He considered all other non-hornblende-bearing assemblages as part of an "ultramafic complex."

A common variant is tremolite-actinolite schist (Fig. 2). In the field, these schists appear as dark-green, moderately to well-foliated rocks, with local stringers of vein quartz. Amphibole crystals are up to several millimeters in length and have bladed to acicular shapes, which typically define foliation. Curving whisps and sprays of tremolite commonly form outside the plane of foliation. Amphiboles locally include small trails of opaque minerals that lie in the plane of foliation. In thin section, the typical colorless amphiboles indicate that tremolite dominates over actinolite, which suggests an Mg-rich/Fe-poor protolith. Talc and chlorite are present in minor amounts.

Talc-tremolite, and less common talc-dolomite schists are developed towards the core of the BGB (Fig. 2). Foliation is less well defined because of the small crystal size of the talc. Talc forms the dominant mineral phase and in thin section consists of small tightly interlocking sheets. Tremolite crystals are similar to those described above. Dolomite typically forms cm-scale, irregular, orange blobs within the talc. Trails of opaque minerals are found in the talc-dolomite schists. Chlorite is present in trace quantities.

Greenstones that consist dominantly of fine-grained chlorite + tremolite + talc + brucite layers that enclose anhedral crystals of altered olivine occur near the southern contact of the BGB and surrounding gneisses at the confluence of the Runde and Ngezi rivers (Fig. 2). Olivines range in size from ~1 mm to 2 cm and weather as red brown or dark gray spheres to prolate ellipsoids that stand in positive relief.

Rare greenstones near the core of the BGB have not had their pre-metamorphic fabrics obliterated. One consists of a mafic breccia whose actual thickness is not

certain, but has a map thickness of ~30 m. The rock possesses two textural components: 1) a matrix that consists of tremolite schist, and 2) a framework that consists of rounded clasts of finer-grained silicified tremolite? schist (mafic) and chert (now recrystallized quartz). Mafic clasts outnumber chert clasts by ~4:1. The matrix is clearly strained and wraps around framework clasts. Clasts vary in size from several millimeters to 16 cm in long dimension. Many mafic clasts have generally prolate shapes, which most likely resulted from regional deformation (Chapter 3). Most clasts are typically rounded to well rounded, however, angular clasts are not rare. Distinctive layering based on grain-size variation was not observed.

The other occurrence consists of a single, well-defined and probably many poorly defined layers of spinifex-textured rock (Fig. 6). The well-defined layer consists of several subunits similar to some of the komatiite flows described by Pyke et al. (1973) from the komatiites in Munro Township, Ontario. The base of the flow is difficult to recognize, but outcrop begins with ~1 m of talc schist, with locally preserved cumulate textures. The overlying spinifex-textured subunit consists of four laterally interfingering, upward-converging fans of primary olivine plates (now altered) that are up to 2 m in length (*cf.* Donaldson, 1982). The spinifex fans are capped by > 1 m of random pyroxene (Fig. 7) and olivine spinifex. Chrysotile and chlorite are the dominant alteration minerals, and tremolite represents minor, late, metamorphic-mineral growth. Similar spinifex fans (cones in their exposures) have been recognized from komatiites in the Nondweni greenstone belt, South Africa (Wilson et al., 1989; 1994). There, the cones are intercalated with pillows that yield a consistent younging direction correlative with younging toward the apex of the cone/fan. Broken, small exposures of greenstones with recognizable spinifex texture continue upsection (downstream) for ~100 m.

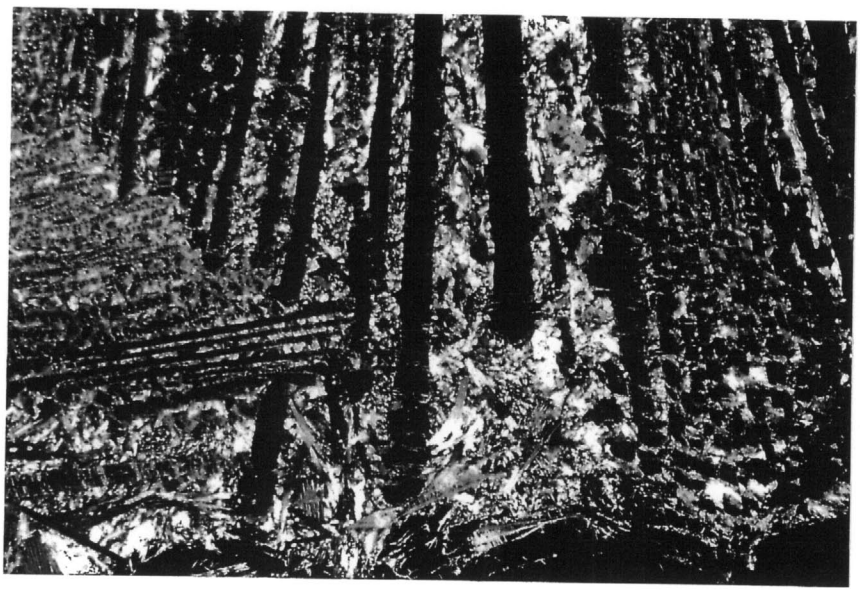

Figure 7. Photomicrograph of random pyroxene spinifex texture from the subunit above the giant fans. Present mineralogy is Mg-chlorite and chrysotile. Cross-polarized light. Length across bottom of photo is ~6 mm.

Metachert ?

Metachert ? forms a significant proportion of the eastern association. Continuous sections of up to ~100 m of metamorphic quartzite are present in the bed of the Runde River near the northern contact of the BGB with surrounding gneisses (Fig. 2). All outcrops of metaquartzite occur in very high strain zones, contain strong L and S fabrics, and are probably best considered mylonites. At one locality, metaquartzite and altered greenstone are intercalated at a decimeter scale.

Quartz and mica form the major minerals in the metachert ? (Fig. 8), with trace quantities of metamorphic amphibole and rare zircon. At a scale of ~5 mm, more micaceous layers commonly alternate with mica-poor layers. Quartz varies greatly in texture and crystal size, with a pronounced negative correlation between quartz crystal size and mica abundance. Mica content ranges from ~1 to 15 %. Crystal size varies from 50-200 μm in samples rich in mica to over 600 μm in mica-poor samples. Aspect ratios of quartz vary from 1.5:1 to 4:1. Similarly, grain boundary textures vary from jagged and irregular to serrated to straight with 120° junctions. Several samples contain distinct crystallographic (lattice) preferred orientations and grain-shape preferred orientations. Straight extinction is more common than undulose extinction.

The micas, which define the visible foliation, consist of muscovite, fuchsite, and biotite in decreasing order of abundance; chlorite is rare. Micas tend to occur as isolated crystals, or less commonly as crystal bundles with straight extinction. There is a distinct bimodal distribution of crystal sizes in the metaquartzites (Fig. 8); the most volumetrically abundant mica ranges in size from 20-100 μm wide by 100-300 μm long, and forms single crystals or anastomosing patterns along quartz grain boundaries. The minor micas occur as ~5 x 40 μm isolated inclusions in quartz.

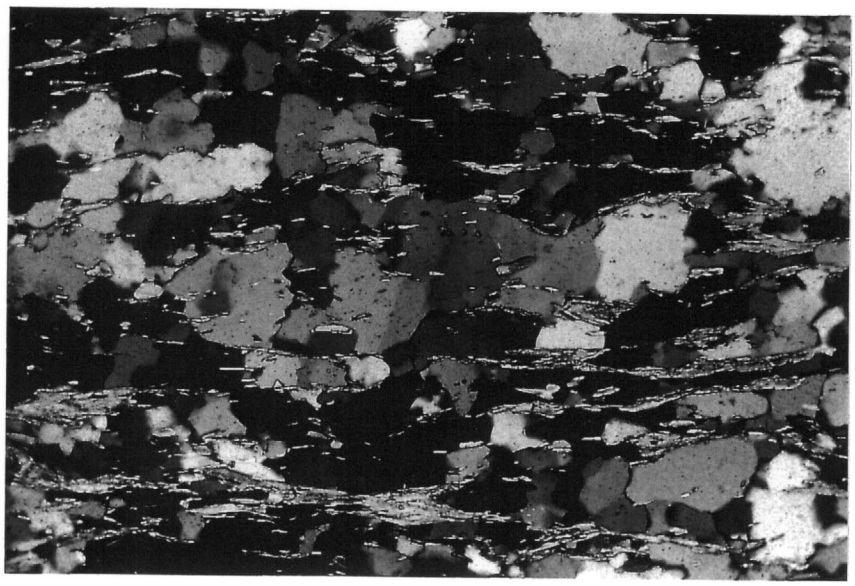

Figure 8. Photomicrograph of metachert from the basinal association. Foliation is defined by muscovite orientation. Note that micas included in quartz are smaller than those at grain boundaries. Cross-polarized light. Length across bottom of photo is ~1.3 mm.

Several trace minerals are found in the metaquartzites. Tremolite blades that are found almost certainly represent metamorphic mineral growth, as nearby greenstones consist dominantly of tremolite. Euhedral to subhedral metamorphic garnets appear in two samples; in one of those examples, the garnets are associated with calcite, biotite, apatite, and quartz. Rare examples of zircon and allanite (?) are found in the metaquartzites.

Iron-Formation

Deformed iron-formation occurs at several places in the eastern association (Fig. 6). Thicknesses reach ~50 m, but poor exposure severely limits accurate thickness measurement. Quartz and opaque iron-oxides comprise the essential mineral phases and are arranged in mm-scale alternating bands (Fig. 5B). Layers are commonly planar, although isoclinal intrafolial folds indicate tectonic overprint. Near the base of the measured section in the Runde River, ~30 m section of iron-formation shows cm- to dm-scale (amplitude and wavelength) folds possibly related to initial slumping or soft-sediment deformation. Crystals in quartzose layers are commonly ~400 μm long by 200 μm wide. Different samples show crystals with straight or serrated boundaries, and these textures are associated with straight and undulose extinction, respectively. Opaque-rich layers contain as little as 5 % opaque minerals, which exist as a fine dust scattered between and included within quartz crystals. Quartz crystal size is distinctly smaller than in quartz-only layers, with typical dimensions ~50 x 200 μm. Opaques form anhedral elongate crystals with a common grain-shape preferred orientation. In layers where opaques form only a minor component, euhedral shapes are common.

Other Rocks

Three other lithologies are present in the basinal association. A 20 m-thick section of metaquartzite occurs approximately 120 m from the northern margin of the BGB in the Runde River (Fig. 2). This lithology differs from other metaquartzites in that it consists of distinct overlapping lenses of coarsely recrystallized quartz with micas (< 1 mm thick) that anastomose around the lenses. Quartz is by far the predominant mineral and lenses typically have oblate shapes and lie in the plane of foliation. Aspect ratios in planes approximately equal to the YZ plane of the strain ellipsoid can exceed 20:1. Full foliation surface views are not exposed, so X and Y dimensions remain uncertain, although we estimate them to be on the order of 10 cm.

Further south in the measured section and along strike in the Ngezi River (Fig. 2), ~25 m of dark-gray, quartz-rich rock consists of alternations of chlorite, mixed fine-grained quartz and chlorite, and less common monomineralic quartz layers, which locally show cm-scale isoclinal intrafolial folds. Opaques occur in trace quantities.

Higher in the section, schist is interleaved with the dark-gray rock and contains prominent quartz ellipsoids. Ellipsoid density varies from tightly packed to floating, although typically ellipsoids do not touch. The ellipsoids are highly flattened in the foliation plane and have either rounded or "winged" terminations. Size varies, but 40-50 cm long by 1-5 cm wide is common. Rarely, the quartz forms stringers deformed into west-plunging "z" folds. In one instance, the quartz has a tablet shape 5 cm thick and > 1 m long and wide. Chlorite forms the matrix material in all analyzed thin-sections.

Protoliths of the Basinal Association

Lithologies comprising the eastern association have been affected by differing metamorphic conditions with the most intense ductile deformation and metamorphism concentrated at the margins of the BGB. Protolith analysis is restricted to the degree to which compositional trends and primary fabrics can be recognized. Protoliths of the metamorphosed mafic breccia, komatiite, and iron-formation will not be considered further.

Some of the greenstones at Buhwa are similar to the metamorphosed Archean mafic and ultramafic rocks from the Abitibi region, Canada (*cf.* Jolly, 1982). Tremolite-actinolite schist and cummingtonite + garnet schist most likely represent mafic to ultramafic volcanic rocks. Jolly (1982) suggested an olivine-cumulate lava as protolith for the assemblage dominated by tremolite+actinolite at greenschist facies and either an olivine-cumulate or basalt protolith for cummingtonite-dominated assemblages at amphibolite facies.

The talc-tremolite and talc-dolomite rocks are more difficult to interpret. Jolly (1982, Table 17.1) has recognized that tremolite and talc (+ carbonate) may both form from actinolite-grade greenschist facies through cummingtonite-grade amphibolite facies in Abitibi mafic lavas. Another possibility is that these schists represent the relics of carbonate metasomatized greenstones, as in the Barberton Greenstone Belt (e.g. de Ronde et al., 1994). Talc-tremolite and talc-dolomite could also represent possible assemblages from metamorphosed siliceous dolomites or limestones (Tracy and Frost, 1991; Yardley, 1989).

The metacherts ? represent either original detrital (sandstone) or chemical (chert) rocks. A number of characteristics favor a chert protolith. Ductilely deformed clastic rocks can preserve enough initial textures, such as cross-laminations, to be recognized

as detrital (e.g. Kusky and De Paor, 1991; Shelley, 1993). Also, quartzarenites typically contain a stable heavy mineral assemblage of zircon, tourmaline, and rutile (Hubert, 1962). Such a stable assemblage, including rounded zircon cores with euhedral zircon overgrowths, led Eriksson et al. (1988) to suggest a detrital origin for quartzites of the Archean Beitbridge Group of South Africa. By contrast, recrystallized cherts typically lack a stable heavy mineral assemblage and are commonly associated with shale interbeds (Tucker, 1991). All textural evidence suggests that the present quartz crystal size in the metachert ? is a function of recrystallization (ie. crystal coarsening); no ghost grain outlines have been recognized. Micas included in quartz crystals are evidence for grain coarsening, where original quartz crystals were no larger than the spacing between phyllosilicates (Shelley, 1993); we favor an analogous situation for the Buhwa metaquartzites. The overall abundance of micas, including fuchsite which may have an exhalative origin (Schreyer et al., 1981), are interpreted as relics of intercalated shaley partings.

A protolith of interbedded chert and shale is also favored for the last three examples of quartz and mica-rich rocks described above. In these examples, the various-sized ellipsoids of recrystallized quartz are interpreted as boudins, which formed upon attainment of sufficient rheological contrast between chert and shale. The major difference between these rocks and the more quartzose metacherts is the proportion of shale to chert.

PALEOENVIRONMENTS

The abundant cross-stratification in Q1 arenites is interpreted as the product of migrating sinuous- and straight-crested sand waves, which indicate the prolonged operation of traction currents. The presence of symmetrical and interference ripples

on many bedding surfaces suggests reworking of the sand waves in a shallow-water setting by surface waves (*cf.* Collinson and Thompson, 1982). The dearth of fine-grained sediments in the arenites indicates continual current winnowing, which is consistent with an above fairweather wave-base environment. A wave-swept shoreface to inner shelf environment similar to those described by Eriksson et al. (1981) for the ~2.9 Ga Lower Witwatersrand Supergroup, Beukes and Cairncross (1991) from the ~2.9 Ga Mozaan Group, and by Simpson and Eriksson (1989) from the Lower Cambrian Chilhowee Group of the eastern United States are appropriate analogs, both of which accumulated on stable platforms. The shales of Q1 perhaps represent more offshore deposits, although the abundance of ripple trains and hummocky cross-stratification in quartzarenite interbeds suggests deposition above storm wave base.

The three subunits of S1 probably represent different environments, but the overall character of S1 indicates drowning of the underlying sand-dominated shelf. Limited exposures of S1A are consistent with a mud-dominated shelf environment below fairweather wave base. The reported presence of stromatolitic carbonate indicates at least one episode of shoaling.

The quartzarenites and debris flows of S1B indicate significant lowering of base level and the disconformable progradation of coarse sediment onto the marine shelf; this is characteristic of lowstand wedge deposits in a passive-margin setting (Van Wagoner et al., 1988). A eustatic fall as the cause of base-level change is favored because all clasts are of intrabasinal origin; reactivation of hinterland sources would likely provide extrabasinal detritus such as feldspars, granites, and gneisses. The deposition of coarse-grained debris flows on a relatively flat shelf does present some problems. One possibility is that the debris flows represent collapse of incised valley

walls. Another alternative is that intrabasinal faulting, similar to the Tertiary of the Texas Gulf Coast (*cf.* Bruce, 1983), cut through this thick, muddy, shelf succession yielding a fault scarp from which intrabasinal clasts could be derived. The overlying laminated shales of S1C suggest reestablishment of low-energy depositional conditions as a result of relative sea-level rise. An outer-shelf setting is favored over a protected inner shelf because no distinct sands that might represent barrier deposits are present. Local wave ripples suggest that storm wave base occasionally reached bottom.

The thick jaspilite (IF1) reflects the cessation of siliciclastic influx and the production of orthochemical sediments. By comparison with Phanerozoic transgressive shelves, the iron-formation is analogous to the carbonate part of the succession in the sense that siliciclastic debris was no longer delivered to the shelf; although, the Buhwa iron-formation represents deeper-water deposition. A below storm-wave-base, pelagic environment is suggested by the laterally persistent submillimeter scale bands of chert and oxides and the association with S1C (*cf.* Eriksson, 1983; Beukes and Klein, 1992).

Intercalated shales (S2) at the top of IF1 and the overlying mixed lithlogies (G1) are difficult to interpret because of the limited exposure, although the association of shale and iron-formation is consistent with rocks below. The ~3 m thick metaquartzite could represent subsequent shoaling or deposition of chert.

Most lithologies in the transitional deposits are considered to represent more basinward equivalents of the western association and thin fingers of the eastern association. Perhaps the most notable transition is the gradual fingering out of Q1 along the northern limb of the fold (Fig. 2). The extent to which all the thinning is stratigraphic, rather than tectonic, has not been fully ascertained, but an increase in

abundance of shale is apparent. Most of the transitional association is considered to represent a shelf marine mudstone. The abundance of shale coupled with the presence of iron-formation similar to that of the eastern association, IF1, and locally developed black shales indicates below-wave-base conditions. These transitional deposits are critical for connecting the eastern and western associations, which otherwise might be considered as totally separate (spatially and temporally) entities.

Lithologies of the eastern association represent the consistently deepest-water deposits in the BGB. The presence of spinifex-texured lavas support the interpretation that the greenstones were in part eruptive. The mafic breccia represents an eruptive lithology in which mafic magmas incorporated fragments of chert and greenstone. Some greenstones could represent primary deposition of carbonate or perhaps hydrothermally carbonated lavas.

Most modern cherts accumulate on the ocean floor as siliceous oozes (Tucker, 1991). These very deep-water deposits make poor analogs for Precambrian cherts because of the presumed absence of silica-secreting microorganisms (Simonson, 1985). In their absence, Eriksson (1983) and Simonson (1985) noted that ambient SiO_2 concentrations in Precambrian seawater would have been elevated, leading to abiotic precipitation of chert as background pelagic fallout. Most workers favor a volcanic source for the elevated concentrations of silica (e.g. Eriksson, 1983; Simonson, 1985; Beukes and Klein, 1992). Both pelagic fallout and volcanogenic mediation may have played a significant role in the formation of chert (and iron-formations) at Buhwa as thick cherts accumulated only in a basinal setting deprived of siliciclastic influx and in association with mafic volcanism.

A PREVIOUSLY UNRECOGNIZED STABLE-SHELF SUCCESSION IN ZIMBABWE

Considerable controversy has centered around the paleotectonic affinity of Archean greenstone belts, with most workers favoring either: 1) that greenstone successions developed in oceanic settings such as volcanic arcs (e.g. Card, 1990), or ophiolites (e.g. de Wit et al., 1987), or oceanic plateaus (e.g. Kusky and Kidd, 1992) or 2) that greenstone successions are ensialic and erupted through continental crust (e.g. Blenkinsop et al., 1993; Bickle et al., 1994). Unlike most greenstone belts, the supracrustal rocks at Buhwa consist mostly of terrigenous clastic sediment with intercalated "greenstone" rocks. Thus, the interpretation of paleotectonic setting here sheds light on tectonic setting of greenstone belts.

Several lines of evidence support a stable-shelf tectonic setting for the cover succession preserved in the Buhwa Greenstone Belt. The transgressive lithologic assemblage of quartzarenite, shale, and chemically precipitated sediment of the western association is reminiscent of Phanerozoic transgressive shelves including the well studied Cambro-Ordovician passive-margin section of the eastern United States (Simpson and Eriksson, 1990), which formed during a first order sea-level rise. The noticable lack of correlative shelf deposits of this age in the craton interior, perhaps suggests that a passive-margin interpretation is appropriate.

The extreme mineralogic maturity of the quartzarenites and stable heavy-mineral suite in the quartzarenites of the western association also is consistent with prolonged sediment reworking in a stable tectonic setting (e.g. Eriksson et al., 1988). Johnsson et al. (1988) cautioned against the use of sandstone composition to infer tectonic affinity, noting that first-cycle quartzarenites can form in a variety of geodynamic settings, especially in response to intense chemical weathering. This concern applies

to the sediments at Buhwa because shales in the BGB have major element trends consistent with a high degree of chemical weathering (Chapter 4). Even so, the source area must have been capable of providing substantial coarse-grained quartz detritus.

Based on stable and heavy mineral composition in the quartzarenites, general age, and geographic proximity, we suggest that the Tokwe segment formed the stable granitic platform upon which the Buhwa cover succession was deposited and from which the sediments were derived. Preliminary interpretations of rare earth element patterns from Q1 interbedded shales suggest a source dominated by tonalitic-granitic crystalline rocks with less abundant mafic volcanic rocks (Chapter 4). The Tokwe segment consists dominantly of banded gneisses and less abundant ~3.5 Ga greenstones (Wilson, 1990; Blenkinsop, in press), from which the sediments at Buhwa could have been derived. Alternatively, Dodson et al. (1988) suggested that the zircons in Q1 could have come from the Sand River gneisses in the Central Zone of the Limpopo Belt, which have recently been dated between ~3.2-3.3 Ga (U-Pb zircon, Retief et al., 1990). Although of proper age, this source is separated from the Zimbabwe Craton by at least two significant structural discontinuities, a factor that could cast doubt on the Sand River gneisses as a source.

Based on our present data set, a stable-shelf paleotectonic setting is assigned to the entire succession at Buhwa. The mafic and ultramafic volcanics of the eastern association indicate some crustal instability in an offshore setting, and it seems likely that the volcanics are associated with rifting, or perhaps even ocean-floor formation, although such close proximity with stable-shelf deposits would be unlike modern passive-margins. Aspects of the foredeep model (Hoffman, 1987) have similarities with the cover succession at Buhwa, but the lack of a thick axial turbidite succession, fluvial molasse, or deformation associated with an advancing fold and thrust belt

suggests that this model is an inappropriate analog for the cover succession of the BGB.

That mafic and ultramafic lavas are intercalated with mature sediments deposited in a depositionally up-dip shelf setting suggests it is possible for greenstones to form on stable, ensialic, continental crust.

CORRELATION

The sediment-dominated cover succession at Buhwa is unique compared with other greenstone belts in the Zimbabwe Archean craton in two major ways: 1) age and 2) stratigraphy. Three major phases of typical greenstone development have been recognized in the Archean of Zimbabwe (Wilson et al., 1978; Wilson, 1979). The oldest is the ~3.5 Ga Sebakwian Group, which consists of highly deformed amphibolites infolded into the poorly understood Tokwe gneisses. At ~2.9 Ga, the Zimbabwe Craton experienced extensive tonalitic plutonism and associated volcanism. Volcanic units range from andesitic to ultramafic in composition (Orpen et al., 1993) and are referred to as the Lower Bulawayan (Lower Greenstones; Mtshingwe Group in the Belingwe Greenstone Belt). Bickle et al. (1993) noted that blocks in an agglomerate at the base of the section are petrologically and isotopically similar to the 2822 $\pm$ 64 Ma Chingezi tonalite (Pb/Pb whole rock), and suggested the two may be cogenetic. The last and most extensive age of greenstone deposition occurred at ~2.7 Ga. This collection of mafic and ultramafic lavas is referred to as the Upper Bulawayan (Upper Greenstones; Ngezi Group in the Belingwe Greenstone Belt).

The cover succession of the BGB has traditionally been correlated with the Lower Bulawayan (e.g. Wilson et al., 1978); however, the ~3.0 Ga depositional age and

lithologic dissimilarity of the BGB and Lower Bulawayan greenstones precludes that correlation and suggests a previously unrecognized phase of "greenstone" development. The craton-wide ~2.7 Ga Upper Bulawayan event may be represented at Buhwa by the Mashaba-Chibi dyke that intrudes the BGB. The thick cover of quartzarenites, shales, iron-formation, chert, and greenstone may have prevented magma penetration through the belt forcing it to spread along contacts, such as that between the Chipinda batholith and quartzarenites.

There are no known stratigraphic equivalents of the cover succession at Buhwa exposed anywhere in the Archean Zimbabwe Craton. As noted above, most greenstone belts possess the tripartite stratigraphic subdivision discussed above, whereas the section at Buhwa is sediment dominated. The thin, stable-shelf Manjeri Formation at the base of the Ngezi Group is a potential lithologic correlative; however, age constraints indicate that the Manjeri Formation is ~300 m.y. younger than the strata at Buhwa.

On a more regional scale, lithologic assemblages similar to Buhwa and of approximately the same age (~2.9-3.0 Ga) are present in the granulite-facies central zone of the Limpopo Belt (Beitbridge Group, Eriksson et al., 1988) and in the Kaapvaal Craton (Mozaan Group, Beukes and Cairncross, 1991; Lower Witwatersrand Supergroup, Eriksson et al., 1981; Beukes and Cairncross, 1991; and Eriksson and Fedo, in press). Although it is still unclear as to how all the parts of the Limpopo Belt and the Zimbabwe and Kaapvaal cratons were assembled, the time period between 2.9-3.0 Ga was seemingly characterized by tectonic stability dominated by mature and stable-shelf sedimentation across large parts of southern Africa.

CONCLUSIONS

The ~3.0 Ga Buhwa Greenstone Belt of southern Zimbabwe is the only major greenstone belt in the Zimbabwe Craton directly adjacent to the well-studied Late Archean Limpopo orogenic belt. It is also located near a fragment of early Archean ensialic crust that comprises part of the Zimbabwe Craton. This, first ever, stratigraphic analysis of the cover succession of the Buhwa Greenstone Belt has yielded several clonclusions.

1) The cover rocks can be divided into shelf and basinal associations with a zone of transitional deposits that provides a critical connection between the two. The shelf association is ~4 km thick and consists predominantly of quartzarenite, shale, and iron-formation representatve of inner-shelf through below wave-base environments. Transitional deposits consist of green, tan, and less common black shales, iron formation similar to that in both the western and eastern associations, and muddy sandstones. These deposits represent lateral, more offshore outer-shelf equivalents to the western association. Much of the basinal association is ductilely deformed, which has obliterated most primary fabrics. The association consists mostly of tremolite/actinolite schists (mafic-ultramafic lavas) and talc-tremolite or talc-dolomite schists (mafic lava or carbonate), with less abundant metaquartzite (chert), and iron-formation. We interpret this association to be a deep-water deposit.
2) A maximum age for the cover succession is given by the age of detrital zircons from quartzarenites (3.05-3.8 Ga). Xenoliths of quartzarenite contained within the surrounding granitoids suggests that the cover succession was intruded. Based on preliminary isotopic ages and lithologic similarity with the nearby Mashaba tonalite, the age of intrusion is taken to be ~2.9 Ga, which provides the minimum

age for the deposit. Thus the depositional age of the cover succession is bracketed between ~3.05-2.9 Ga.

3) A stable tectonic setting such as an intracratonic shelf or passive margin is supported by the extreme maturity of the quartzites and stratigraphic development of the western association.

4) While there are no correlative deposits elsewhere in the Archean Zimbabwe Craton, similar successions (lower Witwatersrand Supergroup; Mozaan Group) deposited between 2900-3000 Ma are found in several places in southern Africa suggesting a period of tectonic stability and widespread shelf sedimentation at ~3.0 Ga.

CHAPTER 3

Geologic History of the Archean Buhwa Greenstone Belt and Surrounding Granite-Gneiss Terrane, Zimbabwe with Implications for the Evolution of the Limpopo Belt

ABSTRACT

The Buhwa Greenstone Belt, and surrounding granite-gneiss terrane, of southern Zimbabwe, is the only major greenstone belt in the Archean Zimbabwe Craton directly adjacent to the granulite-facies rocks that constitute the Northern Marginal Zone of the Limpopo Belt. Its deformational history and assembly sheds light on the evolution of the Northern Marginal Zone-Zimbabwe Craton transition.

Assembly of the region began with deposition of the dominantly sedimentary, quartzose, cover succession at ~3.0 Ga on top of banded gneisses that dominate the ~3.5 Ga Tokwe segment. At ~2.9 Ga the northern margin of the greenstone belt experienced ~12 km of oblique-slip dextral shearing. This shear zone was later intruded by the ~2.9 Ga Chipinda batholith, which varies from granite to tonalite in composition. The remaining events recognized in the region took place during the time span 2.9-2.5 Ga. NW-directed thrusting of the NMZ over the Zimbabwe Craton took place along a collection of discrete, typically m-wide shear zones that dip S and have a steeply pitching to down-dip stretching lineation with reverse-sense kinematic indicators; these shears correlate along strike with other similar structures for 200 km and collectively form the tectonic break between the Zimbabwe Craton and the NMZ. In response to thrusting, the cover succession and surrounding granitoids were folded

and underwent regional greenschist-facies metamorphism. The dominant structure in the region is the main fold that deforms the Buhwa Greenstone Belt and surrounding granitoids. This strongly asymmetric synformal syncline plunges at 28° toward 088°, has an interlimb angle of 66°, and an axial surface oriented at 086°/86°S; a very strong axial planar cleavage is associated with the fold. The strongly linear ENE-trending southern margin of the belt is the result of sinistral-sense shearing along the contact between the greenstones and enclosing crystalline rocks. Two suites of potassic granites were emplaced north and south of the greenstone belt towards the end of thrusting. These events were followed by conjugate faulting related to continued NW compression and later filling of these fractures by the Great Dyke of Zimbabwe and its satellites. The last group of events may have occurred at this time or more recently and include sinistral shearing, transecting cleavage formation, and open folding as a result of NE-directed crustal shortening.

INTRODUCTION

Events culminating in the assembly of the Archean Zimbabwe Craton and the Limpopo Belt have been poorly understood until recent investigations centered mostly in the Limpopo Belt. These investigations have shed considerable light on the metamorphic and tectonic evolution of the belt (e.g. Rollinson and Blenkinsop, in press). The Limpopo Belt is a 700 km by 250 km zone of polymetamorphosed granulite-facies continental crust that separates the Archean Kaapvaal craton to the south and the Zimbabwe Craton to the north (Fig. 9). The belt is divided into: a central zone (CZ) flanked by northern and southern marginal zones (Cox et al., 1965; NMZ, SMZ), which bear some resemblance to their adjacent Archean cratons (e.g. Tankard et al., 1982). However, the tectonic evolution of the dominantly low-grade

Figure 9. Simplified geologic map showing the southern part of the Zimbabwe Craton, the Limpopo Belt, and the northern part of the Kaapvaal Craton. Greenstone belts in the Zimbabwe Craton: B - Buhwa, Be - Belingwe, Mw - Mweza, Ma - Masvingo. Inset map shows the southern horn of Africa and the regional geologic setting of the Zimbabwe and Kaapvaal Cratons and the Limpopo Belt. Redrawn from Rollinson and Blenkinsop (in press).

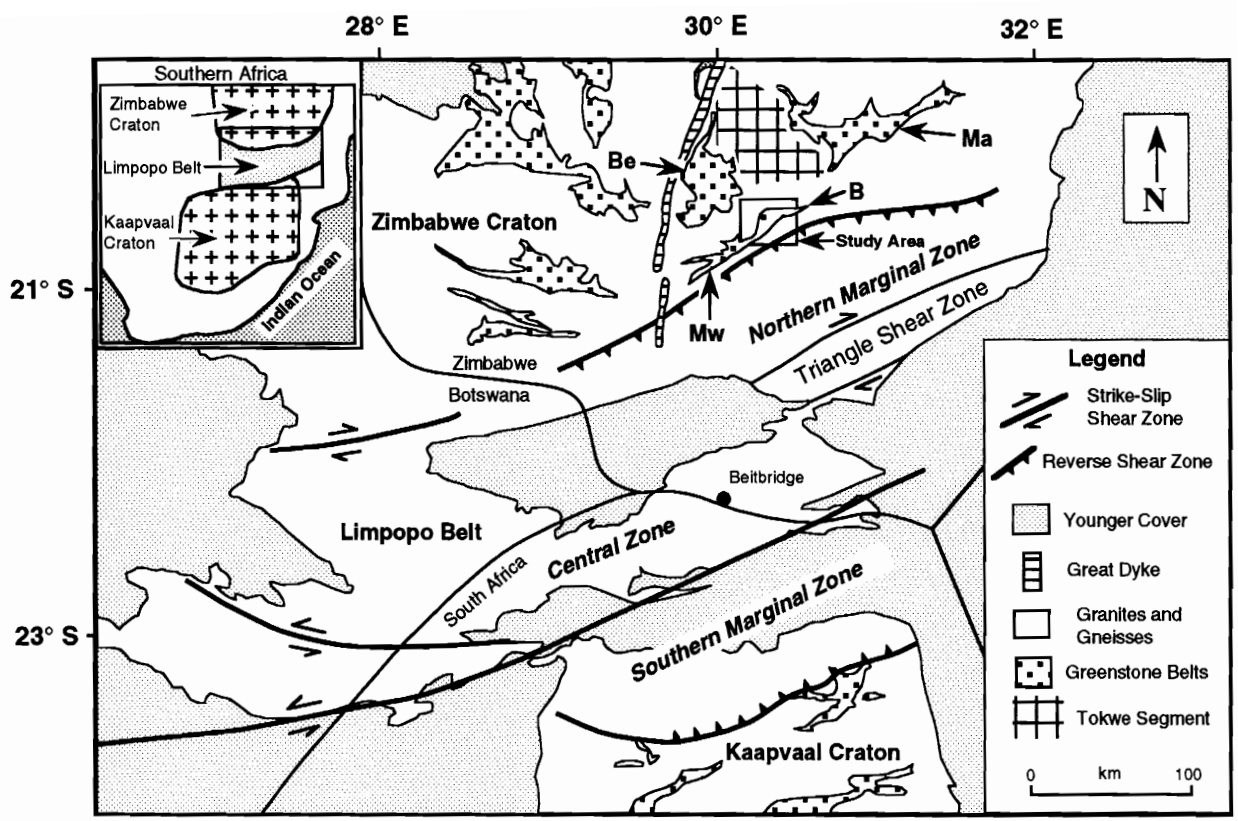
28° E
30° E
32° E
21° S
23° S
Southern Africa
Zimbabwe Craton
Limpopo Belt
Kaapvaal Craton
Indian Ocean
Be
Ma
B
Study Area
Mw
Northern Marginal Zone
Triangle Shear Zone
Zimbabwe
Botswana
Beitbridge
Limpopo Belt
South Africa
Central Zone
Southern Marginal Zone
Kaapvaal Craton
N
Legend
Strike-Slip Shear Zone
Reverse Shear Zone
Younger Cover
Great Dyke
Granites and Gneisses
Greenstone Belts
Tokwe Segment
0
km
100

craton margin remains unknown because strain markers are not abundant in the dominantly isotropic granitoids. Genetic models for the Limpopo Belt have favored a Himalayan-style continental collision between the Kaapvaal and Zimbabwe Cratons (Roering et al., 1992; Treloar et al., 1992). However, new work has established that the shear zone separating the CZ and NMZ was active at 2.0 Ga (Kamber et al., in press), which contrasts with the age of deformation of the NMZ-Zimbabwe Craton transition at ~2.6 Ga (Mkweli et al. in press). Thus, a simple unified model for the Limpopo Belt no longer exists.

This paper documents, for the first time, the structural and tectonic history of the ~3.0 Ga Buhwa Greenstone Belt (BGB; Figs. 9, 10). Because no other greenstone belt in the Archean Zimbabwe Craton is close to the NMZ of the Limpopo Belt, an understanding of the geologic history of the BGB may shed light on the events that resulted in their juxtapositioning. Additionally, this study of the Buhwa region provides a database for comparison of craton-margin and intracratonic deformation patterns.

EVOLUTION OF THE BUHWA REGION

Based on the distribution of lithologies and structures, cross-cutting features, and available absolute ages, an historical outline documenting the development of the Buhwa Greenstone Belt and surrounding granite-gneiss terrane can be established (Table 1). The evolution of the Buhwa Greenstone Belt and surrounding granites and gneisses took place during three, or possibly four, distinct time periods: 1) ~3.0 Ga and earlier, 2) ~2.9 Ga, 3) 2.9-2.5 Ga, and 4) ~2.0 Ga.

Figure 10. Geologic map and cross section of the Buhwa Greenstone belt and surrounding granite-gneiss terrane. Lithologic contacts modified from the mapping of Worst (1962).

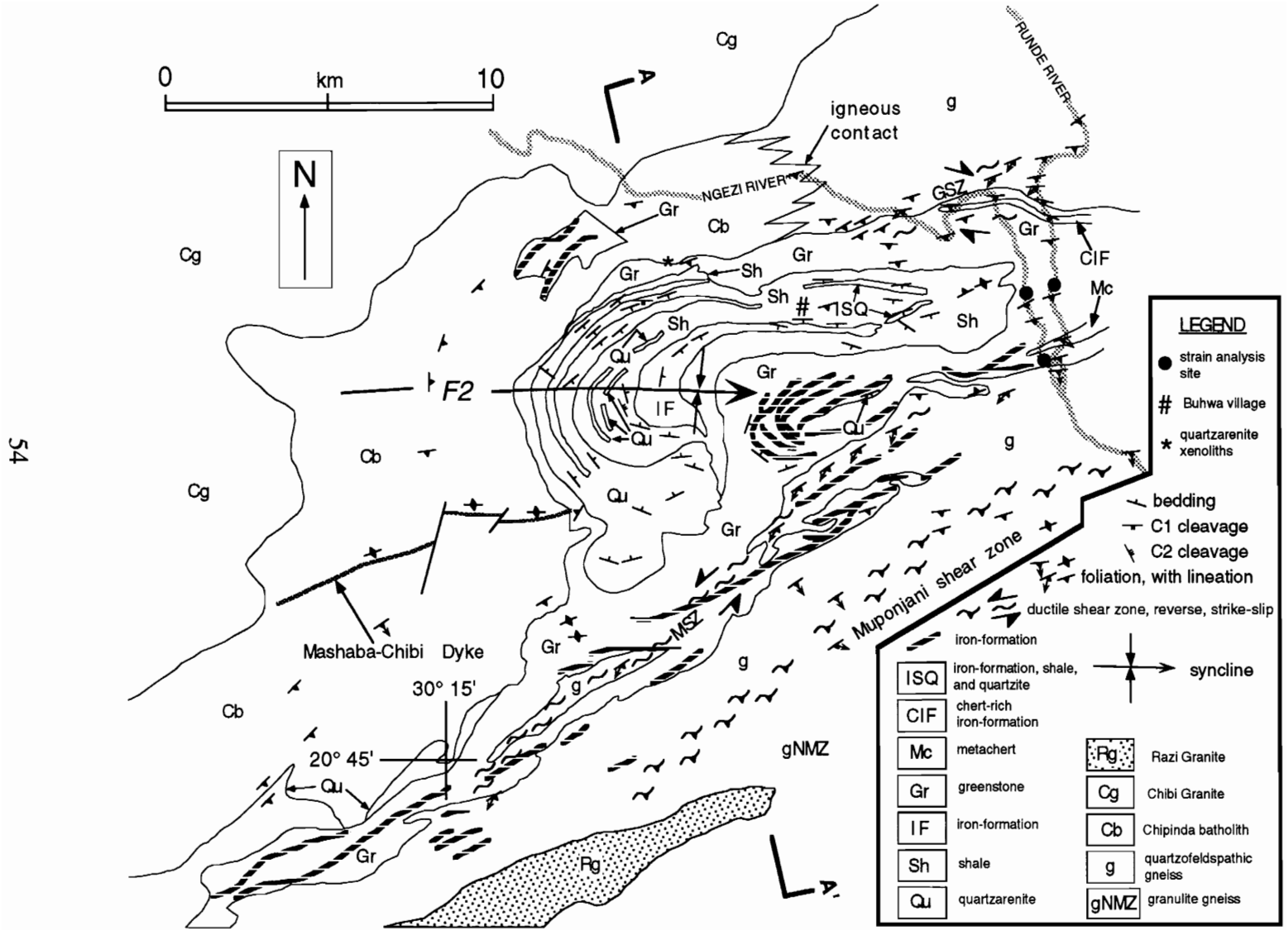
0
km
10
N
RUNDE RIVER
NGEZI RIVER
igneous
contact
Cg
g
Cb
Gr
GSZ
CIF
Mc
Sh
ISQ
Qu
F2
IF
Mashaba-Chibi Dyke
MSZ
Muponjani shear zone
30° 15'
20° 45'
gNMZ
Pg
LEGEND
strain analysis site
Buhwa village
quartzarenite xenoliths
bedding
C1 cleavage
C2 cleavage
foliation, with lineation
ductile shear zone, reverse, strike-slip
iron-formation
syncline
ISQ iron-formation, shale, and quartzite
CIF chert-rich iron-formation
Mc metachert
Gr greenstone
IF iron-formation
Sh shale
Qu quartzarenite
Pg Razi Granite
Cg Chibi Granite
Cb Chipinda batholith
g quartzofeldspathic gneiss
gNMZ granulite gneiss

Figure 10. Continued.

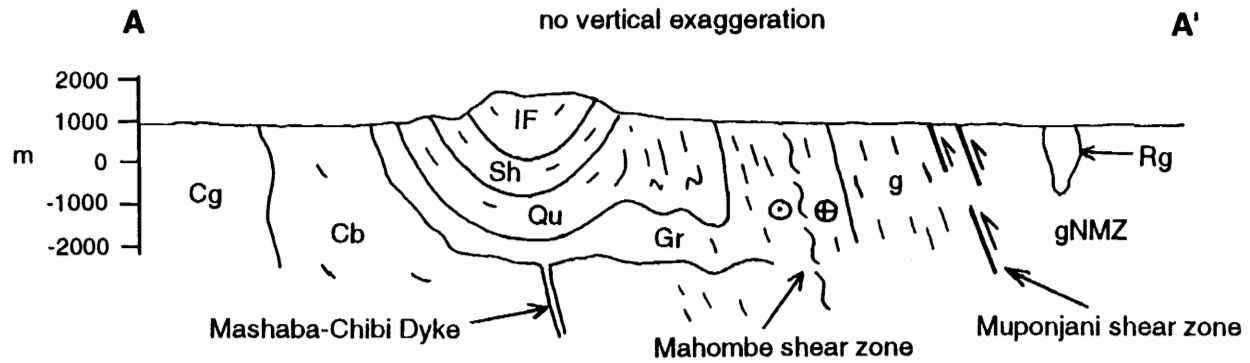
A
no vertical exaggeration
A'
2000
1000
m
0
-1000
-2000
IF
Sh
Qu
Gr
Cg
Cb
g
Rg
gNMZ
Mashaba-Chibi Dyke
Mahombe shear zone
Muponjani shear zone

Table 1. Summary of Events in the Buhwa Greenstone Belt Region

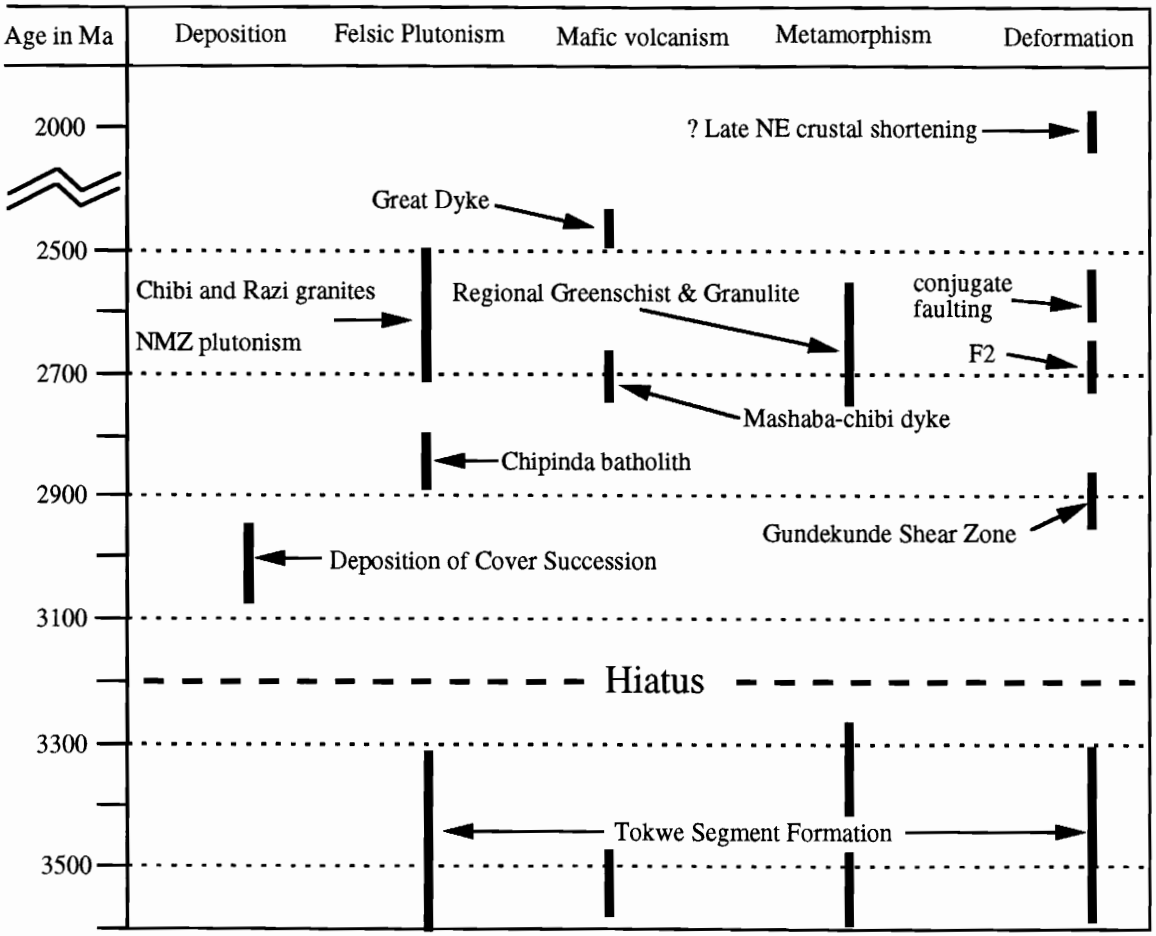

3.0 Ga and Earlier Record

The oldest events in the Buhwa region are related to the accretion/assembly of the roughly triangular-shaped ~3.5 Ga Tokwe segment (Fig. 9), which represents an ancient stabilized portion of sialic crust in the core of the more widespread Archean Zimbabwe Craton (Wilson, 1990). This composite terrane consists dominantly of multiply intruded and deformed banded tonalitic gniess with less abundant early Archean greenstone remnants and the ~2.7 Ga Mashaba-Chibi dykes (Wilson et al. 1987; Wilson, 1990). Although no conclusive correlatives of the Tokwe segment have been located in contact with the BGB, the dominantly sedimentary cover succession that comprises the BGB (Fig. 10) is interpreted to have originally been deposited on the Tokwe segment (Chapter 2).

Thusfar, no workers have recognized any geologic events following construction of the Tokwe segment by ~3.2 Ga and before deposition of the Buhwa cover succession at ~3.0 Ga. Presumably some subsidence mechanism, possibly related to rifting or thermal sagging, initiated sedimentation. A minimum depositional age of ~2.9 Ga for the BGB is indicated by xenoliths of the BGB contained within the ~2.9 Ga Chipinda batholith (Chapter 2). Detrital zircons in the BGB quartzarenites have concordant ages that range from 3.05-3.8 Ga, and provide a maximim age for the cover rocks (Dodson et al., 1988). The cover rocks are interpreted as a thick stable-shelf succession, either passive-margin or cratonic-basin, that shows a transition from shallow-marine to below-wave-base environments (Chapter 2). Shallow shelf environments are best preserved in the main F2 fold-closure region, whereas deeper water sediments and volcanics are more common in the Runde-Ngezi river area.

~2.9 Ga Record

Plutonism

The BGB is surrounded on its northern margin by an elongate composite batholith (Chipinda batholith) whose composition varies from granite to tonalite. The contact between the BGB and Chipinda batholith is very poorly exposed, except at a few locations. Most commonly the contact separates granitoids from talc schist, which in turn is in contact with quartzarenites and shales that form most of the cover succession. To the east, the Chipinda batholith intrudes relics of the Gundekunde shear zone (see below).

At two locations (one in the map area (Fig. 10) and the other just west of the detailed map area), xenoliths of quartzite are contained within masses of tonalite. Elsewhere, essentially strain-free tonalite is in contact with foliated talc schist. These two relationships suggest that the Chipinda batholith intruded the BGB.

A preliminary single-crystal zircon U-Pb age of ~2.9 Ga for zircons (Chapter 2) is interpreted as the crystallization age for the Chipinda batholith. This ~2.9 Ga age for tonalitic rocks is common in the southern Zimbabwe Craton (e.g. Hawkesworth et al., 1979; Bickle et al., 1993). No absolute dates are available from the area directly south of Buhwa, however, Hickman (1978) reported an age of 2880 ± 74 Ma (Rb-Sr whole-rock 13-point errorchron; recalculated using λ (^{87}Rb) = 1.42 x 10^{-11} a^{-1}) from gneisses in the NMZ, which was thought to represent a metamorphic age.

Deformation

The majority of the contacts between greenstones and crystalline rocks along the northern margin of the BGB are igneous. However, the contact in the vicinity where the Ngezi and Runde rivers pass over the greenstone belt is a major ductile shear zone,

referred to here as the Gundekunde Shear Zone (GSZ; Fig. 10). The GSZ, which is ~500-1000 m wide and has a mapped strike of ~8 km, consists of L>S and LS protomylonites and mylonites developed in the crystalline rocks that surround the greenstone belt (in BGB lithologies also); the strongest fabrics are found in the gray gneiss directly adjacent to the BGB. Foliation orientation in the GSZ varies in response to the shape of the strain trajectory and strain intensity. By contrast, lineation orientation is more constant because linear fabrics are best developed in the high-strain shear plane, which dips steeply to 205° based on map interpretation (Figs. 10, 11). A noticeable low-to-high strain gradient is associated with the transition from NE-striking to E/W-striking foliations. Lineations typically plunge moderately to the WSW (average plunge is 39°), which suggests oblique-slip movement on the GSZ assuming the entire block has not been reoriented.

In map view, foliations curve in an orientation consistent with dextral-sense shearing. Dextral-sense slip is supported by the majority of kinematic indicators including deflected foliations, σ porphyroclasts, mica fish (Fig. 12), small-scale Z folds in a boudinaged chert, and a high-angle quartz grain-shape preferred orientations (Means, 1981) in several layers of iron formation. In most thin-sections, quartz behaves crystal-plastically (strong grain shape preferred orientations) while feldspars behave brittlely. However in one example of gneiss from near the shear plane, 2-5 mm long microcline crystals have distinctly bent twins, poorly developed core-mantle structures, and internal subgrain formation; feldspar grain shape preferred orientations are common in the surrounding matrix. All of these feldspar-plastic characteristics suggest that deformation temperatures reached at least 450 °C (DePaor and Simpson, 1993).

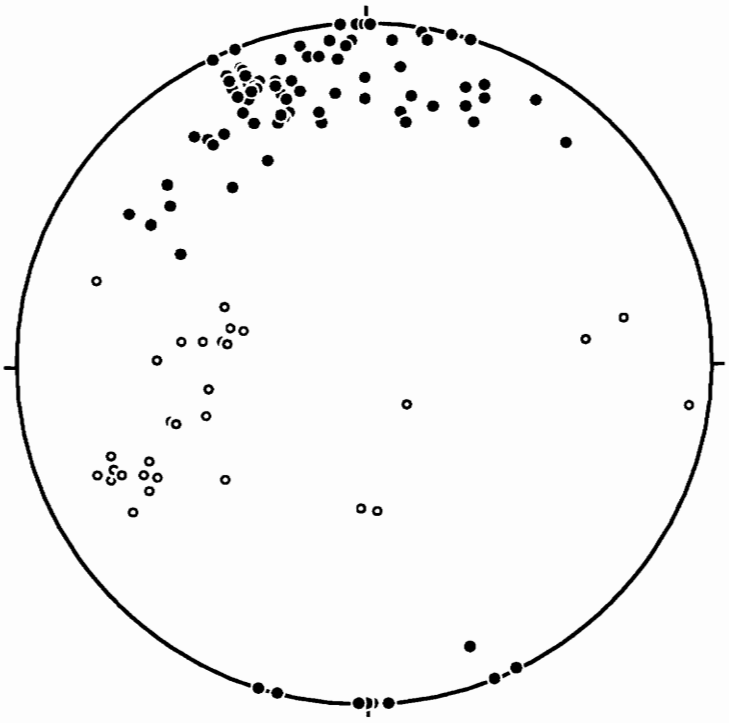

Figure 11. Lower hemisphere, equal-area stereographic projection of poles to foliation (filled circles, 78 data points) and stretching lineations (open circles, 30 data points) in the Gundekunde Shear Zone.

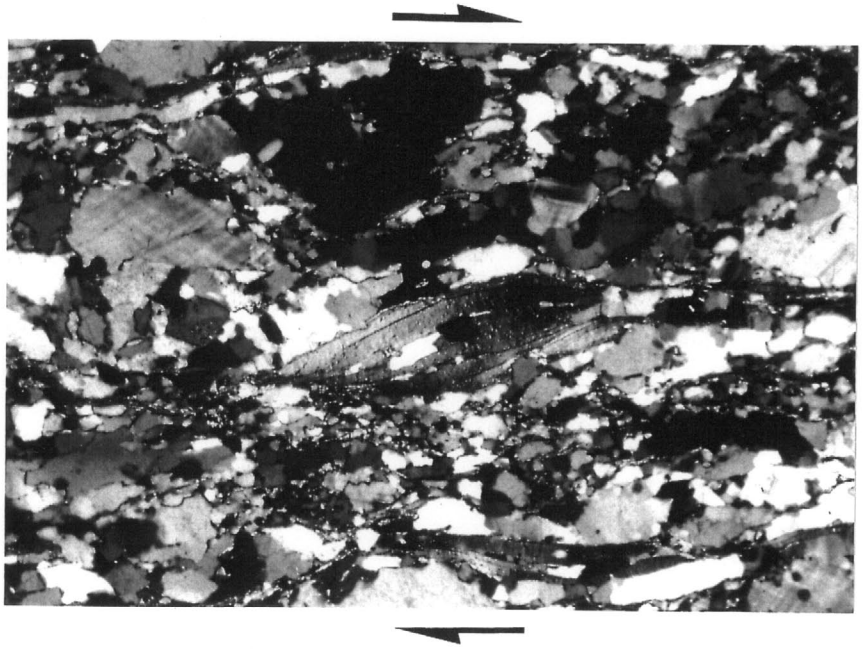

Figure 12. Photomicrograph of a classical mica fish showing dextral-sense displacement from the Gundekunde Shear Zone. Length across bottom of photo is ~3 mm.

Because a strain trajectory for the GSZ is apparently so well preserved, some estimations regarding the displacement can be calculated (following the methods of Ramsay and Graham, 1970; Ramsay and Huber, 1983). Two alternatives can be envisioned: First, a preexisting regional foliation that strikes ~065° was deflected by motion on the shear zone. The horizontal component of displacement for this alternative is estimated at 3.5 km. Second, the observed foliation is exclusively the product of shear zone activity (e.g. Ramsay and Graham, 1970). For this alternative, displacement was determined in two ways (Fig. 13): 1) displacement was calculated using shear strain measurements plotted against distance from the shear zone boundaries (which are poorly defined), with a resulting displacement of 11.8 km; 2) given the lineation orientation (average plunge of 39°), the appearance of feldspar-plastic textures, and a possible geothermal gradient of 44 °C km^{-1} for Archean continental crust (Allègre, 1982), displacement is calculated at ~15 km. If the geothermal gradient was lower than that postulated above (England and Bickle, 1984), for example 25 °C km^{-1}, displacement on the GSZ increases to ~29 km. This calculation assumes that the gneisses with feldspar-plastic textures were uplifted along the GSZ and not some later unmapped structure. The convergence of results between 10-15 km, leads us to suggest that the preserved fabrics are dominantly the result of ductile shearing under relatively elevated thermal conditions.

The timing of the Gundekunde Shear Zone and the age of its protolith is a problem in the historical development of the area. The Chipinda batholith intrudes the GSZ along the northern margin of the BGB. Whether the fabrics associated with the GSZ developed during an *earlier* ~2.9 Ga event similar to the relationship between the ~2.9 Ga Mashaba tonalite and ~2.9 Ga Chingezi gneisses near the Belingwe greenstone belt

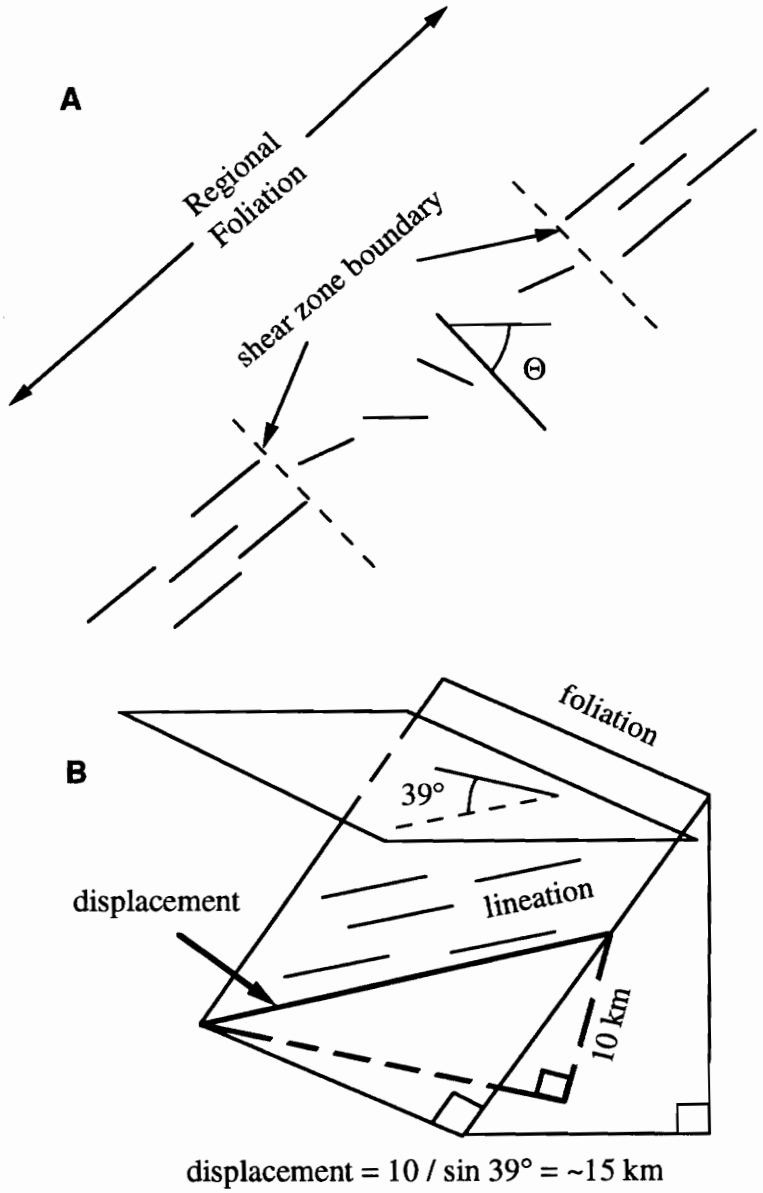

Figure 13. Different methods for calculating displacement on the Gundekunde Shear Zone. A. Calculating angular shear strain (γ) at different points between shear zone boundaries. The illustration shows the field geometry for a deflected foliation. The same principle was used for calculating displacement assuming all the foliation was related to shearing. B. Geometric relationships showing the displacement calculation using ~10 km of vertical uplift along the average lineation.

(Hawkesworth et al., 1979), or formed as part of the ~3.5 Ga Tokwe segment remains uncertain at this time.

2.9-2.5 Ga Record

The time bracket between 2.7-2.5 Ga is the most complicated in the area because it incorporates events including ductile thrusting, regional folding, regional and local metamorphism, intrusion of deep-to-shallow-level granitoids and ultramafic rocks, and brittle faulting. Many of these events overlap in time and current geochronology does not separate all episodes of assembly.

Shear Zones

Thrust Shear Zones. Approximately 2 km SW and parallel to the southern margin of the greenstone belt, is a set of discrete, typically meter-to-tens of meters wide, shear zones here termed the Muponjani Shear Zone, whose combined map thickness exceeds 2 km (Fig. 10). These shears dip steeply to the SE and deform banded tonalitic/Ksp-megacryst granitic gneisses that experienced granulite-facies metamorphism (Rollinson and Blenkinsop, in press). Shear zones have essentially down-dip mineral stretching lineations (Fig. 14) best preserved in the finer grained tonalitic layers; foliation orientation is largely constant. Several examples of σ porphyroclasts with top-to-the-north (reverse-sense) displacements were observed.

Although exposures of the Muponjani Shear Zone south of Buhwa are poor, strike projections permit some regional correlation. To the east in the bed of the Runde River, several meter-thick shear zones separate domains of less-strained gneiss. Most porphyroclasts with asymmetrical tails similarly yield reverse-sense displacements. Other workers (e.g. Worst, 1962; James, 1975; Odell 1975; Ridley, 1992) have

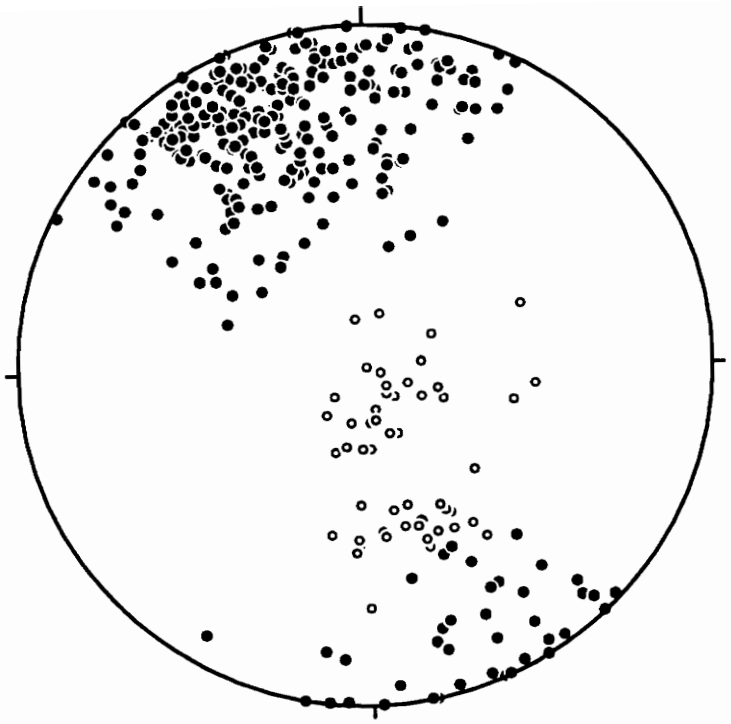

Figure 14. Lower hemisphere, equal-area stereographic projection of poles to foliation (filled circles, 289 data points) and stretching lineation (open circles, 52 data points) in the Northern Marginal Zone and Muponjani Shear Zone.

recognized or inferred a similar structural break. Mkweli and Blenkinsop (1992) and Mkweli et al. (in press) have demonstrated the occurrence of a low-angle reverse-sense shear zone (Umlali Shear Zone), with a maximum of several kilometers of displacement south and west of the Mweza Greenstone Belt (Fig. 9). In that region, the Razi Granite partly obscures the break, but was intruded during the waning phases of shearing and thus is locally deformed.

We suggest the reverse-sense Muponjani Shear Zone correlates with all these structures and represents part of the major tectonic break that separates the Northern Marginal Zone of the Limpopo Belt from the Zimbabwe Craton (Rollinson and Blenkinsop, in press; Mkweli et al., in press), a contact that has traditionally been recognized as the orthopyroxene-in isograd. Because much of the NMZ consists of charnockites and enderbites, which represent primary plutonic bodies that crystallized under granulite-facies (anhydrous) conditions (Ridley, 1992), we conclude that the "opx-in isograd" no longer has relevance as a tectonic domain boundary.

Strike-Slip Shear Zones. The southern margin of the BGB is distinctly linear, with a trend of ~060° (Figs. 9, 10). This trend is parallel with regional foliation in the granulites of the Northern Marginal Zone of the Limpopo Belt (Rollinson and Blenkinsop in press; see below). The contact between the BGB and surrounding gneisses is not exposed, however, a strong overprinting tectonic fabric that affects greenstone belt lithologies and adjacent crystalline rocks can be mapped parallel to the edge of the greenstone belt. The rocks consist of L>S and LS protomylonites and mylonites that define the Mahombe Shear Zone (MSZ; Fig. 10).

The MSZ dips steeply (~80°) to the SE, with a strong, shallow SW-plunging mineral stretching lineation (Fig. 15). The MSZ has a mapped strike length of ~20 km

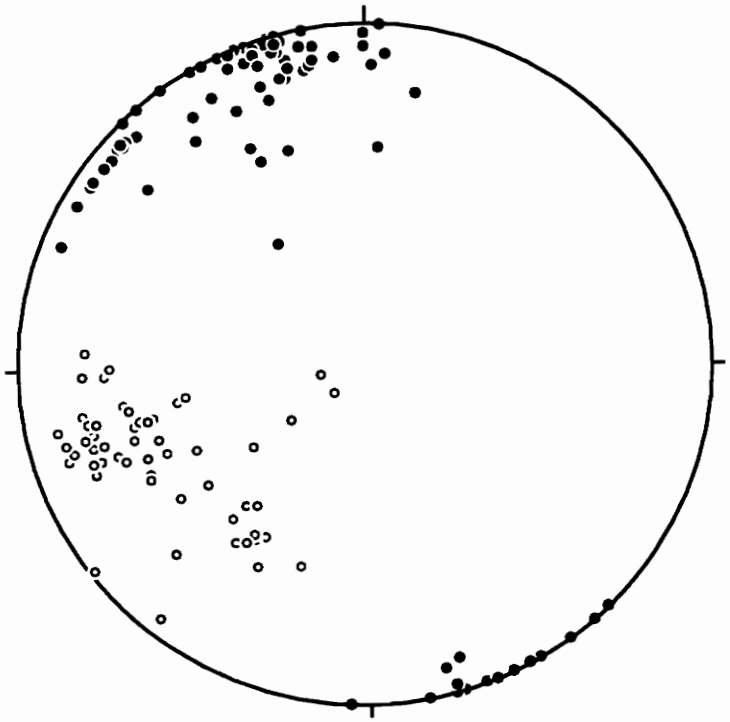

Figure 15. Lower hemisphere, equal-area stereographic projection of poles to foliation (filled circles, 72 data points) and stretching lineation (open circles, 61 data points) in the Mahombe Shear Zone.

and a width of ~1 km, although this width probably represents a combined thickness of discrete shear zones. Fabrics are best preserved in the gneisses. Gneissic foliation is defined by aligned biotite, quartz ribbons and elongate crystals, and trains of fractured feldspars. The essential and accessory mineralogy is identical to the Chipinda batholith, which is the likely protolith (Chapter 2). In the greenstones, foliation is defined primarily by elongate hornblende or cummingtonite crystals, which locally wrap around mm-scale garnets. Lineation is defined by the orientation of elongate amphibole crystals, which suggests new mineral growth during deformation (e.g. Shelley, 1989).

Mesoscopic and macroscopic features associated with shearing are rare and give conflicting shear senses. However, in thin sections oriented parallel to lineation and perpendicular to foliation (see Fig. 15), abundant, distinct, sinistral-sense shear bands cross-cut the foliation (Fig. 16). The shear bands (C or C' surfaces) are defined by aligned fine-grained biotite (common replacement by epidote) and muscovite and quartz crystals with prominent crystallographic and grain shape preferred orientations. Epidote is commonly associated with biotite in the shear bands. The average angle between shear bands and foliation (S surfaces) is 30°. Quartz grain-size reduction is common within shear bands, although abundant phyllosilicate growth (*cf.* Hippert, 1994) commonly obscures quartz textures. The uniform sinistral shear sense on these C surfaces is consistent with less common grain shape preferred orientations in quartz ribbons that also indicate sinistral shear sense (Means, 1981; Lister and Snoke, 1984). By comparison, these fabrics are similar to the "banded type" geometries discussed by Blenkinsop and Treloar (in press) from mylonites in the Mushandike Granite in Zimbabwe.

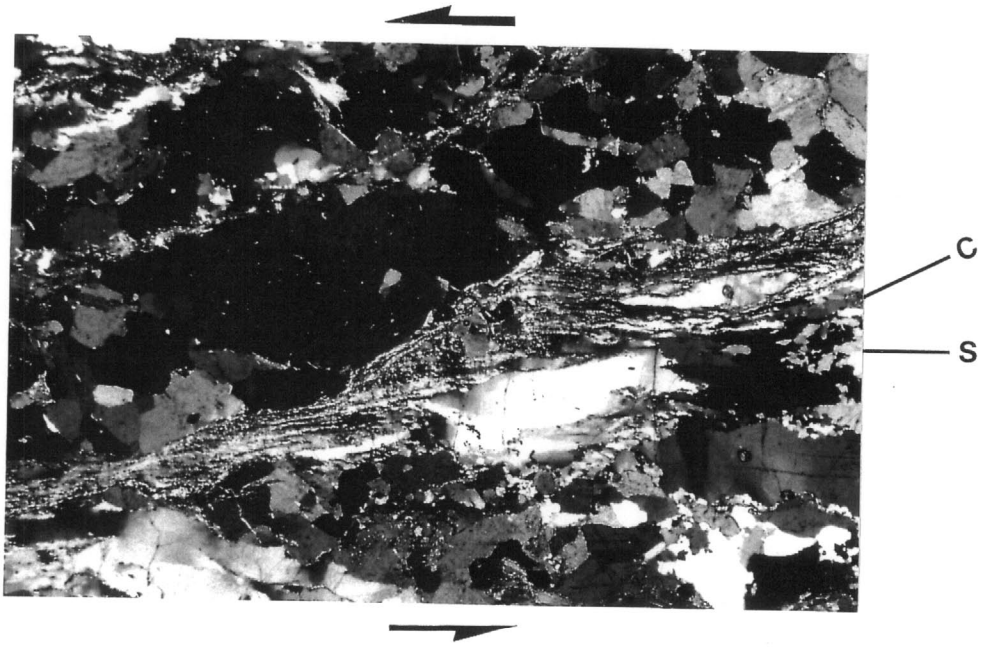

Figure 16. Photomicrograph showing S-C fabrics from the Mahombe Shear Zone. Length across bottom of photo is ~4.3 mm.

Along strike to the east in the vicinity of the confluence of the Runde and Ngezi Rivers (Fig. 10), shallowly-SW plunging linear fabrics typical of the MSZ change orientation significantly to down-dip, steeply east plunging, and shallowly east plunging (Fig. 17). This transition from westerly to down-dip and east-plunging lineations is not exposed and therefore the timing relationships between these fabrics is unclear. Nowhere could either be seen deforming the other. The three distinct lineation orientations in the confluence area are formed on different lithologies, namely metachert (steeply east-plunging), homogenous gray gneiss (down-dip), and banded gneiss (shallow east plunging). We suggest the different lineations formed in the same event because: 1) the orientations are restricted to distinct rock types that are adjacent to each other (map distance of ~600 m), 2) the units display a common foliation, and 3) no overprinting relationships between the lineations has been recorded.

Intrusions

Two suites of ~2.6 Ga K-feldspar granite comprise the youngest major rock type in the Buhwa area. The Chibi Granite forms an elongate batholith subparallel to orogenic strike of the Limpopo Belt and separates the Buhwa Greenstone Belt from the Belingwe Greenstone Belt ~30 km to the northwest. Outcrops of the Razi Granite are found directly north of, straddling, and south of the orthopyroxene-in isograd, which traditionally demarcates the northern margin of the NMZ (Robertson, 1973, 1974; Fig. 1). The Razi Granite is identified by K-feldspar megacrysts and cross-cutting relationships with other lithologies. Although largely undeformed, Mkweli et al. (in press) report a U-Pb zircon age of 2627 $\pm$ 7 Ma for a late-kinematic

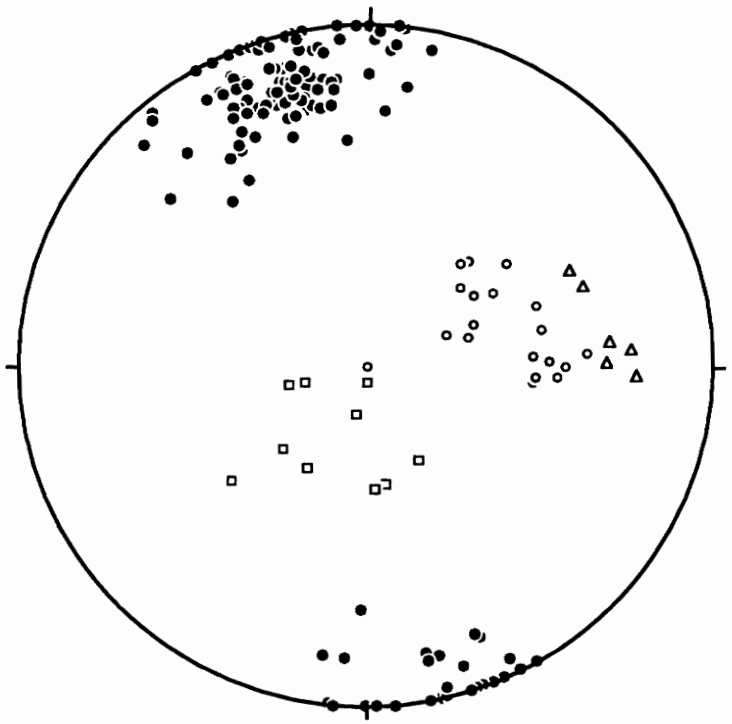

Figure 17. Lower hemisphere, equal area stereographic projection of poles to foliation (filled circles, 117 data points) and stretching lineation (open circles, 19 data points, metachert; open triangles, 6 data points, banded gneiss; open squares, 10 data points, gray gneiss) in the confluence of the Runde and Ngezi rivers.

microgranite associated with the Razi Granite, and infer this to be the approximate age of thrusting.

Approximately 150 m.y. after Chipinda batholith intrusion, the NMZ experienced an extensive phase of charnockite-enderbite plutonism (Ridley, 1992). New ages from this plutonic suite span from 2.58-2.71 Ga (Berger et al., in review). Based on petrologic and numerical modelling, the charnockite-enderbite suite typical of the NMZ is interpreted to have crystallized at depth from a convecting magma "ocean" (Kramers and Ridley, 1989; Ridley and Kramers, 1990). The K-rich, Razi and Chibi granites accompanied intrusion of the charnockite-enderbite suite.

A prominent, vertical, ENE-striking mafic dyke cross-cuts the Chipinda tonalite and intersects the BGB near the fold-closure region where it spreads as a sill along the intrusive contact (Fig. 10). Mafic dykes of this orientation and relative age, regionally, have been termed Mashaba-Chibi dykes and are thought to represent filling of the feeder conduits to ~2.7 Ga Ngezi Group mafic and ultramafic lava flows (Wilson et al., 1987; Wilson, 1990). Fabrics in the dyke vary from mylonitic to virtually undeformed, with preserved foliation parallel to the dyke walls. Such an orientation is consistent with NW-directed crustal shortening. Strain is typically much greater in the dyke than in surrounding older granitoids, a characteristic which is attributed to rheological differences.

Folds

Four fold sets deform all or part of the BGB; three of these also affect the surrounding granitoids and gneisses. Relative ages have not been resolved for F2 and the intrafolial folds (no definitive cross-cutting relationships); these may have formed as part of a single deformational episode.

F1 Folds. Disharmonic folds within different iron-formation units are designated F1. These folds are typically upright, although variable in orientation and vary from cm- to m-scale in amplitude and wavelength. In the Runde River, iron-formations of the designated basinal association (Chapter 2) are trapped in a high-strain zone (Gundekunde Shear Zone); these folds have been modified by later ductile deformation. Other F1 folds occur at the eastern terminus of the main iron-formation unit (Fig. 10), where the folds are meter-scale and are associated with intense microfaulting (offsets typically < 1 cm). Fold hinges have variable orientations, although locally numerous axes plunge gently towards the west, with steeply dipping axial surfaces commonly oriented east/west. Bedding above and below the iron-formation is not folded.

Based on their disharmonic nature, F1 folds are interpreted as slump folds related to gravitational collapse on a slope prior to lithification (e.g. Reineck and Singh 1980, p. 485). The cover succession at Buhwa is interpreted to have formed on a depositional ramp, with shallow-water facies near the fold-closure region and deeper water sedimentation to the east (Chapter 2). The position of F1 folds in a deeper water setting (Chapter 2) may indicate the ramp slope where sediments became gravitationally unstable and prone to slumping. These folds are likely to have been modified into present orientations during later crustal shortening.

Alternatively, the competency contrast between adjacent quartzite/greenstone and the iron-formation was sufficient to permit early buckling in the finely laminated iron-formation to form F1 folds while other, more massive, units experienced layer-parallel strain (*cf.* Ghosh et al., 1993). Adjacent units are not strongly folded, although the quartzites have a series of small-scale, steeply west-plunging (e.g. 60° towards 244°)

folds possibly related to the quartzites warping around a late mafic dyke that separates the quartzites and iron-formation.

F2 Folds. The main fold (Buhwa syncline) is the dominant structure in the area. It deforms the cover succession and surrounding granitoids, and represents F2 deformation in the field. This major F2 fold consists of a single, east-plunging synformal syncline; no adjacent anticline is present (Fig. 10). Further southwest along strike, but outside the study area, F2 folding does contain a synform-antiform pair.

In the Buhwa region, the major synform has an axial trace mapped for ~20 km. The fold is strongly asymmetric, with a long S-dipping northern limb and a short N-dipping southern limb (Fig. 10). Abundant younging criteria (ripple marks, trough cross-stratification, and flame structures) young toward the axial surface of the fold which, when combined with bedding orientations, indicates the structure is a synformal syncline. The best fit great circle through poles to bedding, yields a fold axis that plunges 28° toward 088° (Fig. 18). The scatter of poles about this π-point indicates that the fold is not perfectly cylindrical. Contoured maxima of the poles to bedding yield fold limbs at 046°/38°S and 118°/45°N (Fig. 18). From these data, an interlimb angle of 66° with a bisecting plane passing through the π-point oriented at 086°/86°S were calculated. This bisecting plane is interpreted as an approximation to the axial surface of the fold (*cf.* Davis, 1984). The orientation of the best-fit great circle would change into a more compatible position with respect to the bedding-cleavage intersection lineation if the data located along the periphery (Fig. 18) were excluded; however, because no unifying field relationship permits a way of discriminating out certain points, all data have been used in the analysis. These data indicate the major fold at Buhwa is gently east-plunging, upright, and tight.

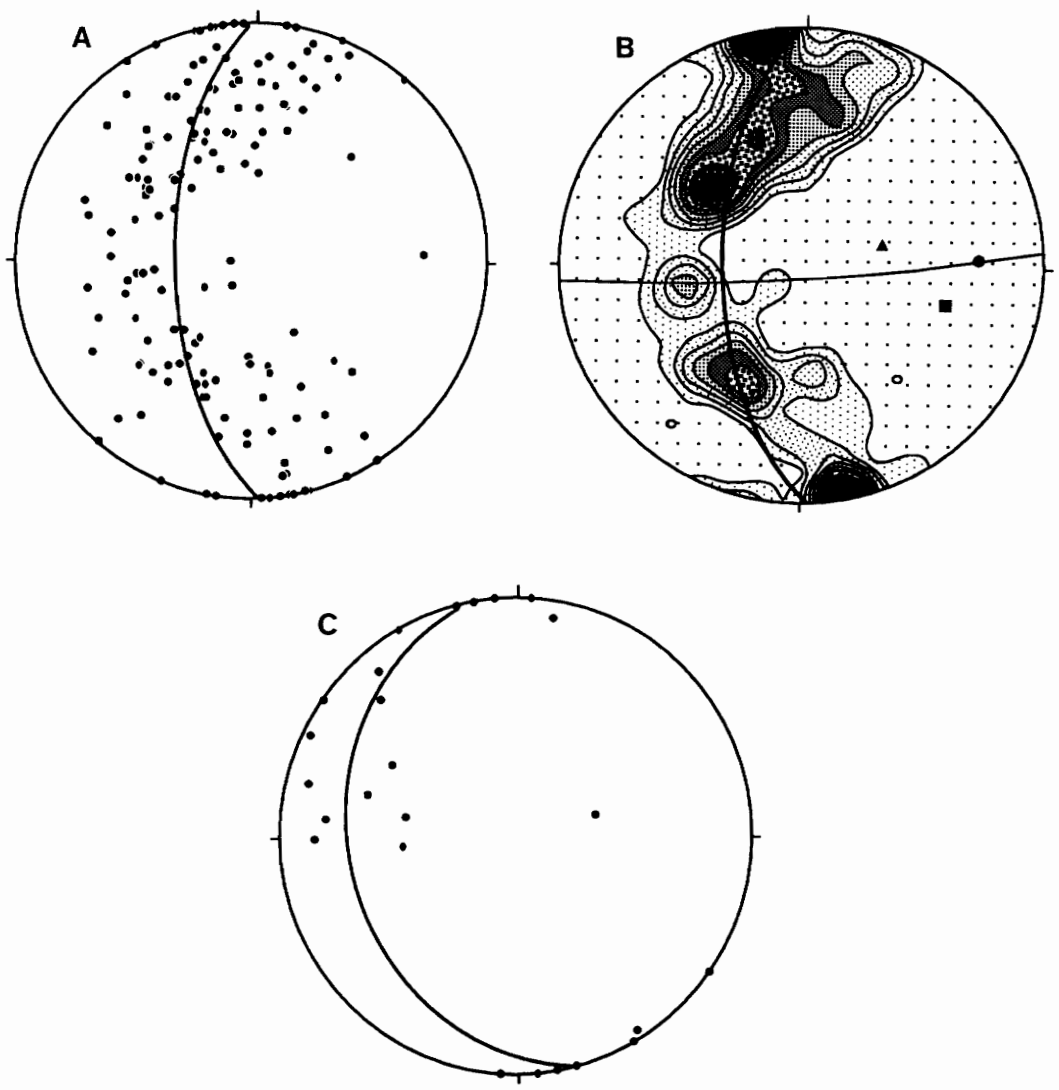

Figure 18. A. Lower hemisphere, equal-area, stereoplot of poles to bedding for F2 showing best-fit great circle and corresponding fold axis; 145 data points. B. Same data contoured at 0.5 times a uniform distribution on the surface of the projection sphere. Low-density stipple pattern is no points; black area is highest density. Filled circle represents average calculated fold axis. Filled square is average cleavage (C1) - bedding intersection lineation from three localities. Filled triangle is average calculated fold axis from poles to foliation in the Chipinda batholith. East-west striking nearly vertical plane represents calculated axial surface. C. Poles to Chipinda batholith foliations with best fit great circle and corresponding fold axis; 17 data points.

A weak foliation in the Chipinda batholith, which is defined by aligned biotites, is mostly concordant with the bedding in the BGB (> 50% of the poles to foliation fall within the contoured data of poles to bedding from the syncline; Fig. 18). There are several alternatives to explain this foliation: 1) The foliation is related to a late set of conjugate faults that affect the entire Zimbabwe Craton. This alternative is unlikely because the observed foliations are not vertical, do not represent high-strain fabrics, and do not grade into shear zones; 2) The foliation is magmatic, and forceful emplacement of the intrusion caused the deformation in the BGB. This alternative is equally unlikely because many of the rocks in thin section contain weak to moderate crystallographic preferred orientations in quartz, locally well-developed grain shape preferred orientations in quartz, and biotites that wrap around larger feldspar crystals. Additionally, we do not see an increase in strain towards the contact, which is typical in forcefully emplaced plutons (Holder, 1979; Bateman, 1985; Ramsay, 1989; Jelsma et al., 1993); or 3) The foliation is a solid-state deformation associated with the stress field that resulted in folding of the BGB. This interpretation satisfies all the observations and indicates that the foliation in the Chipinda batholith represents a solid-state fabric that developed cogenetically with shortening of the greenstone belt.

Out of the study area to the southwest, folds similar in scale to F2 possess notably different orientations as can be seen on satellite images of the region (e.g. fig 3.9 in Nisbet, 1987) or on the reconnaissance geologic map of Worst (1956). These folds are chevron to isoclinal in shape and have axial traces that trend ~060°; such trends are very similar to the trend of orogenic strike as represented by foliations in the granulites of the northern marginal zone (Rollinson and Blenkinsop, in press). The main Buhwa syncline trends 088°, which is noticeably oblique to other folds currently assigned to F2.

We propose that the main F2 folding formed in response to uplift of the NMZ over the Archean Zimbabwe Craton. The variation is F2 fold-axis orientations can be attributed to heterogeneous progressive deformation along the length of the greenstone belts. This may be especially true for the main Buhwa syncline whose axial surface is oblique to the dominant foliation (*cf.* Hudleston and Lan, 1993). Strain measurements in the eastern part of the BGB support this conclusion as well, although some evidence of superimposed NNE-directed shortening is recorded in the Ngezi and Runde river locations.

F3 Folds. F3 is recognized through the interpretation of regional-scale map patterns. F3 folds are long wavelength (> 40 km) folds that have axes oriented perpendicular to orogenic strike of the Northern Marginal Zone (Fig. 9). These cross folds are identified by recognizing apparent polarity reversals in the plunges of F2 folds. On the map of Worst (1956), a "porpoising" fold hinge is apparent from the map pattern of several units, especially several thin iron-formation layers.

The same doubly-plunging geometry, however, could be the result of heterogeneous compressive stress along the length of the greenstone belt as Wood (1974) demonstrated for the Cambrian slate belt of Wales. That F2 folds along the length of the belt possess different orientations may point to strain heterogeneity. Further mapping and structural analysis in the area SW of Buhwa is necessary to resolve the issue.

Intrafolial Folds. The few intrafolial folds principally occur within the cover succession in the Gundekunde Shear Zone (see below). Fold hinges plunge moderately (~25-40°) to the east and west. In the Ngezi River (Fig. 2), several

recrystallized chert boudins are deformed into west-plunging Z folds oriented parallel to the dominant stretching lineation in the adjacent gneisses, suggesting the structures are cogenetic.

Cleavage

Two cleavages are developed in the cover succession of the BGB. The earlier (C1) is a very strong pressure-solution cleavage developed within shales interbedded with quartzarenites (unit Q1B; Chapter 2) and shales of the transitional association along the long northern limb of the main syncline (F2). C1 is also rarely present in cherty bands in the main iron-formation (IF1; Chapter 2). The host lithology was typically very clay rich (now chlorite and sericite) with mm-thick layers of silty or very fine sandy mudstone. C1 slaty cleavage has a domain spacing of much less than 1 mm (Fig. 19). A similar cleavage was not recognized on the short southern limb of the fold .

Homogeneity of host shales, poor exposure, and modest preservation of the cleavage precluded detailed analysis. However, of the three localities where the cleavage is well exposed, the cleavage-bedding intersection lineation falls within the scatter of π points derived from bedding orientations (Fig. 18; average cleavage-bedding intersection lineation is 38° toward 105°). Pending further analysis, we suggest that C1 is axial planar to the main F2 fold.

A later cleavage (C2) deforms a much smaller region; it has been recognized only in the hinge-zone of the map-scale F2 fold in unit S1C shales (Fig. 10; Chapter 2). The spacing between C2 cleavage domains is 1-4 cm. C2 dips steeply to the NE or SW (Fig. 20) and clearly crosscuts the axial surface of F2, suggesting that C2 is a late

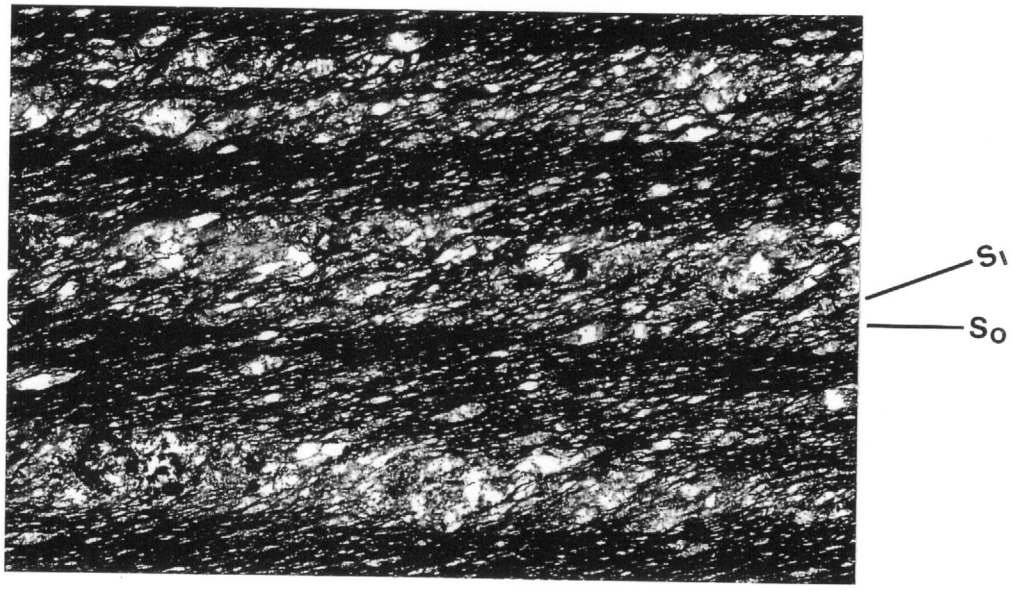

Figure 19. Photomicrograph of C1 penetrative slaty cleavage. So is bedding, S1 is cleavage. Length across bottom of photo is ~4.3 mm.

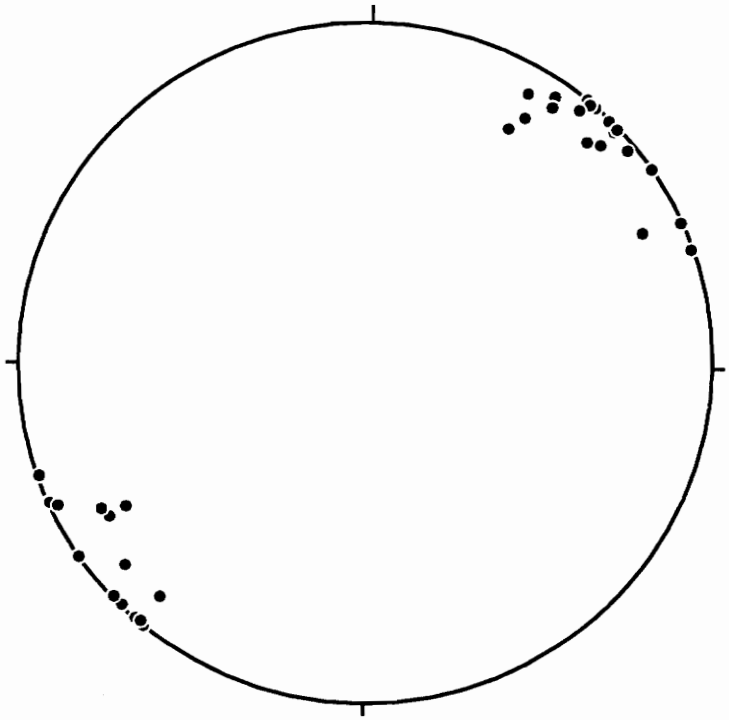

Figure 20. Lower hemisphere, equal-area stereographic projection of poles to C2 (27 data points).

transecting cleavage. The similarity in orientation with possible F4 fold axial surfaces suggests that C2 could be axial planar to F4.

Metamorphism

Some comments on the metamorphic history based on field observations and thin-section analysis (mineralogy and textures) warrant consideration. Worst (1962) considered that the BGB suffered greenschist-facies metamorphism, while Dodson et al. (1988) suggested that the same rocks reached at least lower amphibolite-facies metamorphism. Our work suggests that the distribution of metamorphic conditions is considerably more variable and complex than previously recognized and we see evidence for regional metamorphism and local metamorphism associated with ductile shear zones.

Regional Metamorphism. Where the rocks of the BGB and adjacent crystalline rocks of the Zimbabwe Craton are not in isolated ductile structures such as the Mahombe and Gundekunde shear zones, the metamorphic grade is at greenschist facies, which is typical of the regional metamorphism that affects the entire craton. In shale units, which are >1 km in thickness in the main F2 fold closure (Chapter 2), yellow and green chlorite and sericite are the main metamorphic minerals; this assemblage is typical of the chlorite zone for low-grade metamorphism of pelitic rocks (Yardley, 1989). In several samples, original clays have not been converted to metamorphic minerals. In the Chipinda batholith, epidote, which typically replaces biotite, and fine-grained micas are the common metamorpic minerals. Chlorite and rare tremolite are the dominant metamorphic minerals in the low-grade core of the greenstone belt east of the major F2 fold. In an example of perfectly preserved

spinifex-textured lava, Mg-chlorite and chrysotile form the metamorphic mineral assemblage, with rare tremolite.

Metamorphic grade and strain increase from the core of the BGB towards the southern margin, where greenstone belt lithologies are in contact with gneisses of the Mahombe and Muponjani shear zones and NMZ (Fig. 10). Although not regional in extent, this narrow band of amphibolite-facies rocks developed in response to regional thrusting of granulite-facies rocks over the Zimbabwe Craton and provides insights to the timing of regional deformation and metamorphism. Greenstones form the dominant rock type in this area and consist of: 1) hornblende + cummingtonite + plagioclase + quartz schist, 2) cummingtonite + garnet $\pm$ plagioclase $\pm$ quartz $\pm$ opaque schist, or 3) brucite + chlorite + olivine schist.

Cummingtonite + garnet schists located more towards the center of the belt have smaller garnets with inclusion trails of cummingtonite that define a weak foliation; a strong foliation wraps around the garnets (Fig. 21A). These textures suggest that metamorphic growth of garnets commenced at the earliest stages in the development of the strong tectonic foliation (*cf.* Vernon et al., 1993). By contrast, garnet-bearing schists at the margin of the BGB have garnets that enclose a strong foliation of opaques, quartz, and cummingtonite (Fig. 21B). These garnets themselves are enclosed by a strong foliation that typically deflects around the garnets. Such textures indicate that tectonism both preceeded and outlasted metamorphism at the edge of the greenstone belt.

In the brucite + chlorite + olivine schists, olivine commonly forms 1-5 mm altered, spherical porphyroblasts with inclusions of opaques enclosed by very fine-grained matrix. We suggest this assemblage represents prograde mineral growth under greenshist- to amphibolite-facies conditions. Metaperidotites that consist of antigorite

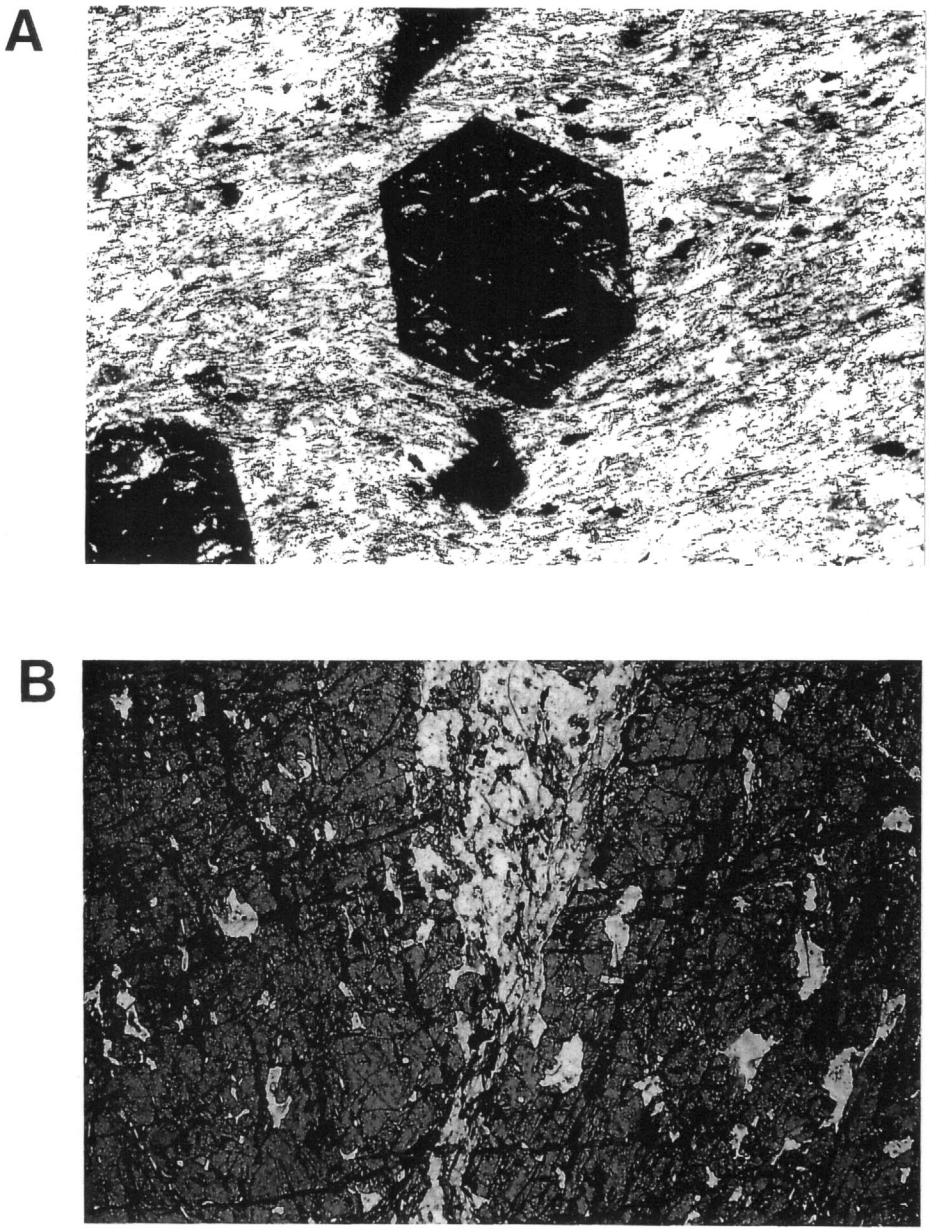

Figure 21 A. Garnets overgrowing a weak foliation of cummingtonite and surrounded by strongly foliated cummingtonite. B. Garnets overgrowing a strong early foliation of quartz, opaques, and amphibole. Length across bottom of photo in A is ~1.3 mm; Length across bottom of photo in B is ~6 mm.

+ brucite produce forsterite essentially isothermally (350-400 °C) over a range of pressures from under 0.5 kb to 5 kb (Tracy and Frost, 1991).

The highest grade of regionally metamorphosed rocks occurs in the Northern Marginal Zone directly south of the BGB (Fig. 10). Rocks of the NMZ have a considerably more complicated history than previously considered (reviewed in Rollinson and Blenkinsop, in press). Although much of the NMZ consists of plutonic rocks (e.g. Ridley, 1992), supracrustal remnants in the NMZ have been metamorphosed to granulite-facies twice (Rollinson and Blenkinsop, in press), with peak metamorphic conditions between 5.1-8.4 kb and 740-850 °C (Rollinson, 1989; Tsunogae et al., 1992). The granulite-charnockite assemblage is raised to current structural levels along the multiple shears of the Muponjani Shear Zone and its correlatives. Closer to the BGB, the Muponjani Shear Zone involves high-grade remnants of iron-formation and greenstone. Iron-formations now consist of quartz + magnetite + cummingtonite schists, in which quartz crystals are very coarse grained (0.25-0.5 mm) and commonly strain free, with 120° junctions. Interspersed greenstones in this sheared region commonly are hornblende amphibolites, although one example has a mineralogy distinct from others nearby in that it consists of pargasitic hornblende, olivine (in part altered to iddingsite), Mg-chlorite, spinel, and orthopyroxene. This represents a prograde granulite-facies mineral assemblage where Mg-chlorite breaks down to form olivine + spinel + orthopyroxene (e.g. Fawcett and Yoder, 1966), a reaction that occurs at about 700 °C and above about 5 kb (Tracy et al., 1984). Such temperatures and pressures are consistent with the thermobarometric estimates noted above. A similar prograde mineral assemblage for ultramafic remnants occurs in the Southern Marginal Zone of the Limpopo Belt (Van Schalkwyk et al., 1992). The presence of these granulite-facies greenstones at Buhwa clearly

demonstrates that some supracrustal remnants in the NMZ are likely to be related to lithologies of the Zimbabwe Craton. Rollinson and Lowry (1992) have drawn the same conclusion based on geochemical similarities of some metabasic rocks in the two areas.

Regional metamorphism and folding are likely be synchronous based on two lines of evidence. First the chlorite and sericite typical of the low-grade shales is commonly axial-planar to F2, and therefore could have grown during shortening of the cover succession. This interpretation is further substantiated on geochemical grounds. Major- and trace-element analysis of the shales indicates that they were enriched in potassium at some point (Chapter 4). The most geologically plausible source of potassium for later enrichment is in association with intrusion of the late, syntectonic Razi and Chibi granites. Although the data do not require so, it is permissible that the sericites acquired their composition at ~2.6 Ga during the waning phases of thrusting. Second, an early tectonic event is documented by the garnets that enclose a strong opaque + quartz + cummingtonite foliation in the area near the southern margin of the BGB. Towards the center of the belt, garnets enclose only a weak foliation, which suggests that the main foliation-producing event(s) followed. These garnet-matrix relationships indicate that metamorphism commenced following the onset of crustal shortening and terminated prior to final tectonic burial.

Metamorphism Associated with Shear Zones. Metamorphic assemblages generated during ductile deformation events punctuate the overall low-grade nature of the BGB and Zimbabwe Craton. In general, shear zones in the BGB area deform rocks that have a granitic protolith, and thus are poor recorders of the metamorphic conditions because mineral phases are not subject to great changes even at relatively

high metamorphic grades. However, "aureole" effects penetrate into the greenstone belt lithologies; these effects are also associated with decreasing strain gradients.

Deformation temperatures for the Gundekunde Shear Zone are constrained by the presence of plastically deformed feldspar in coarse-grained gray granitic gneiss. The greenstones adjacent to this gneiss consist of coarse tremolite + talc + opaque schist and associated layers of iron-formation have strong crystallographic and grain shape preferred orientations. Tremolite-dominated schist has a map width of ~1 km; less common greenstone types include talc + dolomite and talc + tremolite schists (Fig. 22).

Only minor metamorphic mineral growth accompanied shearing along the Mahombe shear zone. Some greenstones in this shear zone consist of hornblende amphibolites, in which the long-axes of hornblende grains parallel a mineral stretching lineation (e.g. quartz rods), suggesting that shearing developed at amphibolite facies.

Conjugate Faults

Two prominent sets of faults, best preserved in the Chibi Granite several kilometers north of the BGB, cross cut the field area (Robertson, 1974). One set strikes NNE (017°) and shows apparent sinistral-sense off-set, while the second set strikes NW (323°) and shows apparent dextral-sense off-set; dips on both sets are vertical or nearly so. A roughly east/west vertical mafic dyke correlated with the Mashaba-Chibi dyke swarm (Chapter 2) that intrudes the Chipinda batholith (Fig. 10) is offset ~1 km by one of the NNE faults. In several examples interpreted from satellite images, the NNE set of faults is crosscut by the NW set.

Wilson (1990) recognized a similar pair of fault sets at the craton-scale in his analysis of the Zimbabwe Craton. The NNE-striking, sinistral faults, termed the

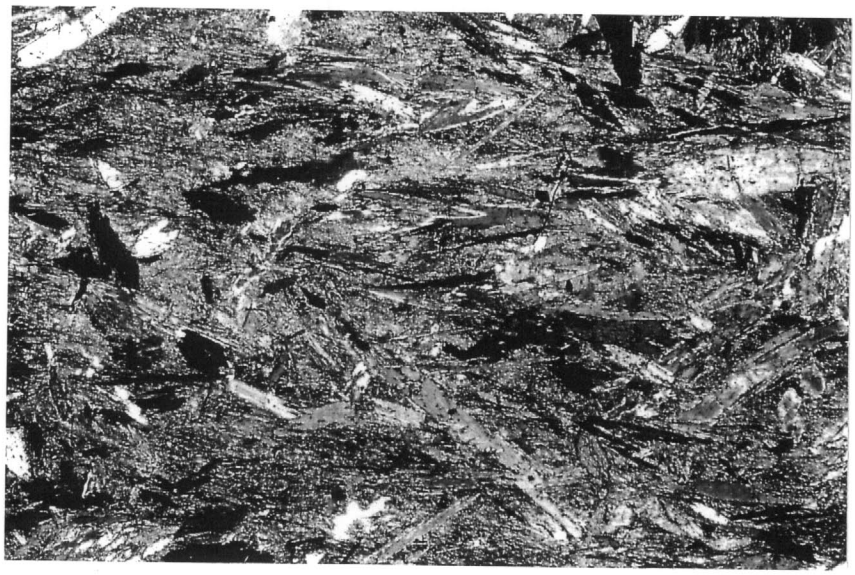

Figure 22. Photomicrograph of talc-tremolite schist. Length across bottom of photo is ~6 mm.

Popoteke set, occupy a significant orientation in that it represents the orientation of the Great Dyke of Zimbabwe, which perhaps intruded one of these faults. The Popoteke fault itself has a strike-length > 400 km and apparent displacements up to 3 km. The NW-striking, dextral faults, termed the Mchingwe set, typically offset the earlier Popoteke set, and the Great Dyke, with apparent displacements up to 4 km.

We suggest that by orientation, sense and magnitude of displacements, and relative age relationships, that the faults cross-cutting the Chibi Granite in the map area correlate with the Popoteke and Mchingwe fault sets. Furthermore, the close spatial proximity and similarity in displacements in the Chibi area are consistent with them forming as a conjugate pair (Wilson, 1990). Fault strikes taken from Robertson (1974) and a satellite image provide the data for a fault analysis. The bisector of the acute angle between the fault sets yields a $\sigma 1$ with an orientation of 350° (Fig. 23). This orientation is similar to that calculated by Wilson (1990) for his "stage 1" in the development of the Great Dyke fracture pattern (σ_1 = 338°) and is parallel to regional deformation patterns in the BGB and NMZ.

Timing of the faulting is bracketed by the age of the ~2.6 Ga Chibi Granite and the ~2.5 Ga Great Dyke of Zimbabwe and satellites (Hamilton, 1977), which most likely fill fractures from Popoteke faulting.

Strain Analysis

In order to estimate strain symmetry and intensity, the long and short axes of 374 deformed clasts of metabasite and chert were measured from a minimum of three flat surfaces in a mafic breccia at three localities in the eastern part of the greenstone belt (Fig. 2; Table 2). The measurements were made along strike on the Runde and Ngezi rivers in the core of the belt, and at their confluence in the south of the belt. Strain

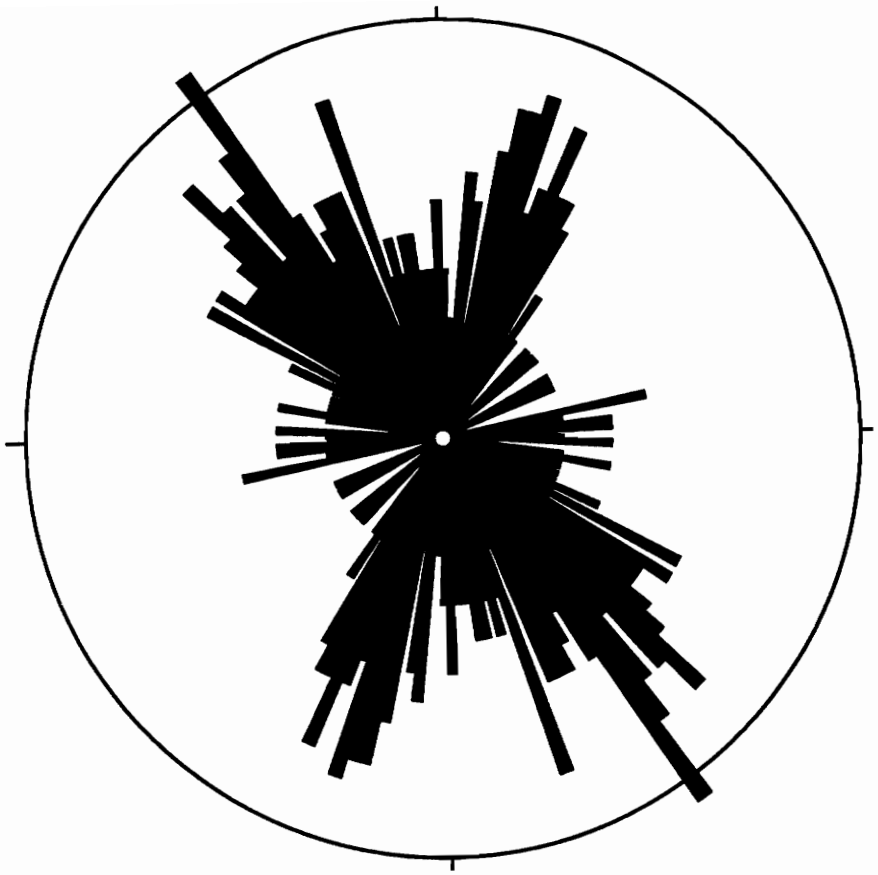

Figure 23. Rose diagram showing the distribution of conjugate faults. 251 data points, all from Chibi Granite. Circle represents 5% of data; class interval is 2°.

Table 2. Results of strain analysis

Location	x	y	z	k	d
Ngezi River	1.51	1.03	0.64	0.76	0.77
Runde River	1.79	1.22	0.47	0.27	1.66
Confluence Area	2.26	1.06	0.42	0.73	1.89

ellipse ratios and orientations for each surface were calculated by the method of Shimamoto and Ikeda (1976), and the measurements were combined into the best-fit strain ellipsoid by the method of Owens (1984). All three localities show strains that fall within the flattening field on a Flinn plot (k = 0.76 Ngezi River, k = 0.27 Runde River, k = 0.73 confluence) with varying strain intensities (d = 0.77, 1.66, 1.89 respectively; Ramsay and Huber, 1983, p. 202, eq. 11.13). Although k and d values differ markedly in the three localities, principal strains have similar orientations in the Ngezi and Runde river localities (Fig. 2): the maximum principal strain is subvertical and the minimum principal strain is subhorizontal in a NNE-SSW direction. At the confluence, the maximum principal strain plunges gently east and the minimum principal strain is subhorizontal in a NNW direction. A poorer fit between the measurements and calculated ellipsoid was obtained at this locality and the result is regarded with less confidence. The minimum principal strain at all three localities is ~0.5, which indicates that the eastern part of the BGB could have been shortened by up to 50%. The shortening is likely to be variable through this area, with values in the core of the belt less than the margins.

~2.0 Ga Record?

Development of the Mahombe shear zone, C2, and F3? record evidence of late NE-directed compression and could have taken place during the 2.7-2.5 Ga period or may be significantly younger. These structures clearly post date F2 and metamorphism, but because of limited magnitude and extent, do not show obvious cross-cutting relationships with other rocks or structures. An interesting possibility is that these structures developed at ~2.0 Ga, an age that has recently proven to be of great geologic significance in the evolution of the Limpopo Belt (e.g. Kamber et al., in

press). Van Breeman and Dodson (1972) first described ages at ~2.0 Ga from the Limpopo Belt *and* from along the NMZ-Zimbabwe Craton contact SW of Buhwa.

The dominant structure associated with this NE shortening is the Mahombe Shear Zone, which strikes at ~065°. NE-SW shortening is consistent with the orientation and displacement sense of the MSZ. Related to this shortening is the late C2 transecting cleavage that cross-cuts all F2 fold elements, and possibly the F3 fold axial surfaces, which share a similar orientation. Our strain measurements from the Runde and Ngezi river sites indicate a minimum principal strain orientation of NNE, which suggests a component of shortening possibly associated with the MSZ and C2. This late NE crustal shortening has not been documented in other areas of the craton or NMZ.

DISCUSSION

The results of this study have particular relavance to two popular hypotheses that explain the deformation patterns recognized in the Limpopo Belt and adjacent Archean Kaapvaal and Zimbabwe Cratons: 1) Himalayan-style continental collision (e.g. Treloar et al., 1992 and references therein), and 2) mantle recycling and "vertical" tectonics (Ridley and Kramers, 1990). Details of the structural geology and tectonic history of the Buhwa Greenstone Belt and surrounding granite-gneiss terrane conflict with these views on the tectonic history of the region.

The most widely accepted model at present is the continent-continent collision theory. Treloar et al. (1992) draw analogies between Archean crustal growth and deformation in southern Africa and Himalayan - Tibetan deformation patterns, in which late phases of deformation include crustal shortening and lateral extrusion. While there is evidence for crustal shortening at Buhwa, there is little evidence that the

shear zones represent escape structures. For example, it has been demonstrated here that the two major shear zones in the area are of (potentially very) different ages, one of which (Gundekunde Shear Zone) *predates* folding and metamorphism and reflects oblique- rather than strike-slip motion. Also, we find no evidence for an imbricate fault stack in the supracrustal succession at Buhwa, which is typical of Himalayan deformation (e.g. Coward et al., 1987). Additionally, our work at Buhwa suggests that the uplift of the NMZ took place along high-angle (>50°), rather than low-angle structures as is generally inferred in these models; we see no field evidence to suggest that previously low-angle structures were rotated into their current high-angle position. Seismic evidence indicates that the NMZ is not underlain by the Zimbabwe Craton (Stuart and Zengeni, 1987), which is consistent with high-angle thrusting.

The mantle recycling, or "Marcy", model offers an attractive explanation for the voluminous input of tonalitic magma in the NMZ and Zimbabwe Craton (Ridley, 1992; Rollinson and Blenkinsop, in press). The areally extensive Chipinda batholith, which is in part of tonalitic composition, is consistent with the Marcy model. However, one of the effects of a convecting "magma ocean," as the model predicts, is low-amplitude long-wavelength warps in the topography, with resultant thin, shelf-like, sedimentary deposits (Ridley and Kramers, 1990). In contrast to the ~250 m thick Manjeri Formation in the Belingwe Greenstone Belt, the sedimentary pile at Buhwa exceeds 3 km and resembles Phanerozoic stable-shelf successions (Chapter 2). To what extent the very thick succession at Buhwa limits the use of the Marcy model requires further study.

Aspects of the evolution of the Buhwa Greenstone Belt and surrounding granite-gneiss terrane resemble continent-continent collision when viewed in a modern plate tectonic setting. However, as pointed out above, the differences are significant. Also,

there are some rocks in the Buhwa region that are similar to those predicted by the Marcy model. The details presented in this paper suggest that a single unified model to explain lithologic distribution and deformation patterns, at least for this part of the Zimbabwe Craton, has not yet been established. Similarities with different theories perhaps suggests that hybrid evolutionary models must be established to account for all the recorded observations.

SUMMARY

The ~3.0 Ga Buhwa Greenstone Belt, and surrounding granite-gneiss terrane, in southern Zimbabwe represents the closest greenstone belt in the Archean Zimbabwe Craton to the polydeformed and metamorphosed Limpopo Belt. An understanding of the geologic evolution at Buhwa, therefore provides information relevant to craton-margin deposition and deformation. The history can be divided into three, or possibly four, time periods embracing different geologic events.

The earliest period (3.0 Ga and older) is highlighted by assembly of the ~3.5 Ga Tokwe segment, an early Archean continental nuclei, followed by deposition of the Buhwa Greenstone Belt cover succession on top of the Tokwe segment. At ~2.9 Ga, the northern part of the belt was ductilely deformed then intruded by a batholith of granitic-tonalitic composition. The majority of events in the area took place between 2.9-2.5 Ga. NNW-directed crustal shortening, which resulted in map-scale folding of the cover succession and regional greenschist-facies metamorphism, occurred in response to uplift of the Northern Marginal Zone of the Limpopo Belt over the Zimbabwe Craton. A conjugate fault pair developed north of the greenstone belt with continued NNW-directed shortening. The remaining events could have formed in this 2.9-2.5 Ga time interval, or later and include: sinistral shearing along the southern

margin of the belt, transecting cleavage, and open folding, all of which are consistent with NE-SW crustal shortening.

Two genetic models have been proposed to explain the juxtapositioning of the Limpopo Belt and the Zimbabwe Craton. Most workers currently favor a continent-continent collisional model similar to the Himalayas, whereas other workers infer "vertical" tectonics and magma oceans. Detailed data presented in this study suggest that neither model can account all the features present, but that both can explain different aspects of the geology. This observation suggests that a hybrid model may be necessary to understand the Archean evolution of the region.

CHAPTER 4

Geochemistry of shales from the Archean Buhwa Greenstone Belt, Zimbabwe: Implications for Provenance and Source-Area Weathering

ABSTRACT

Low-grade shale samples from the Archean (~3.0 Ga) Buhwa Greenstone Belt, Zimbabwe, generally define a single group based on major- and trace-element concentrations. The shales are strongly depleted in CaO, Na_2O, and Sr with respect to average Archean upper crust. By contrast, K_2O, Ba, and Rb are enriched several times relative to average Archean upper crust. Transition metals and high field strength elements typically have average Archean concentrations, with two exceptions: one sample shows Cr and Sc enrichment and another shows Cr depletion with enrichment of high field strength elements. Most samples have fractionated LREE patterns with small negative Eu anomalies (average Eu/Eu* = 0.77) and generally flat HREE. Exceptions include a sample with fractionated LREE and no Eu anomaly, one with fractionated LREE and a large negative Eu anomaly, and one with a flat REE pattern that has low ΣREE. The geochemical characteristics suggest that the source consisted of well-differentiated and less well-differentiated felsic rocks and mafic volcanic rocks. A nearby early Archean (~3.5 Ga) continental nucleus has similar geochemical trends and is the probable source. Intense chemical weathering of the source terrane is indicated by an average chemical index of weathering value of 98, nearly complete depletion of CaO and Na_2O, and high Al_2O_3/Na_2O ratios. Fine-grained sediments of comparable age and tectonic setting elsewhere in southern Africa show similar source-

area compositions and weathering trends, which suggests that southern Africa was tectonically stable and had a hostile chemical environment at ~3.0 Ga.

INTRODUCTION

Geochemical studies of fine-grained siliciclastic rocks have provided critical information regarding provenance, source-area weathering conditions, and estimates of upper crustal composition through time. This has been especially true for Archean terranes, for which in many cases source areas have been eroded away or are conjectural. Additionally, geochemical studies have added much to the understanding of the growth of the continents through time (e.g. Taylor and McLennan, 1985).

Of all the major Archean cratons exposed on Earth, only the Zimbabwe Craton (Fig. 24) has not been the focus of detailed geochemical studies of the shales that comprise parts of greenstone successions. Perhaps the thickest accumulations of well-preserved fine-grained sediments in the Zimbabwe Craton are exposed in the ~3.0 Ga Buhwa Greenstone Belt. Unlike other "greenstone" belts in Zimbabwe, Buhwa consists dominantly of sedimentary rocks and does not contain stratigraphic equivalents of the well-studied Lower and Upper Bulawayan groups (~2.9 and ~2.7 Ga, respectively) or the Shamvaian Group (~2.6 Ga; see Blenkinsop, in press). Based on lithology and available geochronology, it is suggested that the unique stratigraphy at Buhwa developed as a stable-shelf succession at or near the margin of the ~3.5 Ga Tokwe segment (Chapter 2), a roughly triangular crustal domain that consists of strongly banded tonalitic gneisses and relics of greenstone belts (Fig. 24; Wilson, 1990). A major goal of this paper is to characterize the composition of the source terrane for Buhwa sediments, to discuss source-area weathering conditions, and

Figure 24. Simplified geologic map showing the southern part of the Zimbabwe Craton, the Limpopo Belt, and the northern part of the Kaapvaal Craton. Greenstone belts in the Zimbabwe Craton: B - Buhwa, Be - Belingwe, Mw - Mweza, Ma - Masvingo. Inset map shows the southern horn of Africa and the regional geologic setting of the Zimbabwe and Kaapvaal Cratons and the Limpopo Belt. Redrawn from Rollinson and Blenkinsop (in press).

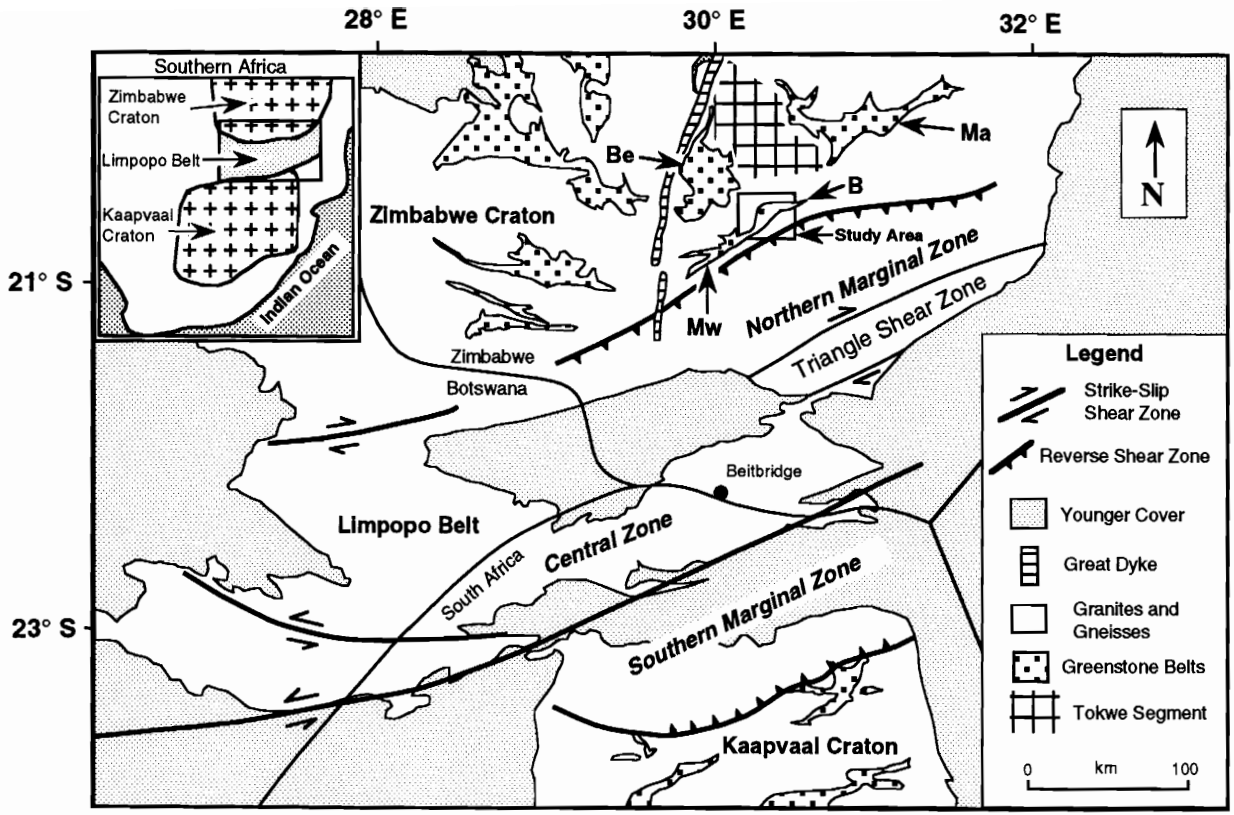
28° E
30° E
32° E
21° S
23° S
Southern Africa
Zimbabwe Craton
Limpopo Belt
Kaapvaal Craton
Indian Ocean
Zimbabwe Craton
Be
Ma
B
Study Area
Mw
Northern Marginal Zone
Triangle Shear Zone
N
Zimbabwe
Botswana
Beitbridge
Limpopo Belt
South Africa
Central Zone
Southern Marginal Zone
Kaapvaal Craton
Legend
Strike-Slip Shear Zone
Reverse Shear Zone
Younger Cover
Great Dyke
Granites and Gneisses
Greenstone Belts
Tokwe Segment
0
km
100

examine post-depositional compositional changes utilizing major-, trace-, and rare-earth element geochemistry.

Deposits of similar age and appearance to the sedimentary rocks in the Buhwa Greenstone Belt are exposed in the granulite-facies Central Zone of the Limpopo Belt (Taylor et al., 1986; Eriksson et al., 1988; Boryta and Condie, 1990) and on the low-grade Kaapvaal Craton in South Africa and Swaziland (West Rand Group of the Witwatersrand Supergroup, Wronkiewicz and Condie, 1987; Mozaan Group of the Pongola Supergroup, Wronkiewicz and Condie, 1989; Fig. 24). A comparison of the geochemical trends of all these units provides valuable information with regard to the composition and weathering of the upper crust in southern Africa at ~3.0 Ga.

GEOLOGIC SETTING

The Buhwa Greenstone Belt is located along the extreme southern margin of the Archean Zimbabwe Craton, where it is juxtaposed against the granulite-facies rocks of the Northern Marginal Zone of the Limpopo Belt (Fig. 25). Details of the structural assembly, metamorphism, and stratigraphy are found elsewhere (Chapter 3). The cover succession at Buhwa has been divided into shelf and basinal associations connected by a belt of transitional deposits (Chapter 2). The shelf association is ~4 km thick and consists of quartzarenite, interbedded quartzarenite and shale, shale, and iron-formation in ascending stratigraphic order (Fig. 26). This area has suffered greenschist facies metamorphism (Chapter 3). Most of the analyzed samples presented in this paper come from the lowest unit (Fig. 26; Q1B of Chapter 2). Transitional deposits, from which the remainder of the analyzed samples come, are dominated by green, tan, and locally black shale (now phyllite), with less abundant iron-formation and muddy sandstone. These lithologies represent more basinward

Figure 25. Geologic map of the Buhwa Greenstone belt and surrounding granite-gneiss terrane. Lithologic contacts modified from the mapping of Worst (1962). Note sample locality sites.

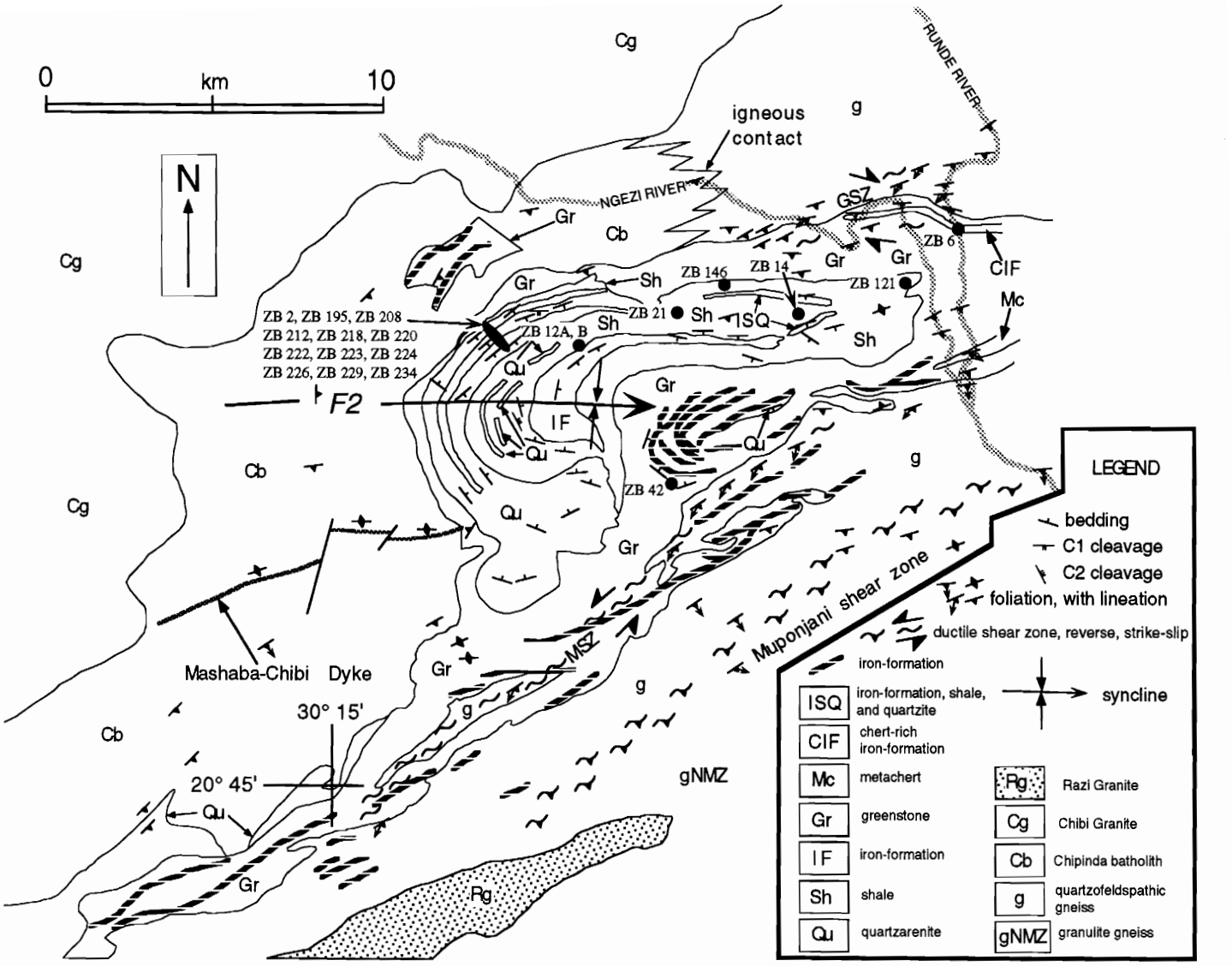
0
km
10
N
RUNDE RIVER
NGEZI RIVER
igneous contact
GSZ
ZB 6
CIF
Mc
ZB 146
ZB 14
ZB 121
ZB 21
ISQ
ZB 12A, B
ZB 2, ZB 195, ZB 208
ZB 212, ZB 218, ZB 220
ZB 222, ZB 223, ZB 224
ZB 226, ZB 229, ZB 234
F2
IF
ZB 42
Mashaba-Chibi Dyke
MSZ
Muponjani shear zone
30° 15'
20° 45'
gNMZ
Cg
Cb
Gr
Sh
Qu
g
Rg
LEGEND
bedding
C1 cleavage
C2 cleavage
foliation, with lineation
ductile shear zone, reverse, strike-slip
iron-formation
syncline
ISQ iron-formation, shale, and quartzite
CIF chert-rich iron-formation
Mc metachert
Gr greenstone
IF iron-formation
Sh shale
Qu quartzarenite
Rg Razi Granite
Cg Chibi Granite
Cb Chipinda batholith
g quartzofeldspathic gneiss
gNMZ granulite gneiss

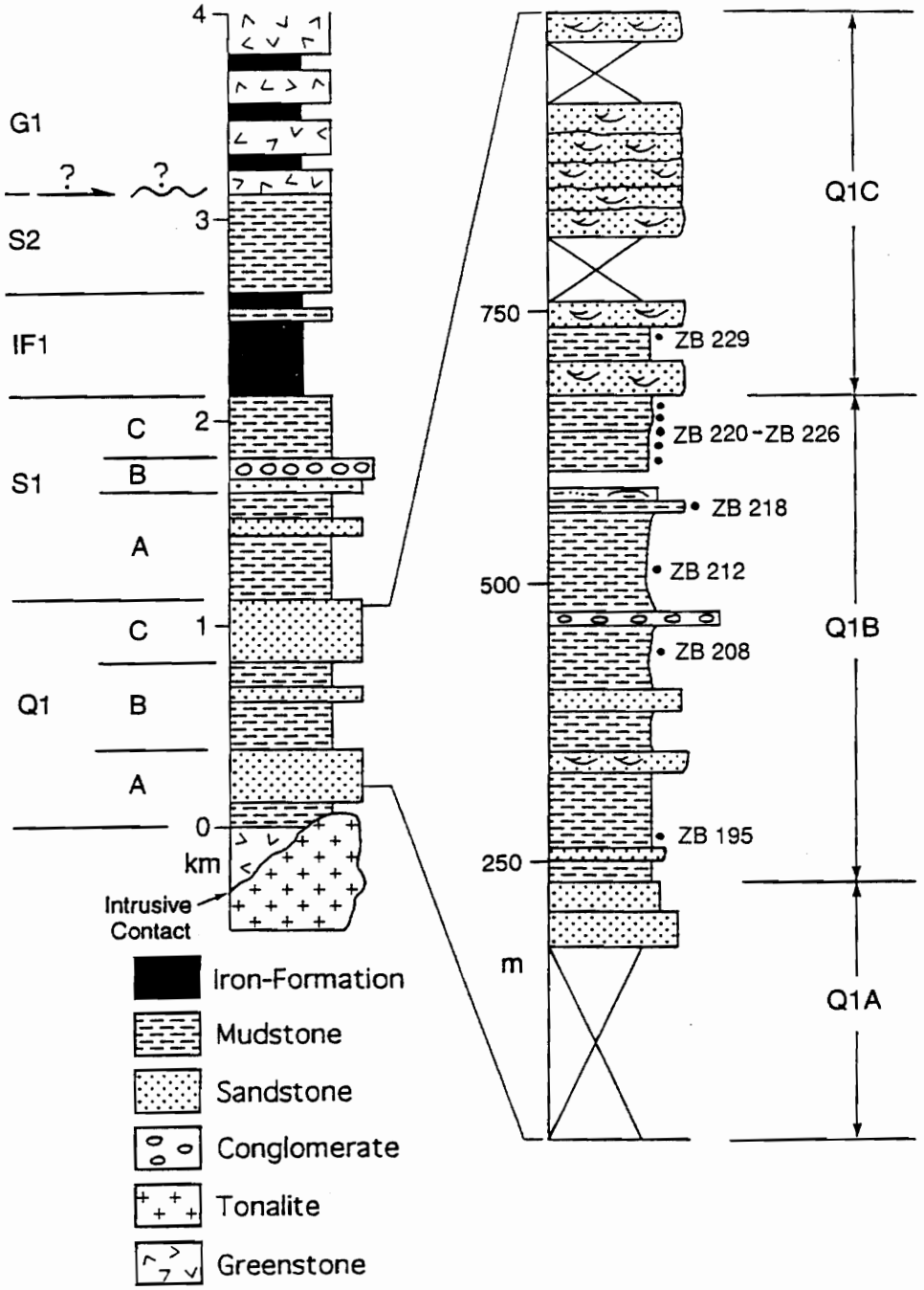

Figure 26. Lithologic column of the shelf association from just NW of the fold axis. Nature of the S2-G1 contact is uncertain. It may be a fault or an unconformity. Expanded column shows details of Q1 and the location of samples referred to in text.

lateral equivalents to the shelf association. The basinal association consists of metamorphosed mafic-ultramafic lavas (including spinifex-textured lava), possible carbonate, recrystallized metachert with intercalations of shale, and iron-formation. Metamorphic grade is at amphibolite facies at the margins of the greenstone belt.

Three major structures deform either part or all of the cover succession and surrounding granitoids at Buhwa: 1) a shear zone that bounds part of the northern margin of the BGB, 2) a shear zone that bounds the southern margin of the BGB, and 3) a regional-scale syncline that deforms the cover succession (Fig. 25; Chapter 3). Areally, both shear zones impart considerable ductile strain into the core of the basinal association. The fold is asymmetric in map view, with a short southern limb and a long northern limb. The fold axis plunges 28° towards 088°, with a nearly vertical axial surface. Younging directions in the quartzites and interbedded quartzites and shales are toward the axial surface of the fold, which indicates that it is a synformal syncline.

ANALYTICAL TECHNIQUES

Twenty samples of fine-grained rock were selected for geochemical analysis. Seventeen of the samples represent shales from the cover succession. Three of the samples (ZB 12A, ZB 12B, ZB 42) have a unique geochemistry suggesting they are not representative of the typical shale. Fresh samples of rock were collected in the field and split by hand to remove any surface staining. The samples were powdered to 200 mesh in an agate swing mill to avoid contamination. Fused-glass discs and pressed-powder discs were prepared for major-element and trace-element analysis, respectively, by X-Ray fluorescence at the Open University with an accuracy of within 10% for all elements (within 5% for most elements). Rare earth elements were

analyzed by isotope dilution at the University of Maryland on an NBS-type single-collector mass spectrometer. Analytical precision is routinely at 0.1%. A new analysis of REE concentration for SCo-1 by isotope dilution is presented here for future reference. REE normalizing factors are from the Leedy Chondrite in Masuda et al. (1973).

GEOCHEMISTRY

Major Elements

Major element concentrations are presented in Table 3. Samples ZB 12A and ZB 12B are chloritic phyllites interbedded with iron-formation and have especially low SiO_2 contents. The iron-formation hosts a major iron-ore deposit, which likely formed by hypogene processes (Chapter 5); corresponding SiO_2 contents are unusually low whereas $Fe_2O_3^t$ contents are unusually high (~30-40 wt. %). ZB 42, an amphibole schist, was analyzed to show variability between shales and metagreenstones. ZB 42 has a low SiO2 content (~49 wt. %) and high MgO (~23 wt. %), Cr (3086 ppm), and Ni (1220 ppm) contents consistent with a mafic volcanic source. These three samples will not be considered any further.

SiO_2 content ranges from ~55.6 % to 77.0% for the shales. As expected there is a negative correlation between SiO_2 and Al_2O_3 (correlation coefficient, r = -0.95), SiO_2 and K_2O (r = -0.90), and SiO_2 and TiO_2 (r = -0.73; Fig. 27). Na_2O, CaO, and P_2O_5 do not systematically vary with SiO_2. MgO and MnO show no correlation with SiO_2. K_2O (r = 0.94), TiO_2 (r = 0.80), Na_2O (r = 0.71, excluding one point), and MgO (r = 0.38) have strong or moderate positive correlations with Al_2O_3 suggesting that illite may have been present at the time of sedimentation (cf. Camiré et al., 1993). Such positive correlations indicate that weathering was an important factor in the source

Table 3. Major and trace element analyses of Buhwa Greenstone Belt shales.

Sample	ZB 2	ZB 6	ZB 12A	ZB 12B	ZB 14	ZB 21	ZB 42	ZB 121	ZB 146	ZB 195
SiO_2	61.07	64.69	39.48	40.45	55.62	69.01	49.37	68.28	70.30	77.00
TiO_2	0.545	0.538	0.606	0.852	0.765	0.226	0.292	0.564	0.571	0.388
Al_2O_3	18.55	18.75	11.374	17.43	21.91	11.42	6.82	14.057	13.58	11.12
$Fe_2O_3{}^t$	6.43	5.33	40.69	29.09	9.06	9.61	11.29	5.90	4.93	1.94
MnO	0.075	0.041	0.097	0.212	0.036	0.027	0.160	0.036	0.034	0.021
MgO	2.96	1.64	3.65	5.31	0.78	2.03	22.84	4.09	1.61	3.74
CaO	0.05	0.03	0.05	0.02	0.04	0.02	4.77	0.03	0.13	0.03
Na_2O	0.10	0.15	0.00	0.02	0.10	0.03	0.17	0.08	3.28	0.07
K_2O	5.75	5.43	0.05	0.22	5.84	4.11	0.01	3.59	3.01	2.58
P_2O_5	0.048	0.050	0.043	0.020	0.021	0.047	0.024	0.043	0.035	0.022
LOI	3.71	3.26	4.37	6.34	5.57	3.01	4.06	3.61	2.07	2.84
Total	99.72	99.91	100.41	99.96	99.74	99.54	99.81	100.28	99.55	99.75
Ba	394	877	15	37	254	615	9	305	833	461
Rb	154	117	4.5	7.3	163	205	0.3	84.4	66.4	37.9
Sr	9.4	25.8	1.5	3.7	7.9	6.9	0.5	7.1	35	6
Y	19.3	16	17.8	12.6	14.2	11.1	11.3	11.9	68.3	15
Zr	122	158	73	89	107	90	17	117	342	406
Nb	8.4	9.5	4.9	5.2	6	5.8	1.1	4.8	15.1	5.9
Th	13	15	5	6	6	9	1	8	18	16
Sc	16	14	13	31	40	8	21	24	8	5
V	112	96	248	298	255	40	155	138	56	35
Cr	276	360	1209	1783	720	97	3086	109	10	180
Co	14	14	64	88	15	6	70	22	12	8
Ni	88	97	271	482	70	118	1220	33	11	49
Cu	14	23	61	121	43	9	43	69	5	10
Zn	30	15	93	139	48	118	71	42	47	16
Ga	23	22	17	18	23	15	8	15	18	12
Cr/Th	21.2	24.0	241.8	297.2	120.0	10.8	3086.0	13.6	0.6	11.3
Co/Th	1.1	0.9	12.8	14.7	2.5	0.7	70.0	2.8	0.7	0.5
Th/Sc	0.8	1.1	0.4	0.2	0.2	1.1	0.05	0.3	2.3	3.2
Cr/Zr	2.3	2.3	16.6	20.0	6.7	1.1	181.5	0.9	0.03	0.4
Cr/V	2.5	3.8	4.9	6.0	2.8	2.4	19.9	0.8	0.2	5.1
moles:										
Al_2O_3	0.182	0.184	0.112	0.171	0.215	0.112	0.067	0.138	0.133	0.109
CaO	0.0009	0.0005	0.000	0.0003	0.0007	0.0004	0.003	0.0005	0.002	0.0005
Na_2O	0.002	0.002	0.000	0.0003	0.002	0.0005	0.003	0.001	0.053	0.001
K_2O	0.061	0.058	0.0005	0.002	0.062	0.044	0.0001	0.038	0.032	0.027
CIA	74	75	n.d.	n.d.	77	71	n.d.	78	60	79
CIW	98	99	n.d.	n.d.	99	99	n.d.	99	71	99

Major elements in wt. %; trace element concentrations in ppm; n.d., not determined; CIA=$[Al_2O_3/(Al_2O_3+CaO^*+Na_2O+K_2O)](100)$ in molecular proportions; CIW=$[Al_2O_3/(Al_2O_3+CaO^*+Na_2O)](100)$ in molecular proportions.

Table 3 . Continued.

Sample	ZB 208	ZB 212	ZB 218	ZB 220	ZB 222	ZB 223	ZB 224	ZB 226	ZB 229	ZB 234
SiO_2	57.99	60.03	59.68	61.37	58.67	56.56	59.73	57.98	67.62	53.97
TiO_2	0.622	0.604	0.640	0.597	0.686	0.624	0.611	0.620	0.619	0.715
Al_2O_3	21.99	20.57	22.58	19.81	22.50	23.26	20.52	22.67	16.98	27.24
$Fe_2O_3{}^t$	5.91	4.70	3.06	5.12	5.87	4.78	5.32	4.27	4.56	1.73
MnO	0.055	0.051	0.021	0.025	0.016	0.022	0.024	0.024	0.014	0.011
MgO	1.96	2.84	2.18	2.01	1.06	2.22	2.27	2.08	1.15	2.09
CaO	0.03	0.02	0.02	0.02	0.03	0.02	0.02	0.03	0.02	0.02
Na_2O	0.18	0.17	0.09	0.18	0.18	0.13	0.11	0.12	0.08	0.18
K_2O	6.26	6.51	7.69	6.26	6.07	7.78	7.13	7.47	5.09	9.38
P_2O_5	0.045	0.051	0.040	0.051	0.047	0.032	0.049	0.041	0.030	0.043
LOI	4.61	4.03	3.54	3.90	4.60	4.27	3.74	4.20	3.54	4.67
Total	99.65	99.58	99.90	99.34	99.73	99.70	99.52	99.50	99.70	99.55
Ba	588	580	506	562	534	586	526	538	446	801
Rb	153	174	162	202	97.3	180	201	218	112	169
Sr	10.3	10.6	12.6	17	14.7	17.6	18.5	19	9.1	15.8
Y	15.4	20.8	23.8	20.9	12.6	17.1	21	21.9	18.6	22.6
Zr	103	139	136	144	152	124	140	124	189	127
Nb	9.4	8.7	8.9	9.3	9.9	9.7	9.1	8.6	8.7	10.4
Th	13	13	14	13	17	17	16	16	12	19
Sc	20	16	18	16	19	18	15	14	10	20
V	136	113	119	117	144	132	120	130	90	142
Cr	343	280	272	287	435	309	287	293	237	331
Co	12	13	7	24	9	16	16	13	7	4
Ni	95	78	31	104	95	81	100	70	112	23
Cu	73	117	67	49	47	51	29	48	61	13
Zn	40	26	18	41	16	28	28	19	12	9
Ga	25	25	28	23	27	27	25	27	19	33
Cr/Th	26.4	21.5	19.4	22.1	25.6	18.2	17.9	18.3	19.8	17.4
Co/Th	0.9	1.0	0.5	1.8	0.5	0.9	1.0	0.8	0.6	0.2
Th/Sc	0.7	0.8	0.8	0.8	0.9	0.9	1.1	1.1	1.2	1.0
Cr/Zr	3.3	2.0	2.0	2.0	2.9	2.5	2.1	2.4	1.3	2.6
Cr/V	2.5	2.5	2.3	2.5	3.0	2.3	2.4	2.3	2.6	2.3
moles:										
Al_2O_3	0.216	0.202	0.221	0.194	0.221	0.228	0.201	0.222	0.167	0.267
CaO	0.0005	0.0004	0.0004	0.0004	0.0005	0.0004	0.0004	0.0005	0.0004	0.0004
Na_2O	0.003	0.003	0.002	0.003	0.003	0.002	0.002	0.002	0.001	0.003
K_2O	0.066	0.069	0.082	0.066	0.064	0.083	0.076	0.079	0.054	0.010
CIA	76	74	72	74	77	73	72	73	75	72
CIW	98	98	99	98	98	99	99	99	99	99

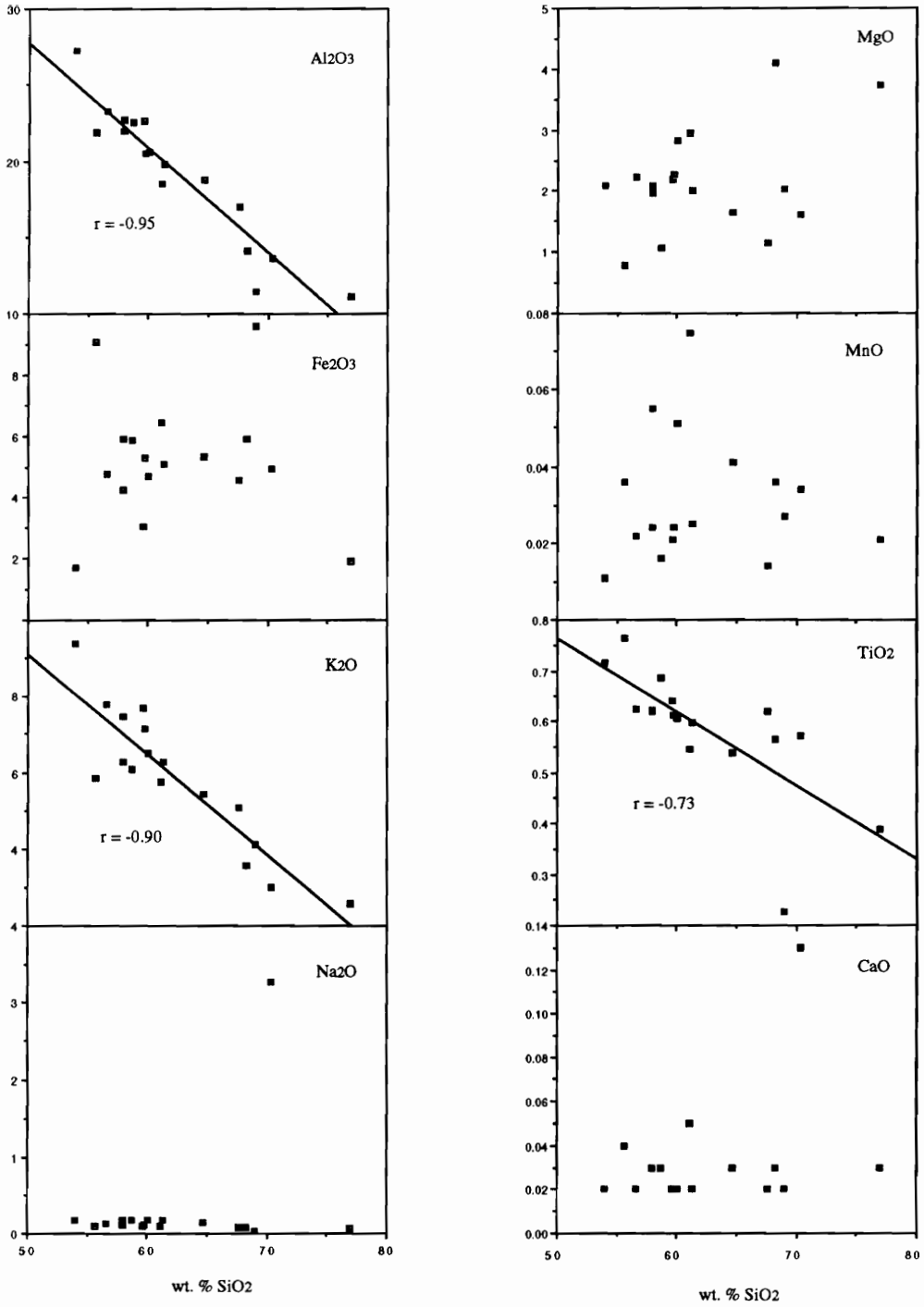

Figure 27. Major oxides (in wt.%) vs. SiO_2 for Buhwa shales, showing calculated regression lines where appropriate.

area, where K and Mg are fixed in clay minerals and Ca is preferentially leached (Nesbitt et al., 1980). Alternatively, these may have been more aluminous clays later enriched in K to form illite.

Large Ion Lithophile Elements

Concentrations of Rb, Sr, and Ba range from 37-218 ppm, 6-35 ppm, and 254-877 ppm, respectively (Table 3). Like potassium, Rb will be incorporated into clays during chemical weathering, in contrast to divalent Ca and Sr, which along with Na tend to be leached (Camiré et al., 1993). This relationship is demonstrated on the spidergram of Figure 28, which shows five samples of Buhwa shales normalized against average Archean upper crust (normalization values taken from Taylor and McLennan, 1985). CaO, Na_2O, and Sr are depleted between 2-3 orders of magnitude relative to average crust, whereas K_2O and Rb, and Ba are at average to above-average concentrations. This pattern is similar to pattern for shales from the Pongola and Witwatersrand Supergroups (Wronkiewicz and Condie, 1987, 1989).

Transition Metals

Feng and Kerrich (1989) noted that Cr, Co, Ni, and Ti-V behave similarly during magmatic processes, but cautioned that they could mutually fractionate during weathering. Similar to Archean shales worldwide, Buhwa shales have elevated Cr and Ni concentrations (averages: 284 ppm and 74 ppm, respectively; Fig. 29). Cr, V, and Sc are all positively correlated with Al_2O_3, suggesting that they are bound in clays and have been variably concentrated during weathering; Co and Ni show no relationship with aluminum. Although Cr may be mobile during weathering, Condie and Wronkiewicz (1990) demonstrated that the Cr/Th ratio can be a very sensitive

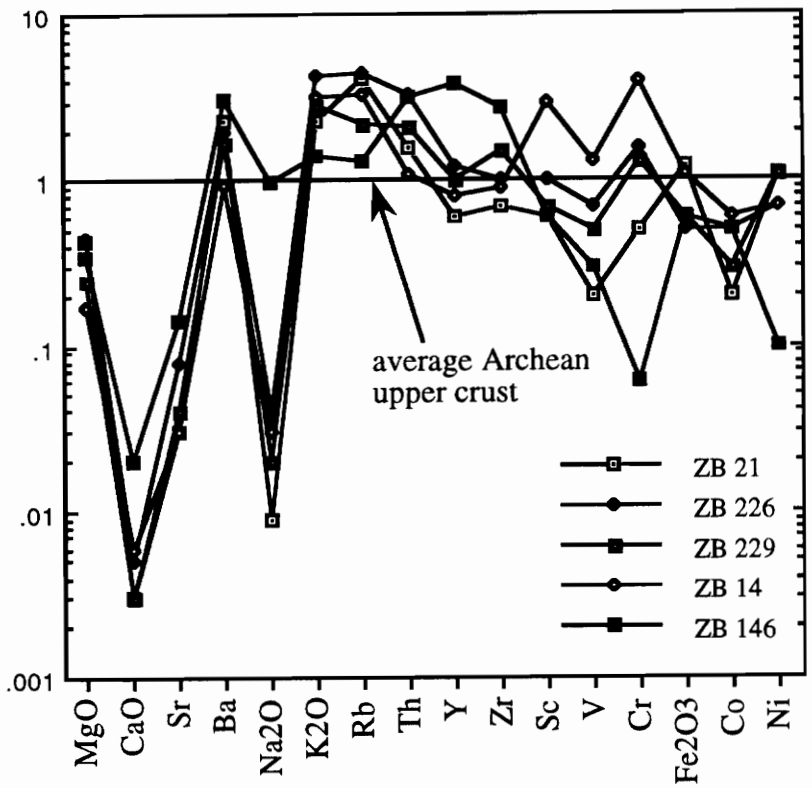

Figure 28. Spiderplot of selected samples of Buhwa shale normalized against average Archean upper crust (values from Taylor and McLennan, 1985). Note strong depletion of CaO, Na_2O, and Sr.

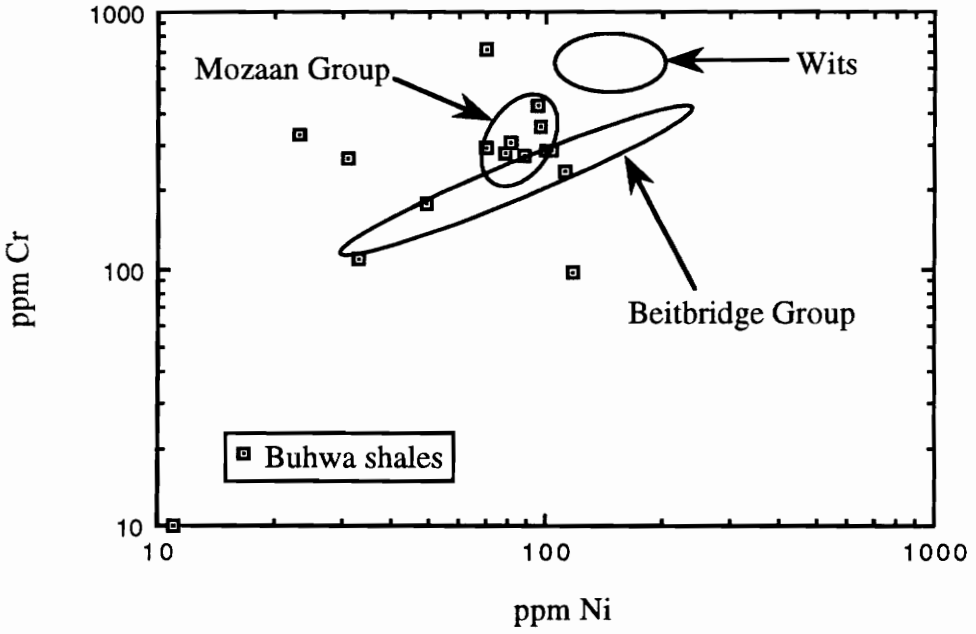

Figure 29. Distribution of Cr and Ni in Buhwa shales. Data for other fields from Condie and Wronkiewicz (1987; Witwatersrand Supergroup), Condie and Wronkiewicz (1989; Mozaan Group), and Taylor et al. (1986) and Boryta and Condie (1990) for Beitbridge Group. Same sources for all succeeding figures.

indicator of provenance. In general, the transition metals are similar to average upper crustal values (Fig. 28), and show minor negative V and positive Cr anomalies.

High Field Strength Elements

Feng and Kerrich (1990) noted that the elements Zr, Nb, Hf, Ta Y, Th, and U behave incompatibly during most igneous events. As a result, these elements are enriched in felsic rather than mafic rocks. Additionally, along with the rare earth elements (REE), these high field strength elements are thought to be immobile during most weathering processes (e.g. Taylor and McLennan, 1985). In Buhwa shales, Y and Zr have normalized values similar to average Archean upper crust, whereas Th, similar to Rb and K_2O, is slightly enriched (2-3 x; Fig. 28, Table 3). Only Zr displays any correlation with SiO2 ($r = 0.72$), suggesting that Zr resides in a more quartzose grain-size fraction where the Zr may be bound in small zircon crystals.

Rare Earth Elements (REE)

Ten shales were selected for REE analysis (Table 4). The features of the REE are somewhat variable but fall into three general trends based on curve shape and degree of europium anomaly (Fig. 30). The most common trend has a small negative Eu anomaly (average Eu/Eu* = 0.77) and some fractionation of the light-REE (LREE; Ce_N/Sm_N = 1.0-2.8, average = 2.2). The second trend is characterized by REE patterns with little or no Eu anomaly (Eu/Eu* = 0.95 and 0.96 for ZB 226 and ZB 229, respectively). These two samples show different fractionation trends in the LREE: ZB 226 shows a high degree of LREE fractionation ($Ce_N/Sm_N = 3.0$) similar to trend one samples, whereas ZB 229 is quite flat ($Ce_N/Sm_N = 1.2$), and has low overall REE cocentrations. The third trend is exemplified by a single sample, ZB 146. This pattern

Table 4. Rare Earth element analyses of Buhwa Greenstone Belt shale.

Sample	ZB 6	ZB 21	ZB 121	ZB 146	ZB 195	ZB 212	ZB 223	ZB 226	ZB 229	ZB 234	SCo-1
Ce	31.6	24.9	17.4	65.6	39.3	18.6	15.6	39	10.8	58.6	55.1
Nd	n.d	n.d	n.d	n.d	n.d.	n.d.	n.d.	n.d.	n.d.	n.d.	n.d.
Sm	3.4	2.1	1.7	10.7	3.53	4.4	1.6	39	2.1	5.42	5.02
Eu	0.8	0.5	0.4	2.0	0.71	1.0	0.49	1.0	n.d.	1.26	1.12
Gd	3.1	1.9	1.5	n.d.	n.d.	3.93	2.2	3.2	2.3	4.6	4.5
Dy	3.2	1.6	2.0	11.3	2.5	3.25	2.7	3.52	n.d	3.9	4.0
Er	1.9	1.0	1.3	7.3	1.7	2.1	1.9	2.3	1.9	2.3	2.4
Yb	2.0	1.1	1.4	7.1	2.0	2.2	n.d	n.d.	2.1	2.1	2.3
Ce_N/Sm_N	2.2	2.8	2.5	1.4	2.6	1.0	2.1	3.0	1.2	2.6	2.6
Gd_N/Yb_N	1.2	1.4	0.87	1.3	n.d.	1.5	0.8	1.2	0.9	1.7	1.5
Ce_N/Yb_N	4.0	5.7	3.2	2.4	4.9	2.2	1.8	4.5	1.3	7.1	6.0
Eu/Eu*	0.79	0.78	0.75	0.57	n.d.	0.76	0.79	0.95	0.96	0.77	0.72

REE concentrations in ppm; n.d., not determined; $Eu/Eu^* = Eu_N/[(Sm_N)(Gd_N)]^{0.5}$

Figure 30. Rare earth element plots for Buhwa shales. A) Trend 1: Fractionated LREE and slight negative Eu anomaly; B) Trend 2: No Eu anomaly; C) Trend 3: Fractionated LREE and significant negative Eu anomaly.

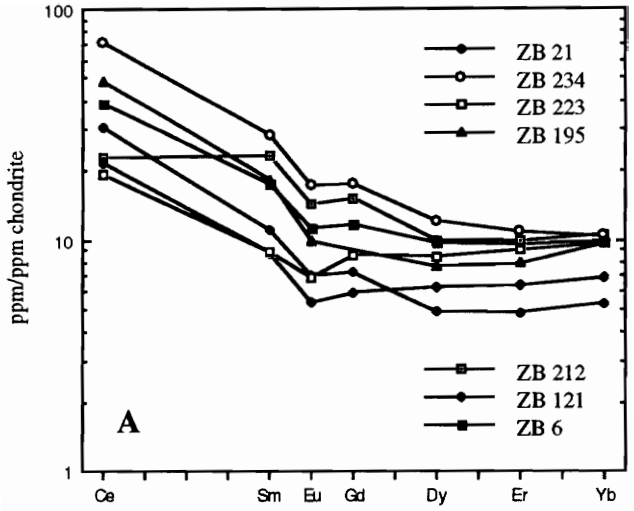
100
10
1
ppm/ppm chondrite
ZB 21
ZB 234
ZB 223
ZB 195
ZB 212
ZB 121
ZB 6
A
Ce
Sm
Eu
Gd
Dy
Er
Yb

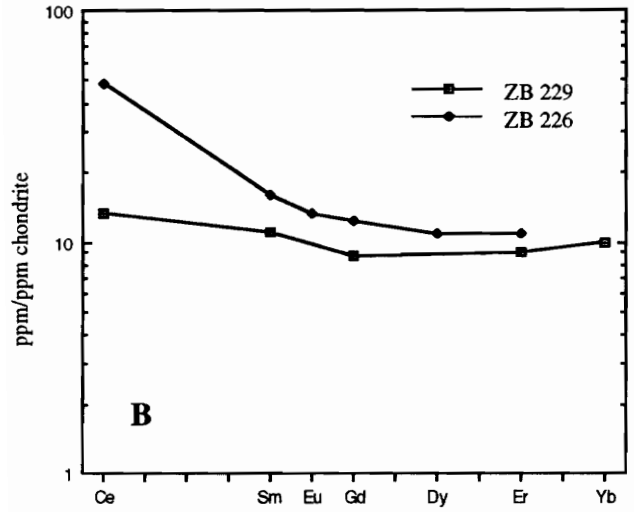
100
10
1
ppm/ppm chondrite
ZB 229
ZB 226
B
Ce
Sm
Eu
Gd
Dy
Er
Yb

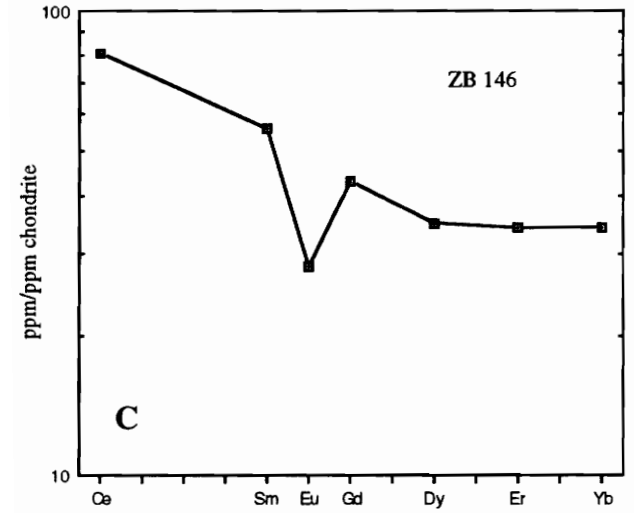
100
10
ppm/ppm chondrite
ZB 146
C
Ce
Sm
Eu
Gd
Dy
Er
Yb

is fractionated in the LREE (Ce_N/Sm_N = 1.5), but unlike other samples fractionated in the LREE, has a prominent negative Eu anomaly (Eu/Eu* = 0.57). Overall REE abundances are significantly higher than in all other samples analyzed. ZB 146 is geochemically unique in all other trace and major element concentrations as well (Table 3).

The heavy-REE (HREE) in all three trends are not strongly fractionated from each other (Gd_N/Yb_N = 0.87-1.7, average = 1.3; Fig. 30), but have both positive and negative slopes. Those samples with positive slopes show Yb enrichment of several times chondrite relative to the other HREE (e.g. ZB 195, ZB 21, ZB 223).

ROLE OF METAMORPHISM

Although most of the shales examined in this study come from the low-grade fold-closure region (Fig. 25), several samples (e.g. ZB 121, ZB 6) come from more eastern areas where metamorphic grade increases (Chapter 3). In these samples, major-, trace-, and rare earth-element concentrations do not show significant variation suggesting that metamorphism did not greatly affect composition. This observation is consistent with other studies of metamorphosed shales ranging from greenschist to amphibolite facies (e.g. Condie and Martell, 1983) and at granulite facies in the Limpopo Belt (Taylor et al., 1986).

PROVENANCE

Source-Area Composition

Numerous factors including source-area composition, source-area weathering conditions, hydraulic sorting, adsorption, diagenesis, and metamorphism will affect the composition of shales. As a result, only the elements least likely to be mobilized

during secondary processes yield reliable insights into the composition of the source area. Taylor and McLennan (1985) and McLennan and Taylor (1991) have suggested that the REE, Th, Sc and the high field strength elements are especially useful elements for monitoring source-area composition. These elements have very short residence times in the water column, and thus are transferred almost quantitatively into the sedimentary record. Additionally, this array includes both incompatible to compatible elements, whose ratios are useful for differentiating out felsic from mafic source components.

Most of the samples analyzed for trace- and rare-earth elements in this study come from a stratigraphic interval between or interbedded with thick accumulations of cross-bedded quartzarenite (Fig. 26). Based on extreme mineralogic maturity and a stable heavy-mineral population dominated by zircon, this succession is consistent with having a felsic plutonic source. However, quartz enrichment may have been due to extreme weathering conditions (see below), and thus, shale geochemistry may add critical information on the source-area composition.

The majority of samples plot as a single group on all trace element discrimination diagrams indicating that a single source provided most of the detritus to the Buhwa shelf. Figure 31 plots six incompatible/compatible trace element ratios against average rock compositions. These ratios were selected because they represent the most fractionation between different lithologies (see Condie and Wronkiewicz, 1990). Lines joining different rock types are arbitrarily drawn. As can be seen, averaged Buhwa shale compositions lie in a field similar to tonalite in composition, however, it must be stressed that the lines connecting rock types could represent mixing lines, such that the shales could represent a homogenization of different sources. Also plotted on Figure 31 are points representing average Archean upper crust. These

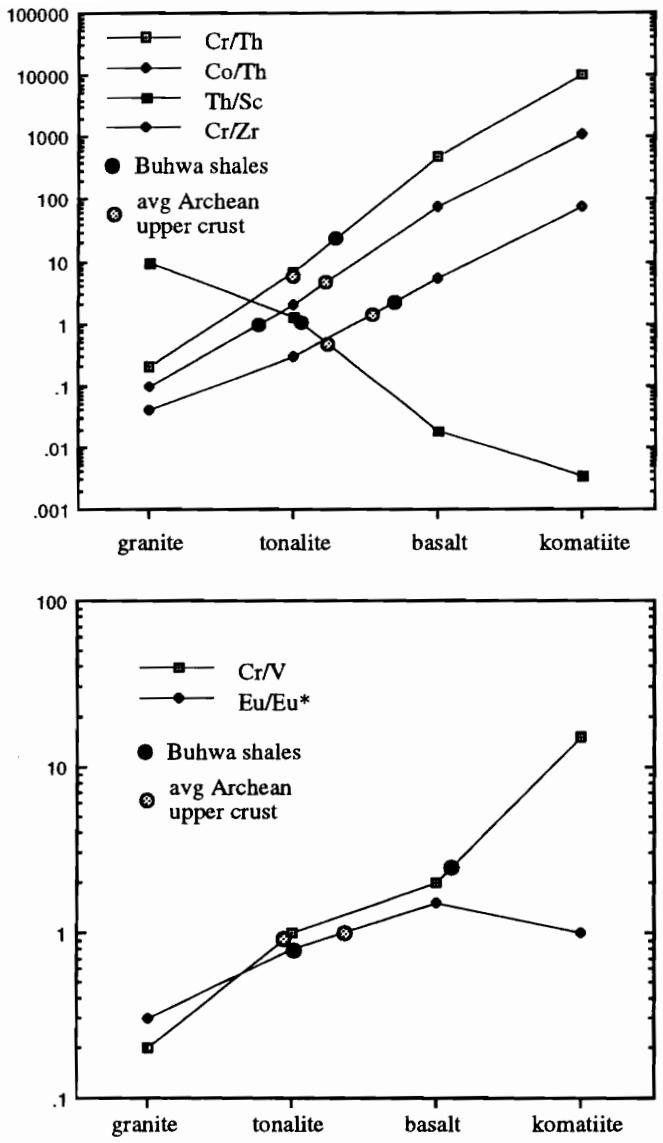

Figure 31. Plots of compatible/incompatible trace-element ratios for Buhwa shales compared against values for average Archean upper crust.

values were assembled by Taylor and McLennan (1985) from greenstone turbidite sequences from different Archean cratons. It is apparent that the two strongly overlap, which is consistent with Buhwa shelf sediments being derived from typical Archean upper crust. By comparison with the North American shale composite (NASC), average Archean upper crust is more mafic, but there is significant overlap.

McLennan and Taylor (1991) suggested that the Th/Sc ratio best reflects the overall bulk composition of the provenance. Figure 32 shows Th/Sc ratio plotted against concentration of Sc for Buhwa shales. The array of Buhwa samples clearly falls outside the well defined clustering of Archean samples as recognized in McLennan and Taylor (1991), and more closely represents the pattern for Phanerozoic or Recent sediments.

Six of nine REE patterns are very similar showing some LREE fractionation and a slight negative Eu anomaly. The presence of an Eu anomaly is traditionally regarded as evidence for a differentiated source (i.e. granite), and it is possible that these patterns represent such a source. However as noted by Condie and Wronkiewicz (1990) in their compilation of Archean igneous rock comppositions, granites have Eu anomalies of ~0.3, whereas tonalites have Eu anomalies of ~0.8. McLennan and Taylor (1991) recognized that shales derived from "cratonic" settings have Eu anomalies ranging from 0.60-0.70. The occurrence of Yb enrichment in some samples is also consistent with a tonalitic source (e.g. Arth and Hanson, 1975)

Although the collection of analyzed samples typically plot as a single group, several samples have a unique geochemistry that need consideration. ZB 14, a black shale, is noticably enriched in absolute abundances of V and Cr with respect to other samples, despite having a simlar Cr/V ratio (Table 3). McLennan et al. (in press) noted that black shales from the Early Proterozoic in the southwestern United States

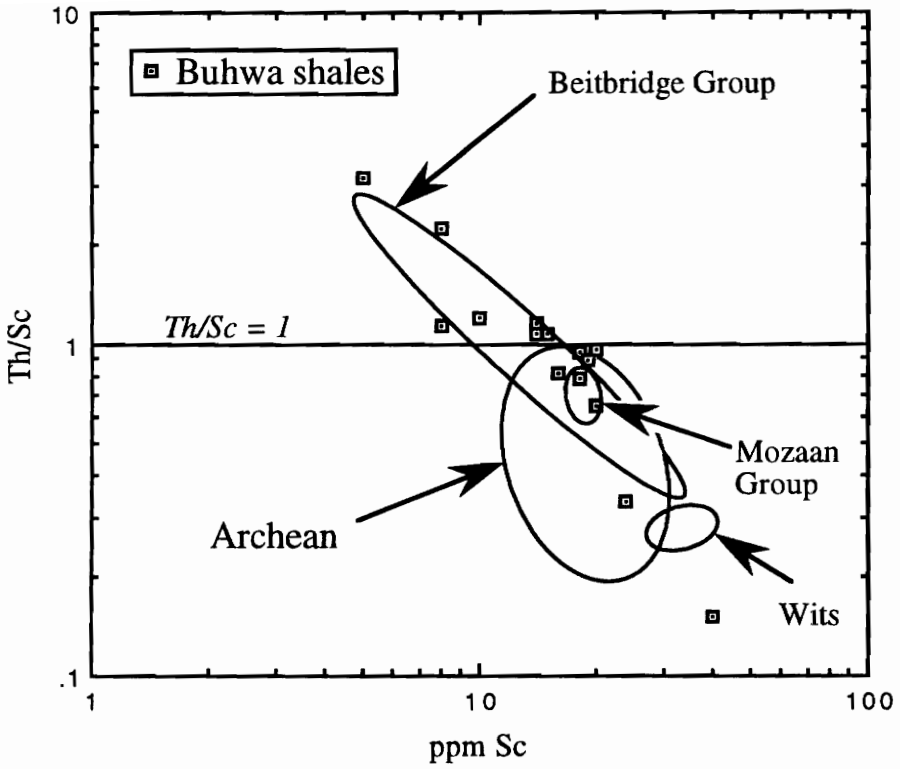

Figure 32. Distribution of Th/Sc vs. Sc for Buhwa shales. Archean field from McLennan and Taylor (1991).

possess several characteristic trace-element variations from typical shales including V enrichment and REE depletion. Chromium may be susceptible to the effects of weathering (Condie and Wronkiewicz, 1990), thus the enrichment in ZB 14 relative to all other samples may be entirely a secondary effect. Given these considerations, ZB 14 adds little to the understanding of provenance.

Another distinct sample is ZB 146, which has a unique REE pattern as mentioned above, as well as unique major- and trace-element concentrations. CaO, Na_2O, Sr, Y, Zr, Nb, and Ba are all significantly enriched, whereas Sc, V, Cr, and Ni are noticeably depleted (Table 3). The enrichment of incompatible elements and depletion of compatible elements favors a felsic source, which is consistent with the REE pattern. Because Eu will substitute for Sr in plagioclase, strong negative Eu anomalies in shales result from sources that underwent intracrustal differentiation processes yielding K-rich granites (Taylor and McLennan, 1985; McLennan and Taylor, 1991). Thus a component of the source terrane consisted of granite or its volcanic equivalent.

Samples ZB 226 and ZB 229 also have unique REE patterns with respect to the main population of Buhwa shales. They are both characterized by having no Eu anomaly. The LREE fractionated pattern in ZB 226 is quite typical of Archean shales worldwide, and probably represents the mixing of undifferentiated felsic and mafic end members (Taylor and McLennan, 1985). In contrast, the low overall abundance of REE and generally flat shape to the REE pattern in ZB 229 is indicative of a mafic volcanic source, a much less common, but persistent, characteristic of many Archean cratonic settings (McLennan and Taylor, 1984, 1991; Taylor et al., 1986).

The preservation of well-defined individual sources within "cratonic" shales is an interesting problem, because of the effeciency of sedimentary reworking in platformal settings. McLennan and Taylor (1991) noted that cratonic sediments from different

Archean cratons show this geochemical diversity and speculated that homogenization was less significant. That sediment-working and -spreading processes on Archean shelves should be no different than on modern shelves, suggests that individual source lithologies occupied large areas, such that homogenization with other rock types was minimal.

Source-Area Location

An early Archean fragment of continental crust within the Zimbabwe Craton that consists of strongly banded gneiss, granite, tonalite, and greenstone-belt relics and termed the Tokwe segment (Wilson, 1990) is a tenable source terrane for Buhwa Greenstone Belt detritus. The age of this continental nucleus is poorly constrained between ~3.09-3.5 Ga (Taylor et al., 1991), and is consistent with the spread of ages for detrital zircons (3.09-3.81 Ga, Dodson et al., 1988) recovered from quartzarenite (Q1 from Chapter 2) in the Buhwa cover succession. Although no direct correlatives of the Tokwe segment are in contact with the cover succession at Buhwa, Tokwe segment outcrops are found only ~30 km to the north (Fig. 24).

The geochemistry and petrogenesis of the Tokwe segment and younger (~2.9 Ga) tonalites and granites were examined in detail by Luais and Hawkesworth (1994). They defined three groups of rocks based on geochemical considerations, of which samples of Tokwe segment form part of all three groups. One important consideration of their work is that rocks loosely referred to as "tonalite" actually represent granite, trondjhemite, and tonalite in a strict sense (Luais and Hawkesworth, 1994). This is relevant to the Buhwa shale geochemistry because the geochemical diversity in the shales indicates that there is more than just a "tonalite" source.

Several of the elemental characteristics of the Buhwa shales overlap enough with Tokwe segment gneisses to suggest that the Tokwe segment could represent the source terrane for Buhwa sediments, but with a mafic component. Two of the three groups defined by Luais and Hawkesworth (1994) show variable REE patterns including samples with no Eu anomalies and others have slightly negative Eu anomalies. Some other trace-element characteristics, such as Cr/Th are not strongly separated between the two groups. Such characteristics are quite similar to the Buhwa shales. The third group of Luais and Hawkesworth (1994) shows the geochemistry of granite, with very low Cr/Th ratios and a strong negative Eu anomaly. These characteristics are very similar to ZB 146. These correlations coupled with the occurrence of ~3.5 Ga greenstones in the Tokwe segment suggest that the lithologic and geochemical diversity within the segment fall within the range of Buhwa shale compositions and could be the source terrane.

SOURCE-AREA WEATHERING

The variable effects of chemical weathering have important effects on the composition of the alkali and alkaline earth elements in siliciclastic rocks, where larger cations (e.g. Rb, Ba), remain fixed in the weathered residue, in preference to smaller cations (Na, Ca, Sr), which are selectively leached (Nesbitt et al., 1980). These chemical trends may be transferred to the sedimentary record (e.g. Nesbitt and Young, 1982; Wronkiewicz and Condie, 1987), and thus provide a useful tool for monitoring source-area weathering conditions.

Nesbitt and Young (1982) defined a chemical index of alteration (CIA) to quantitatively measure the degree of weathering (in molecular proportions), where

CaO* represents the Ca in the silicate fraction only (see McLennan, 1993 for corrections):

$$CIA = [Al2O3/(Al2O3 + CaO^* + Na2O + K2O)]\ 100$$

CIA values for average shales range from 70-75 (of a possibe 100), which reflects the compositions of muscovites and illites. Intensely weathered rock yields mineral compositions trending towards kaolinite or gibbsite and a corresponding CIA of ~100. The vertical dimension on such plots corresponds with values of CIA. CIA values for Buhwa shales range from ~70-~80 with an average of 76 (Table 3; Figure 33A).

Figure 33A plots the data for Buhwa shales on an A - CN - K ternary diagram (in molecular proportions), which is useful for depicting weathering trends of different source rocks (Nesbitt and Young, 1984, 1989). Also shown on the diagram is the positions of idealized minerals, post-Archean Australian Average Shale (PAAS), and average Archean upper crust and a line showing the limit of weathering, to the right of which indicates K enrichment. The long dashed lines with arrows show the weathering trends for tonalite and granite (from Nesbitt and Young, 1989).

The majority of Buhwa shales (except for ZB 146) plot almost on the aluminum - potassium join (1-2 % $CaO^* + Na_2O$) in a position consistent with derivation from highly weathered granite. However, based on immmobile (or less mobile) trace-element constraints, the source is thought to be more tonalitic in nature, with less common occurrences of strict granite. If the interpretation of a tonalite-dominated source is correct, the major element data indicate that there has been significant K enrichment. This is supported by the numerous points that plot to the right of the "limit of weathering" line. We suggest, therefore, that Buhwa shales followed the

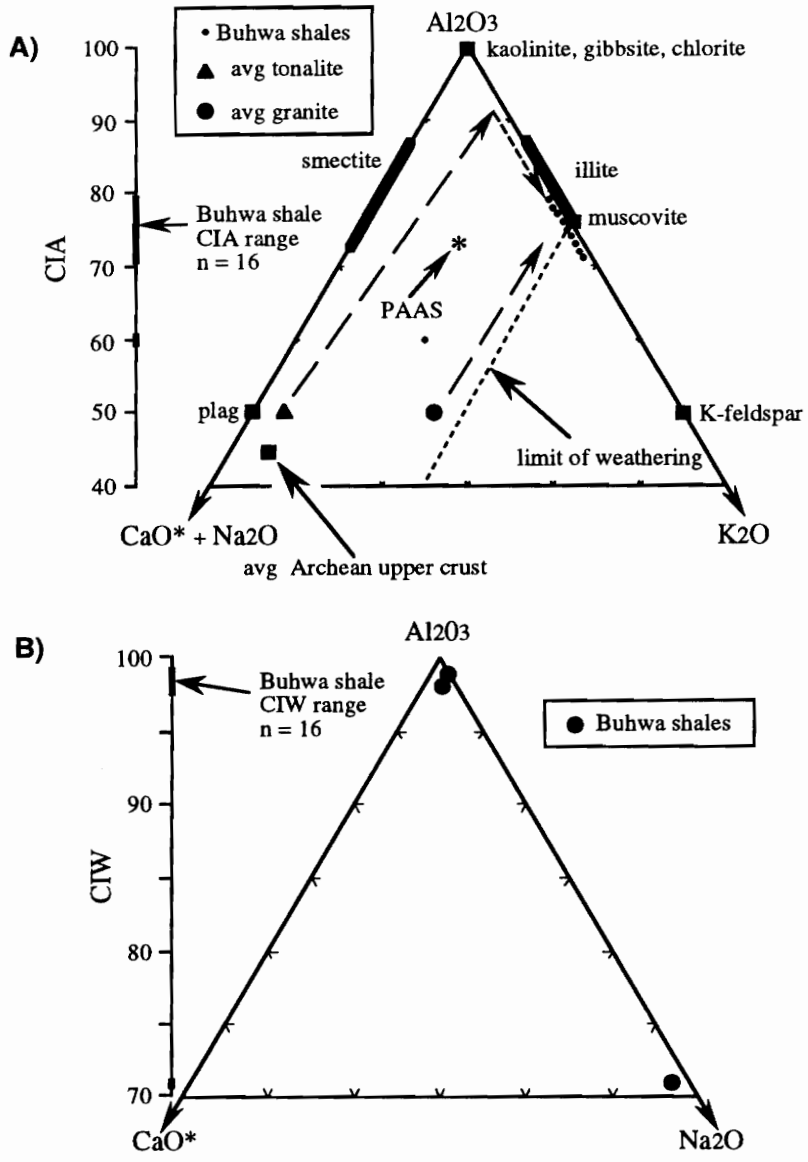

Figure 33. A) A-CN-K diagram for Buhwa shales (in molecular proportions). Note how enrichment of potassium lowers average CIA value. B) A-C-N diagram for Buhwa shales. Note the high average CIW values indicative of intense chemical weathering.

weathering path for tonalite (the spread amongst the data coincides with sources other than strict tonalite) until it nearly reached complete loss of Ca and Na. At some later time, the samples were significantly enriched in K following the short dashed line towards the K pole on the diagram. The exact composition prior to K enrichment cannot be established.

This interpretation has significant bearing on the use of CIA values *alone* as indicators of weathering. Buhwa shales have slightly "above" average CIAs, which would suggest average weathering conditions, but the CIA values of the Buhwa shales have been modified by processes that occurred after source-area weathering and transport. Harnois (1988) proposed a different quantitative weathering index termed the chemical index of weatherng (CIW). This index is identical to the CIA except that it eliminates use of K as a factor in the equation, because the behavior of K can be somewhat variable (Harnois, 1988). Because late K enrichment at Buhwa can be demonstrated, CIW values are calculated for Buhwa shales (Fig. 33B; Table 3); these show significant differences with respect to CIA. The average CIW for Buhwa shales is ~98, which represents a value consistent with intense chemical weathering. Intense chemical weathering is also suggested by the depletion of Ca, Na, and Sr on the spiderplot of Figure 28, which is normalized against average Archean upper crust. On a plot of Al_2O_3 versus Na_2O, Buhwa shales define a field representative of chemical weathering beyond that for Amazon cone muds (Fig. 34). Intense chemical weathering conditons might have been common in the Archean with pCO_2 concentrations at ~10^2 that of present atmospheric levels (Kasting, 1993).

Timing and processes associated with K enrichment at Buhwa are poorly understood. Wronkiewicz and Condie (1989) appealed to the diagenetic breakdown of feldspar or K-rich clays lower in the Pongola Supergroup sedimentary pile with

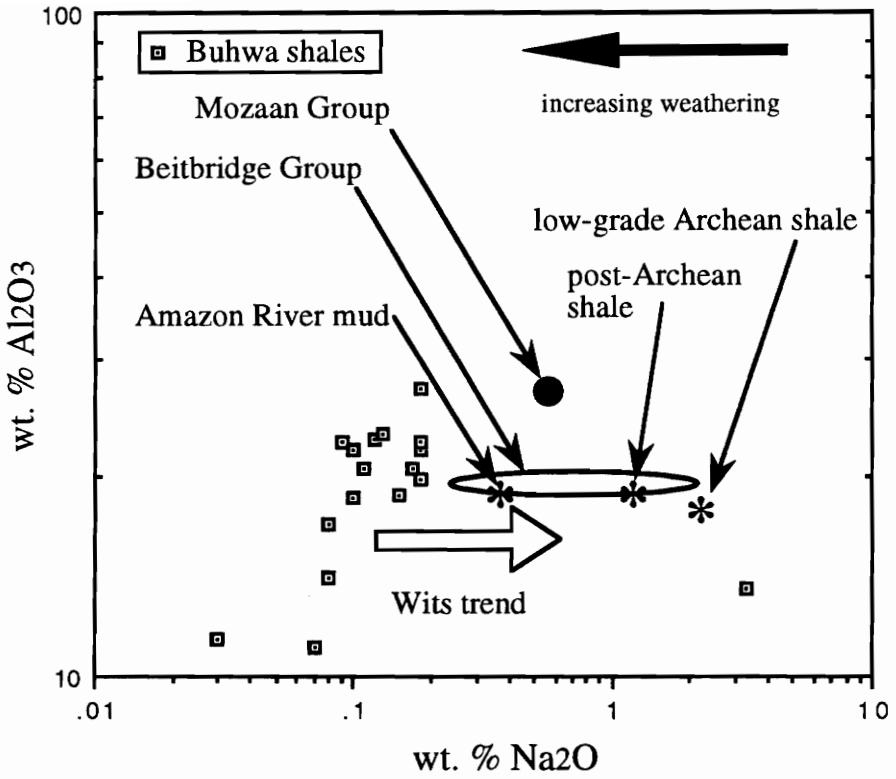

Figure 34. Plot of Al_2O_3 vs. Na_2O for Buhwa shales. Values for Amazon river mud, post-Archean shale, and low-grade Archean shale from Taylor et al (1986).

upward migration of K-rich fluids. This mechanism seems unlikely at Buhwa because 1) there is no textural evidence in thin sections that feldspars were present then dissolved away, and 2) if the CIW values for Buhwa shales are valid, much of the feldspar in the source would have been converted to clays prior to deposition and burial. Although our sampling array only covers ~600 m of vertical section, there is no correlation between K_2O concentrations and stratigraphic height as might be expected if upwardly mobile K-rich fluids passed through the succession.

The two suites of K-rich granites that intude both north and south of the Buhwa Greenstone Belt are potentially attractive sources for K enrichment (Fig. 25). Elsewhere at Buhwa, K-rich pegmatites that intrude the cover succession add noticeable amounts of microcline to metachert layers. Micas and clays, which control the distribution of K in Buhwa shales ($r = 0.94$ for Al_203 and K_2O), presently define a strong axial planar cleavage (Chapter 3) in the major, map-scale F2 fold (Fig. 25). Cross-cutting relationships and partly sheared plutons suggest that the Razi Granite (south of Buhwa), which is dated at 2627 ± 7 Ma, was intruded syntectonically with uplift of the Northern Marginal Zone of the Limpopo Belt (Mkweli et al., in press). The Chibi Granite (north of Buhwa) intruded at ~2.6 Ga (Hickman, 1978; Hawkesworth et al., 1979). Garnet-matrix relationships in Buhwa greenstones indicate that metamorphism and tectonism overlapped in the area, leaving the suggestion that the micas, which define an axial planar cleavage, could have acquired their compositions during intrusion and folding, an interpretation which satisfies all geologic observations. It is, however, possible that K enrichment could have post-dated folding in a metasomatic event for which a K source is not so obvious.

OTHER ARCHEAN STABLE-SHELF DEPOSITS IN SOUTHERN AFRICA

There are several stable-shelf successions deposited between ~2.9 -3.1 Ga in southern Africa that may be time correlatives with the Buhwa shelf, including the lower part of the Witwatersrand Supergroup (Wronkiewicz and Condie, 1987) and the Mozaan Group (Wronkiewicz and Condie, 1989) on the Kaapvaal Craton, and the Beitbridge Group within the granulite-facies Central Zone of the Limpopo Belt (Taylor et al., 1986; Boryta and Condie, 1990). It is useful to compare the geochemistry of these deposits with the Buhwa shelf in order to assess regional source-area conditions.

Most figures in this paper show average points or fields representing these different stable-shelf deposits along with the Buhwa shale data for comparison. In general, source terrane compositions based on trace-element and REE patterns suggest that there is not significant compositional changes between the different sources. For example, the spread of Buhwa shale data for Th/Sc versus ppm Sc is atypical of Archean turbidite deposits (cf. McLennan and Taylor, 1991); however when plotted with all other shelf muds from southern Africa, a single field is defined (Fig. 32). This is especially true for the Bietbridge Group pelites, which almost identically overlap with the Buhwa shales. Although the field is restricted, average Mozaan pelites plot within the main cluster Buhwa data, whereas Witwatersrand pelites appear to have a relatively more mafic source.

The scatter is similar for ppm Cr plotted against ppm Ni (Fig. 29). The main cluster of Buhwa samples strongly overlaps with Mozaan pelites, which have less Cr than the Witwatersrand samples. Beitbridge Group samples show more scatter than the other successions, but still form a single continuous field. Buhwa shale samples plot in a position intermediate between the fields for Early and Late Archean (Taylor

and McLennan, 1985), which is consistent with the mixing of differentiated and mafic undifferentiated sources for Buhwa shales.

REE patterns for Buhwa shales indicate that several rock types provided detritus to the basin. This is quite similar to the findings of Taylor et al. (1986) for Beitbridge Group pelites, which show REE patterns indicative of well-differentiated, less well-differentiated, and mafic volcanic sources. Witwatersrand and Mozaan pelites have REE patterns similar to the main trend of Buhwa samples, having fractionated LREE, slight negative Eu anomalies, and generally flat HREE (Wronkiewicz and Condie, 1987, 1989). It seems that sediment homogenization on these shelves was comparatively better so that less variable REE patterns resulted.

Weathering conditions between the different areas are compared on Figure 34. A distinctive characteristic about the different trends is that the main cluster of Buhwa samples was derived from a more highly weathered source terrane, although the Mozaan and Witwatersrand samples similarly indicate intense chemical weathering. This is also born out in the CIW values. CIA values are not compared because post-weathering K mobility has differentially effected the varying shelf deposits. The average CIW for Buhwa shales is ~98. Mozaan pelites have CIW values that range from 94-97, and Witwatersrand samples range from 90-97 (calculated from data of Wrokiewicz and Condie, 1987, 1989). All data generally points toward fairly intense chemical weathering conditions and tectonic stability in southern Africa during this time.

Beitbride Group CIWs vary significantly. The low-Al group of Boryta and Condie (1990) has an average CIW of 65, whereas the average CIW for the high-Al group is 96. The average CIW for the Beitbridge Group samples of Taylor et al. (1986) is 82 with a range of 67-91. This high degree of scatter represents either original variability

in weathering conditions not recorded in the other shelf deposits in southern Africa, or, more likely, major-element mobility during granulite-facies metamorphism.

CONCLUSIONS

Sedimentary features of the cover succession of the Buhwa Greenstone Belt, Zimbabwe are consistent with a stable-shelf origin for at least the western part of the belt. Major-, trace-, and rare earth-element analyses of a suite of shales interbedded with quartzarenites yield several conclusions with regard to local and regional geochemical trends, source-area composition, and source-area weathering conditions:

1) Of the major elements, CaO and Na_2O are significantly depleted with regard to average Archean upper crust. By contrast, K_2O is somewhat enriched. Sr behaves similarly to Ca and Na, whereas Ba and Rb more closely follow K. The high field strength elements and transition metals generally have average Archean concentrations, with two exceptions: one sample, a black shale, is strongly enriched in Cr and Sc, and another sample is depleted in Cr and enriched in the high field strength elements. Most samples analyzed for rare earth elements show LREE fractionation, a small negative Eu anomaly (average Eu/Eu* = 0.77), and generally flat HREE. One sample has a pronounced negative Eu anomaly, fractionated LREE, and larger ΣREE than the other samples. Another sample has a flat REE pattern with low REE abundances.

2) Based on immobile trace-element ratios and REE patterns, the source area is believed to consist of tonalite, granite, and mafic volcanic rocks. Such an array of rock types is found as an early Archean continental nucleus just north of Buhwa,

termed the Tokwe segment. Geochemical characteristics of the granite-tonalite suite in the Tokwe segment are comparable, given some sediment homogenization, with the Buhwa samples.

3) Intense chemical weathering of the source area is indicated by an average chemical index of weathering (CIW) value of 98, nearly complete removal of CaO and Na_2O, and high Al_2O_3/Na_2O ratios. A more conventional weathering index, the chemical index of alteration (CIA), is less useful in this study because late K-enrichment has affected the shale composition, which has spuriously modified CIA values.

4) Fine-grained sediments of comparable age and paleotectonic setting occur at several other places in southern Africa, including the Beitbridge Group in the granulite-facies Central Zone of the Limpopo Belt, and the lower part of the Witwatersrand Supergroup and Mozaan Group in the low-grade Kaapvaal Craton. Source terranes for these different stable-shelf deposits vary somewhat, but all together define a single field that consists of typical Archean upper crust. Source-area weathering conditions for appear to be intense for all the deposits (except for the Beitbridge Group whose major-element chemistry was modified by metamorphism), suggesting that tectonic stability and a hostile chemical environment prevailed over southern Africa at ~3.0 Ga.

CHAPTER 5

Geologic setting and ideas concerning the origin of the iron-ore deposits at Buhwa, Zimbabwe

ABSTRACT

Greenstone belts of various ages are widespread in the Zimbabwe Archean craton. Banded iron formation is a typical lithology in all of them, but Buhwa is one of only two major occurrences of high-grade iron ore. The geologic history at Buhwa includes a major phase of supracrustal deposition, widespread tonalitic plutonism, folding, formation of shear zones, and greenschist- to amphibolite-facies metamorphism. The supracrustal cover sequence can be divided into two associations (1) a deeper-water, mixed chemical sediment and volcanic rock succession, and (2) a siliciclastic-dominated marine-shelf succession that contains a thick jaspilite unit that hosts six iron-ore deposits. Axial ratios of the ore bodies indicate they are oblate ellipsoids in shape. Previous work had established hematite as the primary ore mineral. Of several possible hypotheses concerning the origin of the ore, hypogene processes involving dissolution of chert and replacement by hematite is the most attractive. The uniqueness of the iron ore at Buhwa may be related to the unusually thick sedimentary sequence, from which mineralizing fluids could have been derived.

INTRODUCTION

Greenstone belts are widely distributed across the Archean Zimbabwe Craton and formed at three main ages: ~3.5 Ga, ~2.9 Ga, and ~2.7 Ga (Wilson, 1979). The oldest and least extensive greenstones are called the "Sebakwian," while the ~2.9 Ga

greenstones are commonly referred to as the "Lower Bulawayan" and the ~2.7 Ga greenstones as the "Upper Bulawayan" (Stagman, 1978). This stratigraphy has been recognized in most of the greenstone belts in Zimbabwe. However, the data presented here suggest that the Buhwa greenstone belt (Figs. 35, 36) in southern Zimbabwe does not conform to the "classical" stratigraphy and is unique in several ways, including the occurrence of a high-grade iron-ore deposit whose geologic setting is unlike any other in Zimbabwe.

The Buhwa Greenstone Belt lies < 5 km north of the northern limit of the Northern Marginal Zone of the Limpopo Belt. This boundary was once regarded as the position of the opx-in isograd, but has recently been demonstrated to be a significant reverse-sense ductile shear zone in places (Fig. 35; Mkweli et al., in press; Rollinson and Blenkinsop, in press), including the area south of Buhwa. As such, Buhwa represents the closest greenstone belt in Zimbabwe to the inferred tectonic front of the "Limpopo orogeny" (e.g. Roering et al., 1992); it may represent a position at or near the edge of the ~3.5 Ga gneissic terrane known as the Tokwe segment (see Wilson, 1990 for a description of the Tokwe segment).

Recent field investigations around the Buchwa Mine area have shed considerable light on the complex and unique history of this geologically important greenstone belt (Fedo and Eriksson, 1993a, 1993b). This paper outlines the stratigraphic and structural setting of the iron-ore deposits at Buhwa, briefly describes the ore bodies, and considers alternative models for ore genesis.

Figure 35. Simplified geologic map showing the southern part of the Zimbabwe Craton, the Limpopo Belt, and the northern part of the Kaapvaal Craton. Greenstone belts in the Zimbabwe Craton: B - Buhwa, Be - Belingwe, Mw - Mweza, Ma - Masvingo. Inset map shows the southern horn of Africa and the regional geologic setting of the Zimbabwe and Kaapvaal Cratons and the Limpopo Belt. Redrawn from Rollinson and Blenkinsop (in press).

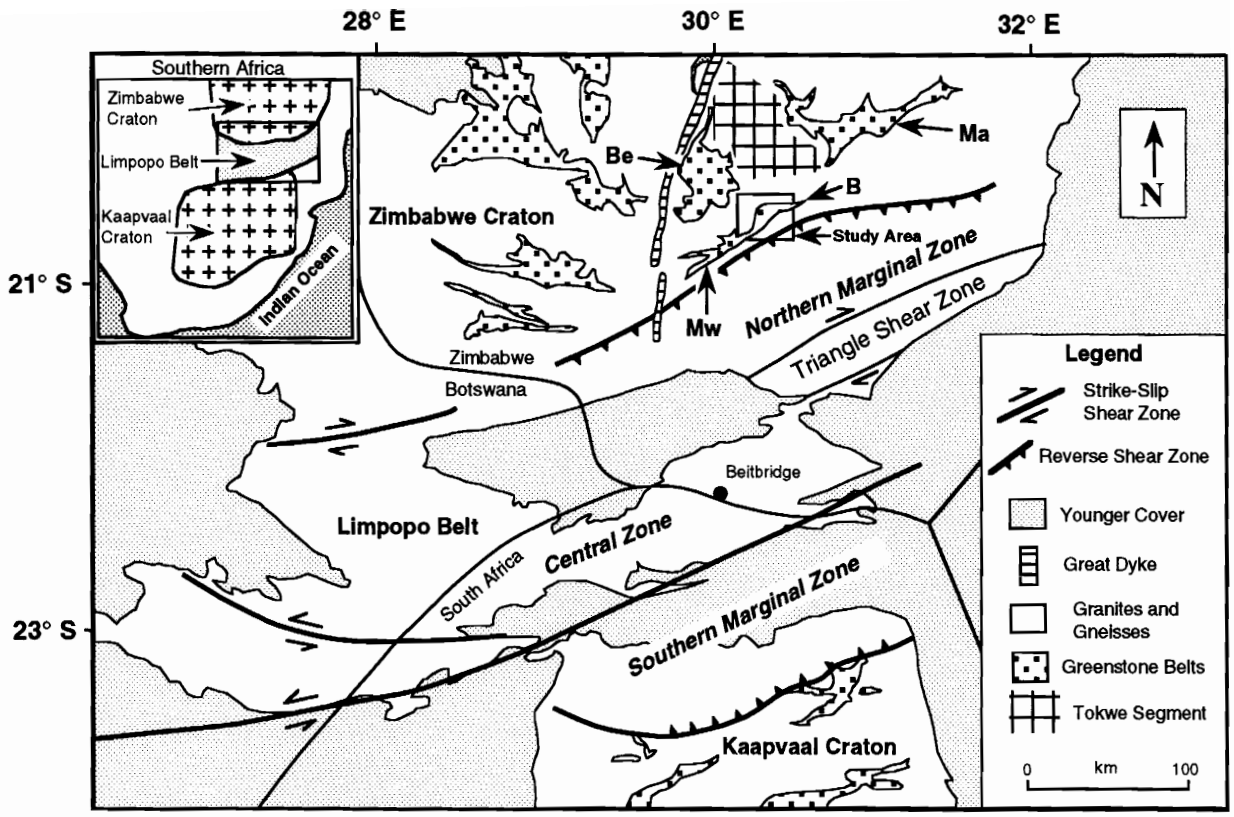
28° E
30° E
32° E
21° S
23° S
Southern Africa
Zimbabwe Craton
Limpopo Belt
Kaapvaal Craton
Indian Ocean
Zimbabwe Craton
Be
Ma
B
Study Area
Mw
Northern Marginal Zone
Triangle Shear Zone
N
Zimbabwe
Botswana
Beitbridge
Limpopo Belt
South Africa
Central Zone
Southern Marginal Zone
Kaapvaal Craton
Legend
Strike-Slip Shear Zone
Reverse Shear Zone
Younger Cover
Great Dyke
Granites and Gneisses
Greenstone Belts
Tokwe Segment
0
km
100

Figure 36. Geologic map of the Buhwa Greenstone belt and surrounding granite-gneiss terrane. Lithologic contacts modified from the mapping of Worst (1962).

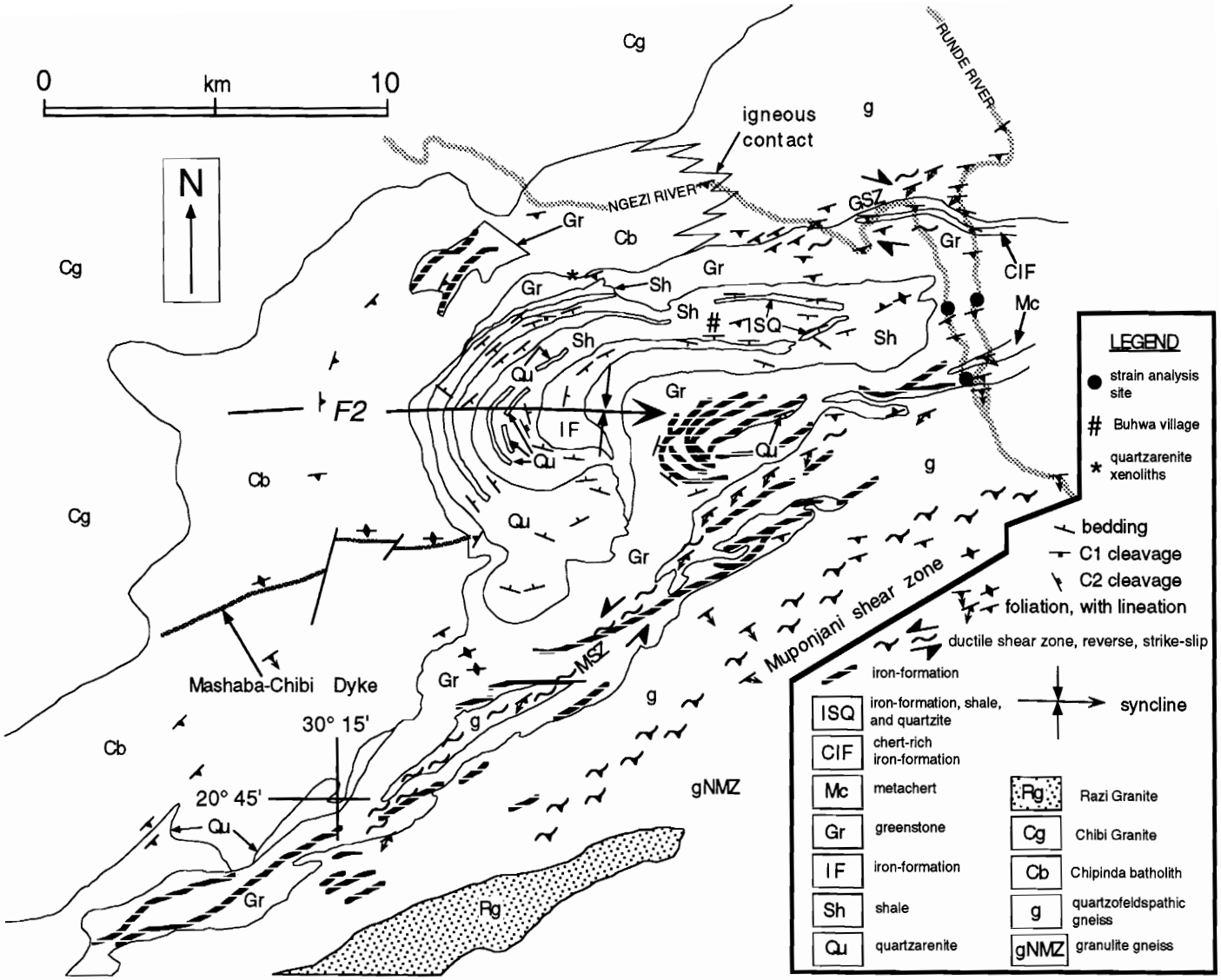
0
km
10
N
RUNDE RIVER
NGEZI RIVER
igneous contact
GSZ
CIF
Mc
ISQ
F2
IF
MSZ
Muponjani shear zone
Mashaba-Chibi Dyke
30° 15'
20° 45'
gNMZ
Cg
Cb
Gr
Sh
Qu
g
Rg
LEGEND
strain analysis site
Buhwa village
quartzarenite xenoliths
bedding
C1 cleavage
C2 cleavage
foliation, with lineation
ductile shear zone, reverse, strike-slip
iron-formation
syncline
ISQ iron-formation, shale, and quartzite
CIF chert-rich iron-formation
Mc metachert
Gr greenstone
IF iron-formation
Sh shale
Qu quartzarenite
Rg Razi Granite
Cg Chibi Granite
Cb Chipinda batholith
g quartzofeldspathic gneiss
gNMZ granulite gneiss

GEOLOGIC SETTING

General History

A wide variety of lithologies and structures of different ages can be found in the area around Buhwa. Potentially the oldest rock type is gneiss, preserved as xenoliths in tonalite that surrounds the belt. The xenoliths, which crop out at numerous localities along the northern edge of the belt, show strong compositional layering similar to classic ~3.5 Ga Tokwe gneiss outcrops in the Tokwe and Runde Rivers. Following greenstone belt formation at Buhwa, the Tokwe basement and Buhuwa greenstone belt were widely intruded by a tonalite batholith, the Chipinda tonalite (Fedo and Eriksson, 1993), whose absolute age is not yet known; a ~2.9 Ga age is tentatively assigned based on regional correlations with the well-studied Chingezi and Mashaba tonalites described by Hawkesworth et al. (1979) and Martin et al. (1993). The correlation with the Chingezi tonalite, coupled with the minimum age of detrital zircons recovered from the quartzites at Buhwa (Dodson et al., 1988) indicates that the Buhwa greenstone belt is older than the tonalite and was deposited between ~2.9 and ~3.1 Ga. A late phase of approximately east/west striking dikes intrudes the tonalite and cover sequence. The culminating events at Buhwa include folding of the region about an east/west-striking axial surface, formation of shear zones in both gneissic and cover sequence lithologies, and amphibolite- (to the south) and greenschist-facies (most of cover sequence including ore bodies) metamorphism. The folded cover sequence is described in more detail because it hosts the iron-ore deposits.

Stratigraphy

Prior to the current investigation little was known about the stratigraphy and sedimentology of the succession exposed at Buhwa, with the only published report being that of Worst (1962). Unlike most greenstone belts in Zimbabwe, the cover sequence is composed dominantly of sedimentary rocks as opposed to mafic and ultramafic volcanic rocks. The cover rocks at Buhwa are divisible into two major associations: the eastern association and the western association, which are linked by an "interfingering zone" located in the vicinity of Buchwa Mine's low-density living quarters.

Eastern Association

The eastern association is best exposed in the river beds of the Ngezi and Runde Rivers ~4 km west of the summit Munaka. The association consists of intercalated metavolcanic rock (greenstone), quartzite (metachert), and uncommon meta-banded iron formation (Fig. 37A).

The metacherts consist mainly of equant, interlocking mosaics of recrystallized quartz. Locally the metacherts contain scattered flakes of mica or bands of scattered opaque minerals so that the rock has a pronounced striped appearance similar to iron-poor banded iron formation. Guilbert and Park (1986) commented on the typical recrystallized nature of chert layers in Archean banded iron formations, noting that many workers have mistakenly called the quartzites "sandstones." These metacherts were previously interpreted by Worst (1962) as lithologic correlatives to the thick detrital quartzite succession of the western association.

Metavolcanic rocks form the majority of the eastern association and consist mostly of actinolite and tremolite schists with less common talc-carbonate schists. Original

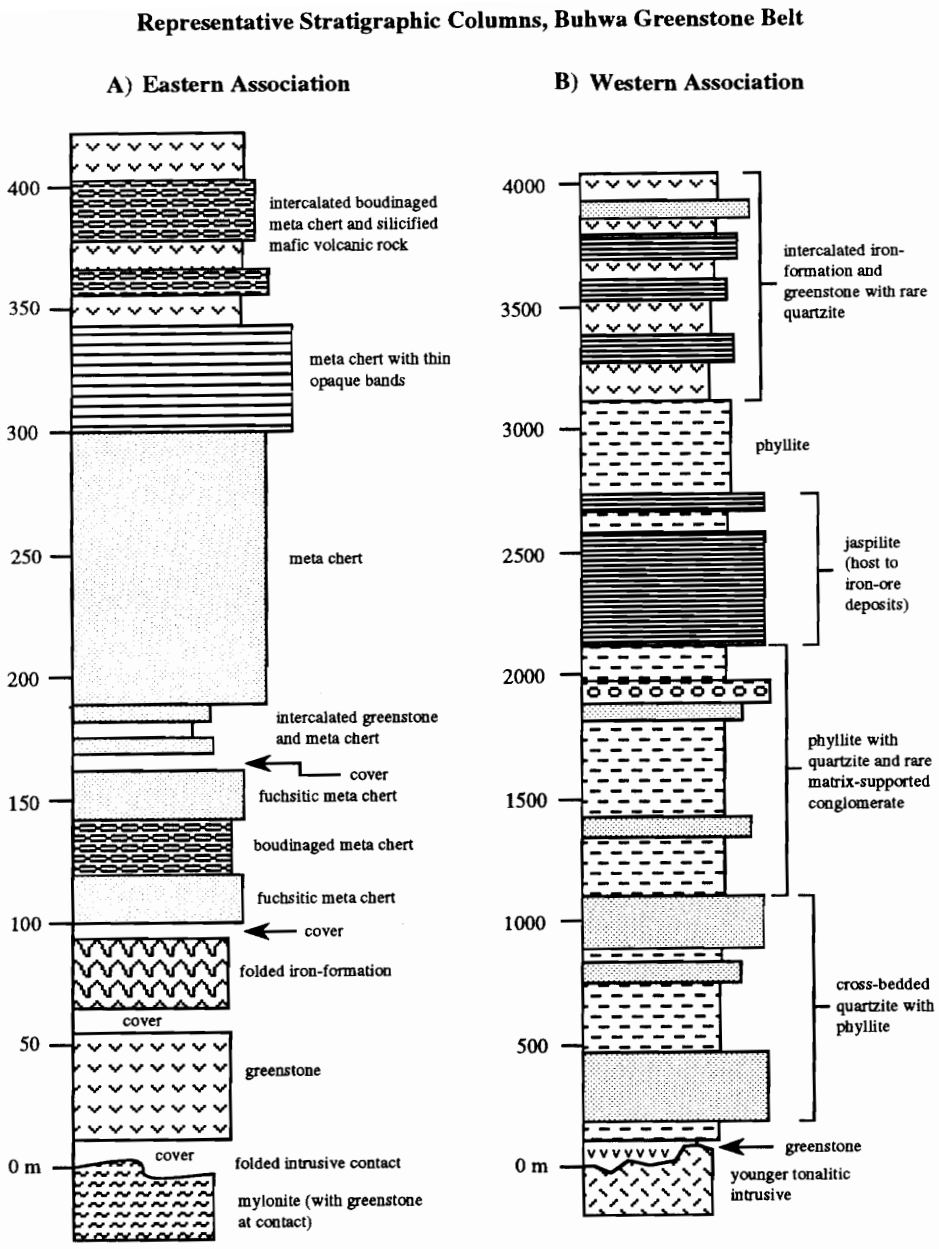

Figure 37. A) representative stratigraphic section of the lower part of the eastern asociation; no way up is implied or inferred; the upper part of the eastern association is dominated by greenstone and less common meta chert. B) representative stratigraphic section of the western association, Buchwa Mine area; note scale change from 3A.

extrusive and/or intrusive textures have been obliterated by metamorphic mineral growth and ductile deformation, except at two localites in the center of the belt where a mafic breccia and spinifex-textured lava flows are preserved.

Few occurrences of meta-banded iron formation are found in the eastern association, where they consist of millimeter- to centimeter-scale, black and white alternations of iron oxides and quartz. They have not been prospected for ore potential, but considering the limited nature and the number of chert bands in both deposits, it seems highly unlikely that ore deposits are developed in them.

Western Association

The western association is best exposed in the fold-closure region near Buchwa Mine (Fig. 36). The association consists dominantly of siliciclastic sedimentary rocks (orthoquartzite, phyllite, and siltstone) and banded iron formation, in which the iron-ore bodies are found (Fig. 37B). Above the main banded iron formation unit, lies a very poorly exposed section of phyllite, then iron formation intercalated with (?intruded by) massive greenstone, and a single thin quartzite unit.

Orthoquartzite, ~1 km thick, forms the preserved basal lithology of the sedimentary succession. The quartzite is divided into three units: a lower and upper quartzite separated by a thick section of interbedded quartzite and phyllite. Quartzites consist of clean quartz sand and local flakes of fuchsite. Good exposures reveal a variety of wave-produced sedimentary structures including trough cross-bedding and symmetrical ripple marks.

An ~1 km thick section that consists mostly of phyllite overlies the quartzite. The lower 500-600 m are very poorly exposed. The upper part consists of flat- and wavy-laminated alternations of mudstone (now phyllite) and siltstone or very fine-grained

sandstone. Nearly 50 m of arenites and rare conglomerate overlie the fine-grained section.

The Buhwa summit ridge consists of banded iron formation, which overlies the phyllites. The extreme topographic relief and dense vegetative cover make it difficult to accurately measure the thickness of the iron formation; however, simple geometric calculations require a thickness in excess of 500 m in the vicinity of Buhwa summit. Along strike, the unit thins to less than 300 m. Non-ore-bearing rocks consist of millimeter- to centimeter-scale alternations of recrystallized white or red chert and hematite. Worst (1962; see discussion therein) considered this distinct banding as characteristic of "jaspilite," and that nomenclature is accepted here. This jaspilite body hosts the iron-ore deposits at Buhwa.

Initial interpretation of the cover sequence at Buhwa is that it represents the transition from stable-shelf to deeper-water sedimentation across the edge of the Tokwe segment. The gneissic xenoliths are tentatively interpreted as relics of the depositional basement upon which the Buhwa cover sequence was deposited, although any evidence of a basement unconformity was obliterated during later tonalitic plutonism. The fining-upward succession in the western sections from coarse- to fine-grained siliciclastic rocks followed by orthochemical sedimentary rocks is reminiscent of a shallow-water Phanerozoic transgressive shelf, with which the Buhwa succession may compare. Eastern sections are more difficult to assess in terms of stratigraphic relationships because of the lack of any facing criteria, lithologic homogeneity, and the convergence of ductile shear zones. Nevertheless, the consistent association of metachert, iron formation, and mafic-to-ultramafic volcanic rocks suggests sub wave-base conditions for the succession.

Structure

The most significant structure is the major fold that strongly deforms the cover succession. The fold is asymmetric in map view, with a short southern limb and a long northern limb, in which all the ore bodies reside (Fig. 36). Jaspilite on the northern limb strikes east/west and dips ~50° to the south, except where the rocks curve into the fold closure. The fold axis plunges ~28° towards 088°, with a nearly vertical axial surface. Several small dikes with the approximately the same orientation are exposed in the current mine workings. Facing criteria in the underlying quartzites show a consistent younging direction toward the jaspilite, which indicates the strata are not overturned and that the fold is a synformal syncline. Minor folds in the region show approximately the same orientation.

IRON-ORE DEPOSITS

General

Iron formations developed mainly in the Archean and the Proterozoic (Guilbert and Park, 1986). There has been a massive amount of literature pertaining to the description and origin of iron formations (e.g. *Economic Geology*, 1973, v. 68; Guilbert and Park, 1986 and references therein). The general definition of iron formation as presented by James (1954) is accepted here: iron formation is typically a thin bedded or laminated chemical sediment that contains >15% iron and commonly has layers of chert. The percent iron to qualify as "iron formation" is placed arbitrarily; however, rocks formed by the same depositional *process* may contain iron contents much less than 15%.

Iron formations have been divided into two main types (Guilbert and Park, 1986). Archean deposits are traditionally called "Algoma" type, which are normally

associated with submarine volcanic rocks; these are exclusively banded iron formations. Proterozoic iron formations are called "Superior" type after the Lake Superior region in the USA, and typically are associated with marine shelf deposits, but not necessarily with volcanic rocks; these are banded or granular iron formations.

In Zimbabwe, banded iron formations have a cumulative strike length of nearly 6000 km (Foster et al., 1986), and occur in all three of the greenstone successions discussed above. The overwhelming majority of iron formations appear in close association with volcanic rocks and commonly carry mineable quantities of gold (Foster et al., 1986; Foster and Gilligan, 1986). There are two main high-grade iron-ore deposits in the country. One of them is located in the Redcliff area of the Midlands greenstone belt near Kwe Kwe and the other is at Buhwa. At Redcliff, most of the iron is extracted from altered and hydrated sulfide-facies iron formation of the Lannes Sedimentary Formation (Cheshire et al., 1980), which is correlated with the Cheshire Formation. The iron formation is underlain by a thick succession of partly pillowed basaltic greenstones and is capped by a comparatively thin section of shales, immature to mature arenites, and pyritiferous chert (Cheshire et al., 1980); all these features point to an Algoma-type occurrence. By comparison, the succession at Buhwa looks quite different. There the iron formation caps a >2 km thickness of detrital sedimentary rocks including thick, supermature quartzarenites and there are no interstratfied volcanic rocks. Such an occurrence seems more common of the Superior-type iron formations. An outline of the general mining history at Buhwa can be found in Worst (1962), Castelin (1980), Rhean (1980), and Acheampong (1982).

Buhwa Iron-Ore Deposits: Description

Iron-ore deposits at Buhwa are primarily controlled by the distribution of the main jaspilite body, whose depositional shape is tabular. The jaspilite, and therefore the ore bodies, is developed only in the western association, particularly above the thickest accumulation of the underlying phyllite-dominated succession, with a strike length of ~13 km. The six ore bodies are wholly contained within the jaspilite and occur at altitudes above 1225 m, except for the Hwi Kwi deposit (see Worst, 1962 for detailed map distribution of the bodies). Five of them occur near the fold closure, stretched out for ~4 km along the northern limb of the fold. The easternmost deposits are located at the eastern end of the exposed jaspilite body near the summit named Hwi Kwi. Ore bodies exposed at the surface presently do not show any preference for a certain stratigraphic horizon, though the bodies near the summit are close to the contact with the underlying phyllite and the Hwi Kwi deposit lies close to the contact with the overlying phyllite. All of the ore bodies occur where the jaspilite is thickest; where the jaspilite thins east of the middle deposit, there are no *in-situ* deposits. Instead, minor, but recoverable deposits of ore occur as loose blocks forming the scree slope on the northern flank of the ridge.

In plan view, the in-situ ore bodies are elliptical in shape with aspect ratios ranging from 5:1 (middle deposit) to 20:1 (summit deposit). Cross-sectional views (in Worst, 1962) are similar; that is, the bodies are elongate in a down-dip direction when compared to their thickness. Aspect ratios range from 2.5:1 to 4:1. However, given the current level of erosion, it is likely that these ratios would perhaps double if their original dimensions were projected above the Earth's surface. Such dimensions indicate that the ore bodies are oblate ellipsoids in geometry. In both plan and cross-sectional views, any single ore body consists of numerous horizons of ore rock that

anastomose around the host jaspilite, and as such does not represent a single uninterrupted concentration of massive hematite. Drilling has shown the ore bodies to be vertical or steeply south dipping (Worst, 1962).

Hematite forms the most abundant ore mineral at Buhwa and was concentrated by the replacement of chert bands by iron oxide (Worst, 1962). Thick sulfide deposits are not present, although scattered isolated grains of, and small patches of pyrite do occur in some layers. Ore grade is variable, ranging from 50% to 67% Fe, with a current average grade at 60.3% Fe (A. Mnyama, personal communication, 1993) Perfectly preserved millimeter-scale bands are present even up to the highest ore grades. Ore-body margins are lower grade than cores because iron-oxide replacement was less complete (Worst, 1962).

Models for Ore Genesis at Buhwa

Based on the above observations, several tenable models can be erected concerning the origin of the iron-ore deposits at Buhwa. First, the possibility that the deposits are syngenetic in origin (or formed immediately after deposition of the jaspilite) must be considered. The fact that the deposits are not truely stratiform, that is, many mineralized zones cross-cut the jaspilite stratigraphy, makes this hypothesis seem unlikely.

Second, the ore could have been formed as a direct result of folding or shearing of the cover sequence. Although the ore bodies do follow the structural grain of the major fold in plan view, this is most likely the result of lithologic control: the mineralization only affected the folded jaspilite. The deposits are *stratabound* not *stratiform* (sensu Guilbert and Park, 1986). Also, the ore bodies show no systematic orientation with respect to the fold, for example, they are not elongated in the plunge

direction. Ore bodies do not show any fabric concordancy with the shear zones at all. Thus a genetic link directly to large-scale structural features seems doubtful. There is the possibility that ore-enriching fluids passed through a conduit of fractures and filled them completely with ore, thus masking their original orientation. It seems unlikely, however, that *all* fractures would have been filled in this way, such that no evidence of cataclasis would be visible. Even at high ore grades millimeter-scale layering is well preserved.

A third possibility relates the later east/west-striking dikes to the emplacement of the ore bodies. In this scenario, fluids associated with the dikes permeated the jaspilite and caused ore enrichment. Although potentially attractive as a source of fluids, this hypothesis is rejected on the following. First, there is no systematic relationship between ore concentration and spatial proximity to the dikes and second, the dikes are relatively small (meter scale) and probably could not carry enough fluids for the widespread mineralization in the fold-closure region.

Ore enrichment by supergene processes is a fourth possibility. In this model, oxidized and heavily leached rocks would overlie the enriched ore bodies. At Buhwa, this could have occurred with the strata at two possible orientations: when the rocks were still flat lying or when the rocks were tilted. The first option would require the leached zone to lie *stratigraphically* above the ore deposits, while the second requires a leached zone to occur at *topographically* higher elevations. Absence of a widespread oxidized-leached zone, as recognized by boxwork or cavity textures, in the host jaspilite makes supergene enrichment an unlikely candidate as the sole ore-enriching mechanism.

The most attractive model for ore emplacement calls on deposition by hypogene processes (Castelin, 1980). This model calls on heated, upwardly mobile, crustal

fluids to have deposited the ore while the strata resided at shallow depths in the crust. In such a setting, fluids migrated through the jaspilite and either dissolved chert leaving a residual, concentrated mass of hematite or replaced chert with hematite filling the voids left by the dissolution of chert. This type of ore enrichment was common in the Lake Superior iron district of the USA, although such high-grade ore has long been mined away (Guilbert and Park, 1986). A prediction of this model is that the ore bodies would cross the jaspilite body. Worst's (1962) observation that the ore bodies are vertical or subvertical seems to be consistent with the model. The distribution of the ore exclusively along the northern limb of the fold may be the result of the relatively simple structural setting, whereby upward fluid transport follows flat, evenly spaced, subvertical bedding planes. Alternatively, an as yet undiscovered ore body may lie at depth in the short southern limb of the fold (see below).

Iron formation, and even jaspilite, is a common feature all along the Buhwa greenstone belt (albeit not as thick as in the Buchwa mine area) and common in all Archean greenstone belts in Zimbabwe. What is unique about the mineralized area near Buchwa mine? Certainly the >2 km thick succession of shelfal siliciclastic sediment that underlies the jaspilite is quite unlike any other occurrence in Zimbabwe, and may be the result of the Buhwa's initial depositional setting at or near the edge of the Tokwe segment. Where did the ore-forming fluids come from? Without any evidence to prove so, it is nevertheless tantalizing to suggest that the fluids escaped during burial, folding, and greenschist-facies metamorphism of the unusually thick, siliciclastic, marine-shelf cover sequence, with the implication that ore enrichment occurred at the same time. The character of the fluids may have been determined by interaction with the cover rocks.

Speculations for Future Exploration at Buhwa

With no new drilling as a tool to guide it, exploration at Buhwa must be conducted utilizing the best available surface geological data and accompanying interpretations. The current study now forms the most comprehensive geological study outside the present mine area, and two major points have arisen concerning the exploration for iron ore at Buhwa.

Curiously all of the ore bodies except Hwi Kwi occur at high elevations in the range as mentioned above. As elevation drops along the northern limb of the major fold, there are no in-situ ore deposits exposed at the surface. Instead, at the lower elevations scree deposits appear on the northern flank of the range, which indicates that iron ore bodies originally extended all along the northern limb of the fold. The known ore bodies pinch at depth, which suggests that mineralizing conditions occurred at constant depth. If this is so, and an original tapering shape is accepted for the tops of the ore bodies as well, the summit body is then predicted to broaden at depth. The model might also predict the possibility of a subsurface ore body in the short southern limb of the fold. Without deep drilling to prove so, perhaps the jaspilite passed through ore-forming conditions at several discreet depths, thereby creating more than one level of ore. If this were so, the structural configuration of the jaspilite as documented by mapping requires that any more iron-ore bodies would lie down dip in Muchipisi valley.

REFERENCES

Acheampong, Y.A. 1982. Buchwa Mine. Chamber of Mines Journal, 24: 25-31.

Allègre, C.J. 1982. Genesis of Archaean komatiites in a wet ultramafic subducted plate. In: N.T. Arndt and E.G. Nisbet (Editors). Komatiites. Allen and Unwin, p. 495-500.

Arth, J.G., and Hanson, G.N. 1975. Geochemistry and origin of the early Precambrian crust of northeastern Minnesota. Geochim. Cosmochim. Acta, 39: 325-362.

Barton, J.M., and van Reenen, D.D. 1992. When was the Limpopo Orogeny? Precambrian Res., 55: 7-16.

Bateman, R. 1985. Aureole deformation by flattening around a diapir during in-situ ballooning: the Cannibal Creek granite. J. Geol., 93: 293-310.

Berger, M., Kramers, J.D., and Nägler, T.F. in review. The Northern Marginal Zone of the Limpopo Belt - 3 models in contest: which will satisfy new petrological, geochemical, and geochronologic data? Lithos.

Beukes, N.J., and Klein, C. 1992. Models for iron-formation deposition. In: J.W. Schopf and C. Klein (Editors), The Proterozoic Biosphere A Multidisciplinary Study. Cambridge University Press, p. 147-151.

Beukes, N.J., and Cairncross, B. 1991. A lithostratigraphic-sedimentological reference profile for the Late Archaean Mozaan Group, Pongola Sequence: Application to sequence stratigraphy and correlation with the Witwatersrand Supergroup. South Afr. Jour. Geol., 94: 44-69.

Bickle, M.J., Nisbet, E.G., and Martin, A. 1994, Archean greenstone belts are not oceanic crust: J. Geol., 102: 121-138.

Bickle, M.J., Orpen, J.L., Nisbet, E.G., and Martin, A. 1993. Structure and metamorphism of the Belingwe greenstone belt and adjacent granite-gneiss terrain: The tectonic evolution of an Archean craton. In: Bickle, M.J., and Nisbet, E.G., (Editors)., The geology of the Belingwe greenstone belt: A Study of the evolution of Archaean continental crust. Geol. Soc. of Zimbabwe Special Publication 2, p. 39-68.

Bickle, M.J., and Nisbet, E.G. (Editors) 1993. The geology of the Belingwe greenstone belt, Zimbabwe: A study of the evolution of Archaean continental crust. Rotterdam, A.A. Balkema, Geol. Soc. of Zimbabwe Special Publication 2.

Blenkinsop, T. in press. Tectonic evolution of greenstone belts the Zimbabwe Craton. In: M.J. deWit and L.D. Ashwal (Editors), Tectonic Evolution of Greenstone Belts, Oxford University Press.

Blenkinsop, T.G., and Treloar, P.J. in press. Geometry, classification and kinematics of S-C and S-C' fabrics in the Mushandike area, Zimbabwe. J. Struct. Geol.

Blenkinsop, T.G., Fedo, C.M., Bickle, M.J., Eriksson, K.A., Martin, A., Nisbet, E.G., and Wilson, J.F. 1993. Ensialic origin for the Ngezi Group, Belingwe Greenstone Belt, Zimbabwe. Geology, 21: 1135-1138.

Bøe, R., and Sturt, B.A. 1991. Textural responses to evolving mass flows: an example from the Devonian Asen Formation, central Norway. Geol. Mag., 128: 99-109.

Boryta, M., and Condie, K.C. 1990. Geochemistry and origin of the Archean Beit Bridge complex, Limpopo Belt, South Africa. J. Geol. Soc. London, 147: 229-239.

Bruce, C.H. 1983. Shale tectonics, Texas coastal area growth faults. In: A.W. Bally (Editor) Seismic Expression of Structural Styles, a Picture and Work Atlas. Studies in Geology Series #15. Am. Assoc. Pet. Geol., p. (2.3.1-1)-(2.3.1-6).

Camiré, G.E., Laflèche, M.R., and Ludden, J.N. 1993. Archean metasedimentary rocks from the northwestern Pontiac Subprovence of the Canadian Sheild: chemical characterization, weathering and modeling of the source areas. Precambrian Res. 62: 285-305.

Card, K.D. 1990. A review of the Superior Province of the Canadian Shield, a product of Archean accretion. Precambrian Res., 48: 99-156.

Castelin, C.A. 1980. Iron ore in Rhodesia. Chamber of Mines Journal, 22: 25-29.

Cheshire, P.E., Leach, A., and Milner, S.A. 1980. The geology of the country between Gwelo and Redcliff. Zimbabwe Geological Society Bulletin No. 86, 300 p.

Collinson, J.D., and Thompson, D.B. 1982. Sedimentary Structures. Allen and Unwin, 194 p.

Condie, K.C., and Martell, C. 1983. Early Proterozoic metasediments from north-central Colorado: Metamorphism, provenance, and tectonic setting. Geol. Soc. Amer. Bull. 94: 1215-1224.

Condie, K.C., and Wronkiewicz, D.J. 1990. The Cr/Th ratio in Precambrian pelites from the Kaapvaal Craton as an index of craton evolution. Earth Plan. Sci. Let., 97: 256-267.

Coward, M.P., Butler, W.H., Asif Khan, M., and Knipe, R.J. 1987. The tectonic history of Kohistan and its implications for Himalayan structure. J. Geol. Soc. London, 144: 377-391.

Cox, K.G., Johnson, R.L., Monkman, L.J., Stillman, C.J., Vail, J.R., and Wood, D.N. 1965. The geology of the Nuanetsi igneous province: Phil. Trans. Royal Soc. London, A 257: 71-218.

Davis, G.H. 1984. Structural Geology of Rocks And Regions. John Wiley and Sons, 491 p.

De Paor, D., and Simpson, C. 1993. New Directions in Structural Geology. 1993 USGS Reston Short Course Notes, 129 p.

de Ronde, C.E.J., de Wit, M.J., and Spooner, E.T.C. 1994, Early Archean (>3.2 Ga) Fe-oxide-rich, hydrothermal discharge vents in the Barberton Greenstone Belt, South Africa: Geol. Soc. Am. Bull., 106: 86-104.

de Wit, M.J., Hart, R.A., and Hart, R.J. 1987. The Jamestown Ophiolite Complex, Barberton mountain belt: a section through 3.5 Ga oceanic crust. J. African Earth Sci., 6: 681-730.

Donaldson, C.H. 1982. Spinifex-textured komatiites: a review of textures, composition and layering. In: N. Arndt and E.G. Nisbet (Editors), Komatiites. Allen and Unwin, p. 213-244.

Dodson, M.H., Compston, W., Williams, I.S., and Wilson, J.F. 1988. A search for ancient zircons in Zimbabwean sediments. J. Geol. Soc. London, 145: 977-983.

England, P., and Bickle, M. 1984. Continental thermal and tectonic regimes during the Archean. J. Geol., 92: 353-367.

Eriksson, K.A. 1983. Archaean iron-formations: Environments of deposition and controls on formation. J. Geol. Soc. Australia, 30: 473-482.

Eriksson, K.A., and Fedo, C.M. in press. Archean synrift and stable-shelf sedimentary successions. In: K.C. Condie (Editor), Archean Crustal Evolution. Elsevier.

Eriksson, K.A., Turner, B.R., and Vos, R.G. 1981. Evidence for tidal processes from the lower part of the Witwatersrand Supergroup. Sed. Geol., 29: 309-325.

Eriksson, K.A., Kidd, W.S.F., and Krapez, B. 1988. Basin analysis in regionally metamorphosed and deformed Early Archean terrains: Examples from southern Africa and Western Australia. In: Kleinspehn, K.L., and Paola, C. (Editors), New Perspectives in Basin Analysis. Springer-Verlag, New York, 371-404.

Fawcett, J.J., and Yoder, H.S. 1966. Phase relationships of chlorites in the system MgO-Al_2O_3-SiO_2-H_2O. Am. Min., 51: 353-378.

Fedo, C.M., and Eriksson, K.A. 1993a. Chronologic evolution of the Archean (3.0 Ga) Buhwa Greenstone Belt, Zimbabwe. 16th International Colloquium of African Geology, p.125-126.

Fedo, C.M., and Eriksson, K.A. 1993b. Evolution of the Archean (~3.0 Ga) Buhwa Greenstone Belt, Zimbabwe, with implications for iron ore distribution. Harare: Zimbabwe, Sub-Saharan Economic Geology Programme with Abstracts. p. 5.

Fedo, C.M., and Eriksson, K.A. in press. Geologic setting and ideas concerning the origin of the iron-ore deposits at Buhwa, Zimbabwe. In: Blenkinsop, T.G., and Tromp, P.L. (Editors), Sub-Saharan Economic Geology 1993. A.A. Balkema, Rotterdam.

Feng, R., and Kerrich, R. 1990. Geochemistry of fine-grained clastic sediments in the Archean Abitibi greenstone belt, Canada: Implications for provenance and tectonic setting. Geochim. Cosmochim,. Acta, 54: 1061-1081.

Foster, R.P., and Gilligan, J.M. 1986. Archean iron-formation and gold mineralization in Zimbabwe. University of Southampton, Department of Geology, Report No. 5, 43 p.

Foster, R.P., Mann, A.G., Stowe, C.W., and Wilson, J.F. 1986. Archaean gold mineralization in Zimbabwe. In: Anhauesser, C.R., and Maske, S. (Editors), Mineral deposits of southern Africa: Geol. Soc. S. Africa, 1: 43-112.

Ghosh, S.K., Mandal, N., Sengupta, S., Deb, S.K., and Khan, D. 1993. Superposed buckling in multilayers. J. Struct. Geol., 15: 85-111.

Guilbert, J.M., and Park, C.F., Jr. 1986. The geology of ore deposits. New York, W.H. Freeman & Co., 985 p.

Hamilton, P.J. 1977. Sr isotope and trace element studies of the Great Dyke and Bushveld Mafic Phase and their relation to early Proterozoic magma genesis in southern Africa. J. Petrology, 18: 24-52.

Harnois, L. 1988. The CIW index: A new chemical index of weathering. Sed. Geol., 55: 319-322.

Hawkesworth, C. J., Moorbath, S., O'Nions, R. K., and Wilson, J. F. 1975. Age relationships between greenstone belts and "granites" in the Rhodesian Archean craton. Earth Plan. Sci. Let., 25: 251-262.

Hawkesworth, C.J., Bickle, M.J., Gledhill, A.R., Wilson, J.F., and Orpen, J.L. 1979. A 2.9 b.y. event in the Rhodesian Archaean. Earth Plan. Sci. Let., 43: 285-297.

Hickman, M. H. 1978. Isotopic evidence for crustal reworking in the Rhodesian Archean craton, southern Africa. Geology, 6: 214-216.

Hippert, J.F.M. 1994. Grain boundary microstructures in micaceous quartzite: Significance for fluid movement and deformation processes in low metamorphic grade shear zones. J. Geol., 102: 331-348.

Hoffman, P.F. 1987. Early Proterozoic foredeeps, foredeep magmatism, and Superior-type iron-formations of the Canadian Shield, In: Kroner, A. (Editor), Proterozoic Lithospheric Evolution. AGU Geodynamics Series 17, 85-98.

Holder, M.T. 1979. An emplacement mechanism for post-tectonic granites and its implications for their geochemical features. In: M.P. Atherton and J. Tarney

(Editors), Origin of Granite Batholiths. Geochemical Evidence. Shiva Press, p. 116-128.

Hubert, J.F. 1962. A zircon-tourmaline-rutile maturity index and the interdependence of composition of heavy mineral assemblages with the gross composition and texture of sandstones. J. Sed. Pet., 50: 489-496.

Hudleston, P.J., and Lan, L. 1993. Information from fold shapes. J. Struct. Geol., 15: 253-264.

James, H.L. 1954. Sedimentary facies of iron-formation. Econ. Geol., 49: 235-291.

James, P.R. 1975. A deformation study across the northern margin of the Limpopo Mobile belt, Rhodesia. Ph.D. Thesis. University of Leeds.

Jelsma, H.A., van der Beek, P.A., and Vinyu, M.L. 1993. Tectonic evolution of the Bindura-Shamva greenstone belt (northern Zimbabwe): progressive deformation around diapiric batholiths. J. Struct. Geol., 15: 163-176.

Johnsson, M.J., Stallard, R.F., and Meade, R.H. 1988. First-cycle quartz arenites in the Orinoco River basin, Venezuela and Colombia. J. Geol., 96: 263-277.

Jolly, W.T. 1982. Progressive metamorphism of komatiites and related Archaean lavas of the Abitibi area, Canada. In: N. Arndt and E.G. Nisbet (Editors), Komatiites. Allen and Unwin, p. 247-266.

Kamber, B., Kramers, J.D., Napier, R., Cliff, R.A., and Rollinson, H.R. 1994. The Triangle shear zone, Zimbabwe, revisited: what remains of the Archaean Limpopo orogeny? J. Petrology, in press.

Kasting, J.F. 1993. Earth's early atmosphere. Science, 259: 920-926.

Kramers, J.D., and Ridley, J.R. 1989. Can Archaean granulites be direct crystallization products from a sialic magma layer? Geology, 17: 442-445.

Kusky, T.M. 1991. Structural development of an Archean orogen, Western Point Lake, Northwest Territories. Tectonics, 10: 820-841.

Kusky, T.M., and DePaor, D.G. 1991. Deformed sedimentary fabrics in metamorphic rocks: evidence from the Point Lake area, Slave province, Northwest Territories. Geol. Soc. Am. Bull., 103: 486-503.

Kusky, T.M., and Kidd, W.S.F. 1992. Remnants of an Archaen oceanic plateau, Belingwe greenstone belt, Zimbabwe. Geology, 20: 43-46.

Lister, G.S., and Snoke, A.W. 1984. S-C Mylonites. J. Struct. Geol., 6: 617-638.

Luais, B., and Hawkesworth, C.J. 1994. The generation of continental crust: An integrated study of crust-forming processes in the Archean of Zimbabwe. J. Petrol. 35: 43-93.

Martin, A., Nisbet, E.G., Bickle, M.J., and Orpen, J.L. 1993. Rock units and stratigraphy of the Belingwe greenstone belt: The complexity of the tectonic setting. In: Bickle, M.J., and Nisbet, E.G. (Editors), The geology of the Belingwe greenstone belt, Zimbabwe A study of the evolution of Archaean continental crust. Geol. Soc. Zimbabwe Special Publication 2, p. 13-37.

Masuda, A., Nakamura, N., and Tanaka, T. 1973. Fine structures of mutually normalised rare-earth patterns of chondrites. Geochim. Cosmochim. Acta, 43: 1131-1140.

McLeannan, S.M., and Taylor, S.R. 1984. Archean Sedimentary Rocks and Their Relation to Composition of the Archean Continental Crust. In: Kroner, A., Hanson, G.N., and Goodwin, A.M. (Editors), Archean Geochemistry: The origin

and eveloution of the Archean continental crust. New York, Springer-Verlag, p. 47-72.

McLennan, S.M., and Taylor, S.R. 1991. Sedimentary rocks and crustal evolution: Tectonic setting and secular trends. J. Geol., 99: 1-21.

McLennan, S.M. 1993. Weathering and Global Denudation. J. Geol., 101: 295-303.

McLennan, S.M., Hemming, S.R., Taylor, S.R., and Eriksson, K.A. in press. Early Proterozoic crustal evolution: Geochemical and Nd-Pb isotopic evidence from metasedimentary rocks, southwestern North America. Geochim. Cosmochim. Acta.

Means, W.D. 1981. The concept of steady-state foliation. Tectonophysics, 78: 179-199.

Mkweli, S., and Blenkinsop, T.G. 1992. A westward continuation of the Zimbabwe Craton-Northern Marginal Zone tectonic break. University of Zimbabwe, North Limpopo Field Workshop Field Guide and Abstracts Volume, p. 43.

Mkweli, S., Kamber, B., and Berger, M. in press. A westward continuation of the Zimbabwe Craton-Northern Marginal Zone tectonic break and new age constraints on timing of the thrusting. J. Geol. Soc. London.

Nesbitt, H.W., Markovics, G., and Price, R.C. 1980. Chemical processes afecting alkalies and alkaline earths during continental weathering. Geochim. Cosmochim. Acta, 44: 1659-1666.

Nesbitt, H.W., and Young, G.M. 1982. Early Proterozoic climates and plate motions inferred from major element chemistry of lutites. Nature, 299: 715-717.

Nesbitt, H.W., and Young, G.M. 1984. Prediction of some weathering trends of plutonic and volcanic rocks based on thermodynamic and kinetic considerations. Geochim. Cosmochim. Acta, 48: 1523-1534.

Nesbitt, H.W., and Young, G.M. 1989. Formation and diagenesis of weathering profiles. J. Geol. 97: 129-147.

Nisbet, E.G. 1987. The Young Earth. Allen and Unwin, 402 p.

Odell, J. 1975. Explanation of the geological map around Bangala Dam. Geological Survey of Rhodesia Short Report , 42.

Orpen, J. L., Martin, A., Bickle, M. J., and Nisbet, E. G. 1993. The Mtschingwe Group in the west: andesite, basalts, komatiites, and sediments of the Hokonui, Bend, and Koodoovale Formations. In: Bickle, M.J., and Nisbet, E.G. (Editors), The geology of the Belingwe greenstone belt: A Study of the evolution of Archaean continental crust. Geol. Soc. of Zimbabwe Special Publication 2, p.

Owens, W.H. 1984. The calculation of a best-fit ellipsoid from elliptical sections on arbitrarily oriented planes. J. Struct. Geol., 6: 571-578.

Pyke, D.R., Naldrett, A.J., and Eckstrand, O.R. 1973. Archaean ultramafic flows in Munro Township, Ontario. Geol. Soc. Am. Bull., 84: 955-978.

Ramsay, J.G. 1989. Emplacement kinematics of a granite diapir: Chindamora batholith, Zimbabwe. J. Struct. Geol. 11: 191-209.

Ramsay, J.G., and Graham, R.H. 1970. Strain variation in shear belts. Can. J. Earth Sci., 7: 786-813.

Ramsay, J.G., and Huber, M.I. 1983. The Techniques of Modern Structural Geology Volume 1: Strain Analysis. Academic Press, 307 p.

Reineck, H.-E., and Singh, I.B. 1980. Depositional Sedimentary Environments (2nd edition). Berlin, Springer-Verlag, 551 p.

Retief, E.A., Compston, W., Armstrong, R.A., and Williams, I.S. 1990. Characteristics and preliminary ages of zircons from Limpopo Belt lithologies. In: D.D. van Reenen and C. Roering (Editors), The Limpopo Belt: A Field Workshop on Granulites and Deep Crustal Tectonics. Rand Afrikaans University, p. 95-99.

Rheam, J. 1980. Iron resources in Zimbabwe. Chamber of Mines Journal, 22: 49-85.

Ridley, J. 1992. On the origins and tectonic significance of the charnockite suite of the Archaean Limpopo Belt, Northern Marginal Zone, Zimbabwe. Precambrian Res., 55: 407-427.

Ridley, J.R., and Kramers, J.D. 1990. The evolution and tectonic consequences of a tonalitic magma layer within Archean continents. Can. J. Earth. Sci., 27:219-228.

Robertson, I.D.M. 1973. Potash granites of the southern edge of the Rhodesian craton and the northern granulite zone of the Limpopo Mobile belt. In: L.A. Lister (Editor), Symposium on granites, gneisses and related rocks. Geol. Soc. South Africa Special Publication 3, p. 265-76.

Robertson, I.D.M. 1974. Explanation of the Geological map of the country south of Chibi. Geological Survey of Rhodesia Short Report 41, 40 p.

Roering, C., Van Reenen, D.D., Smit, C.A., Barton, J.M., De Beer, J.H., De Wit, M.J., Stettler, E.H., Van Schalkwyk, J.F., Stevens, G., and Pretorius, S. 1992. Tectonic model for the evolution of the Limpopo Belt. Precambrian Res., 55: 539-552.

Rollinson, H.R. 1989. Garnet-orthopyroxene thermobarometry of granulites from the Northern Marginal Zone of the Limpopo Belt, Zimbabwe. In: Daley, J.S., Cliff, R.A. and Yardley, B.W.D. (Editors), Evolution of Metamorphic Belts. Geol. Soc. London, Special Publication, 42: 331-335.

Rollinson, H.R. 1993. A terrane interpretation of the Archaean Limpopo Belt. Geol. Mag., 130: 755-765.

Rollinson, H.R., and Blenkinsop, T.G. in press. The magmatic, metamorphic and tectonic evolution of the Northern Marginal Zone of the Limpopo Belt in Zimbabwe. J. Geol. Soc. London.

Rollinson, H.R., and Lowry, D.L. 1992. Early basic magmatism in the evolution of the North Marginal Zone of the Archaean Limpopo Belt. Precambrian Res., 55: 33-45.

Shelley, D. 1989. P, M and G tectonites: a classification based on origin of mineral preferred orientations. J. Struct. Geol., 11: 1039-1044.

Shelley, D. 1993. Igneous and metamorphic rocks under the microscope. London, Chapman and Hall, 445 p.

Shimamoto, T., and Ikeda, Y. 1976. A simple algebraic method for strain estimation from deformed ellipsoidal objects. 1. Basic Theory. Tectonophysics, 36: 315-337.

Shreyer, W., Werding, G., and Abraham, K. 1981. Corundum-fuchsite rocks in greenstone belts of South Africa: petrology, geochemistry, and possible origin. J. Petrology, 22: 191-231.

Simonson, B.M. 1985. Sedimentology of cherts in the Early Proterozoic Wishart Formation, Quebec-Newfoundland, Canada. Sedimentology, 32: 23-40.

Simpson, E.L., and Eriksson, K.A. 1989. Sedimentology of the Unicoi Formation in southern and central Virginia: evidence for late Proterozoic to Early Cambrian rift-to-passive margin transition. Geol. Soc. Am. Bull., 101: 42-54.

Simpson, E.L., and Eriksson, K.A. 1990. Early Cambrian progradational and transgressive sedimentation patterns in Virginia: an example of the early history of a passive margin. J. Sed. Pet., 60: 84-100.

Stagman, J.G. 1978. An outline of the geology of Rhodesia. Geological Society of Rhodesia Bulletin, No. 50, 126 p.

Stuart, G.W., and Zengeni, T.G. 1987. Seismic crustal structure of the Limpopo mobile belt, Zimbabwe. Tectonophysics, 144: 323-335.

Tankard, A.J., Jackson, M.P.A., Eriksson, K.A., Hobday, D.K., Hunter, D.R., and Minter, W.E.L. 1982. Crustal Evolution of Southern Africa, 3.8 Billion Years of Earth History. New York, Springer-Verlag, 523 p.

Taylor, P.N., Kramers, J.D., Moorbath, S., Wilson, J.F., Orpen, J.L., and Martin, A. 1991. Pb/Pb, Sm-Nd and Rb-Sr geochronology in the Archean Craton of Zimbabwe. Chem. Geol., 87: 175-196.

Taylor, S.R., and McLennan, S.M. 1985. The Continental Crust: Its composition and evolution. Blackwell, 312 p.

Taylor, S.R., Rudnick, R.L., McLennan, S.M., and Eriksson, K.A. 1986. Rare earth element patterns in Archean high-grade metasediments and their tectonic significance. Geochim, Cosmoshim. Acta, 50: 2267-2279.

Tracy, R.J., and Frost, B.R. 1991. Phase equilibria and thermobarometry of calcareous, ultramafic, and mafic rocks, and iron-formations. In: D.M. Kerrick (Editor), Contact Metamorphism. Min. Soc. Am., Reviews in Mineralogy v. 26, 207-289.

Tracy, R.J., Robinson, P., and Wolff, R.A. 1984. Metamorphosed ultramafic rocks in the Bronson Hill anticlinorium, central Massachusetts. Am. J. Sci., 284: 530-558.

Treloar, P.J., Coward, M.P., and Harris, N.B.W. 1992. Himalayan - Tibetan analogies for the evolution of the Zimbabwe Craton Limpopo Belt. Precambrian Res., 55: 571-587.

Tsunogae, T., Miyano, T., and Ridley, J. 1992. Metamorphic P-T profiles from the Zimbabwe Craton to the Limpopo Belt, Zimbabwe. Precambrian Res., 55: 259-278.

Tucker, M.E. 1991. Sedimentary Petrology an Introduction to the Origin of Sedimentary Rocks (2nd edition). Oxford, Blackwell Scientific Publications, 260 p.

Van Breeman, O., and Dodson, M.H. 1972. Metamorphic chronology of the Limpopo Belt, southern Africa. Geol. Soc. Am. Bull., 83: 2005-2018.

van Schalkwyk, J.F., and van Reenen, D.D. 1992. High-temperature hydration of ultramafic granulites from the Southern Marginal Zone of the Limpopo Belt by infiltration of CO_2-rich fluid. Precambrian Res., 55: 337-352.

Van Wagoner, J.C., Posamentier, H.W., Mitchum, R.M., Vail, P.R., Sarg, J.F., Loutit, T.S., and Hardenbol, J. 1988, An overview of the fundamentals of sequence stratigraphy and key definitions, In: Wilgus, C.K., Hastings, B.S., Kendall, C.G.St.C., Posamentier, H.W., Ross, C.A., and Van Wagoner, J.C. (Editors), Sea-level changes - An integrated approach. Soc. Econ. Paleo. Mineral. Special Publication 42, p. 39-45.

Vernon, R.H., Collins, W.J., and Paterson, S.R. 1993. Pre-foliation metamorphism in low-pressure/high-temperature terrains. Tectonophysics, 219: 241-256.

Wilson, A.H., Versfeld, J.A., and Hunter, D.R. 1989. Emplacement, crystallization and alteration of spinifex-textured komatiitic basalt flows in the Archaean Nondweni greenstone belt, southern Kaapvaal Craton, South Africa. Contrib. Mineral. Petrol., 101: 301-317.

Wilson, A.H., and Versfeld, J.A. 1994. The early Archaean Nondweni greenstone belt, southern Kaapvaal Craton, South Africa, Part II: characteristics of the volcanic rocks and constraints on magma genesis. Precambrian Res., 67: 227-320.

Wilson, J.F. 1979. A preliminary reappraisal of the Rhodesian basement complex. Geol. Soc. South Africa Special Publication 5, p. 1-23.

Wilson, J.F. 1990. A craton and its cracks: Some of the behavior of the Zimbabwe block from the late Archaean to the Mesozoic in response to horizontal movements, and the significance of some of its mafic dyke fracture patterns. J. African. Ear. Sci., 10: 483-501.

Wilson, J.F., Bickle, M.J., Hawkesworth, C.J., Martin, A., Nisbet, E., and Orpen, J.L. 1978. Granite-greenstone terrains of the Rhodesian Archaean craton. Nature, 271: 23-27.

Wilson, J.F., Jones, D.L., and Kramers, J.D. 1987. Mafic dyke swarms in Zimbabwe. In: H.C. Halls and W.F. Fahrig (Editors), Geol. Assoc. Canada. Special Paper 34, p. 433-444.

Wood, D.S. 1974. Current views of the development of slaty cleavage. Ann. Rev. Earth Plan. Sci. Lett., 2: 369-401.

Worst, B.G. 1956. The geology of the country between Belingwe and West Nicholson. Southern Rhodesia Geological Survey No. 43, 218 p.

Worst, B.G. 1962. The geology of the Buhwa iron ore deposits and adjoining country: Belingwe district. Southern Rhodesia Geological Survey No. 53, 114 p.

Wronkiewicz, D.J., and Condie, K.C. 1987. Geochemistry of Archean shales from the Witwatersrand Supergroup, South Africa: Source-area weathering and provenance. Geochim. Cosmochim. Acta, 51: 2401-2416.

Wronkiewicz, D.J., and Condie, K.C. 1989. Geochemistry and provenance of sediments from the Pongola Supergroup, South Africa: Evidence for a 3.0 Ga-old continental craton. Geochim. Cosmochim. Acta, 53: 1537-1549.

Yardley, B.W.D. 1989. An Introduction to Metamorphic Petrology. Essex, Longman, 248 p.

Vita

Christopher Mark Fedo was born in Los Angeles, California on September 20, 1963. He attended California State University, Fullerton and graduated with a B.S. in Geology in 1988. He went on to Vanderbilt University in Tennessee where he earned his Masters degree in 1990. Chris continued his education at Virginia Tech where he earned his Ph.D. in 1994. His next step is a Post Doctoral Fellowship at the University of Western Ontario.